GEOLOGICAL SURVEY OF CANADA

OPEN FILE 2850

Structural analysis of lode gold deposits in deformed terranes

F. Robert, K.H. Poulsen, and B. Dubé

1994

Natural Resources Canada Ressources naturelles Canada

Canada

STRUCTURAL ANALYSIS OF LODE GOLD DEPOSITS IN DEFORMED TERRANES

F. ROBERT, K.H. POULSEN
Geological Survey of Canada,
601 Booth St., Ottawa, Ont., Canada K1A 0E8

and

B. DUBÉ
Centre Géoscientifique de Québec
2700 Einstein, Ste-Foy, Que., Canada G1V 4C7

OPEN FILE REPORT #2850

Ottawa, April 1994

NOTE

This document contains notes used for a short course on Structural Analysis of Ore Deposits. It represents the first, *unedited* draft of a manuscript to be submitted for publication as a GSC Bulletin. The document is relased as an Open File in its unedited form in order to make it readily available to anyone interested.

TABLE OF CONTENTS

	Page
CHAPTER 1: INTRODUCTION	1
ACKNOWLEDGEMENTS	4
CHAPTER 2: STRUCTURAL CHARACTERISTICS OF GOLD DISTRICTS	5
INTRODUCTION	5
LITHOLOGICAL COMPOSITION	5
PROGRESSIVE DEFORMATION AND STRUCTURAL HISTORY	7
FAULTS AND SHEAR ZONES	14
REGIONAL STRAIN	17
CHAPTER 3: GEOLOGICAL STRUCTURES ASSOCIATED WITH GOLD DEPOSITS	19
INTRODUCTION	19
STRUCTURAL FABRICS	20
SHEAR ZONES	21
Nature and composition of shear zones	22
Internal structure of shear zones	24
VEINS	31
Theoretical considerations	31
Classification of veins	34
Fault-fill veins	36
Internal characteristics	36
Structural significance	42
Extensional veins and vein arrays	42
Internal characteristics	43
Spatial relationships	48
Structural significance	48
Stockworks and breccia veins	49
Stockworks	49
Breccia veins	52
RELATIONSHIPS AMONG VEINS AND SHEAR ZONES	53
Age relationships	53
Age relationships among veins	53
Vein development vs shear zone activity	55
Geometric relationships	57
Plunge of ore shoots	57

CHAPTER 4: THE INFLUENCE OF FAR-FIELD STRESS / STRAIN REGIME 61
INTRODUCTION 61
ANDERSONIAN FAULTING AND STRESS REGIMES 63
AXES OF NETWORKS 64
Determination deposit-scale strain axes from vein and shear zone data 67
STRUCTURE OF DEPOSITS AND THEIR ANALYSIS 69
Ferderber deposit 69
Star Lake deposit 71
Sigma-Lamaque deposit 73

CHAPTER 5: THE INFLUENCE OF STRENGTH ANISOTROPY 79
INTRODUCTION 79
COMPETENCE AND ANISOTROPY 79
Definition 79
Theoretical considerations 80
Strain refraction 84
Summary 89
STIFF LAYERS WITHIN INCOMPETENT MATRIX: THE EXAMPLE OF SILL-HOSTED GOLD DEPOSITS 89
Introduction 89
Norbeau deposit 91
Structural analysis 92
Results and discussion 96
Cooke deposit 98
Structural analysis 100
Influence of strength anisotropy 100
INCOMPETENT LAYERS WITHIN COMPETENT UNITS: THE CASE OF ENFORCED SHEARING 102
Introduction 102
Gold deposits within the Bourlamaque pluton 104
Introduction 104
Dykes and ore relationships 104
Kinematic analysis 107
Determination of deposit-related strain axes within the pluton 108
Summary 108

CHAPTER 6: STRUCTURAL HISTORY OF DEPOSITS 111
INTRODUCTION 111
DEFORMED VEIN GOLD DEPOSITS 112
Overprinting by continuation of shear zone displacement 113
Overprinting vein sets of different generation 115

San Antonio deposit 115
Pervasively deformed vein deposits 118
Orenada deposit 118
DEFORMED SULPHIDIC GOLD DEPOSITS 121
Disseminated au sulfide deposits 121
Greywacke Lake deposit 121
Massive au sulfide deposits 126
Mosquito Creek deposit 126

CHAPTER 1: INTRODUCTION

Structure has long been recognized as an important control of many aspects of lode gold deposits at all scales, ranging from the distribution of deposits to the internal textures and structures of the ore. In deformed terranes, for example, the *geometry*, i.e. the shape and orientation, of virtually all lode gold deposits and the *localization* of a large number of others are strongly influenced by structure. These two attributes are critical in efficient exploration and mining where understanding the structural controls of lode gold deposits in deformed terranes is more than an academic exercise. The understanding of the structural controls of lode gold deposits is achieved by *structural analysis* of deposits, the results of which can also be used in a predictive way in the course of exploration and mining.

Many of the important structural controls of lode gold deposits have been established over 50 years ago, as summarized in special volumes and textbooks such as Newhouse (1942), McKinstry (1948) or CIMM (1948). These early studies emphasized geometric aspects of the deposits, but interpretations of the structural controls were limited by poor kinematic constraints on shear zones and veins which are present in a large number of gold deposits. Most studies were also limited by the consideration of deformation in two dimensions only.

In the last decade, a large number of studies have documented the structural settings and controls of lode gold deposits in deformed terranes (see reviews by Hodgson, 1989; Poulsen and Robert, 1989). In part because they coincided with an explosion of literature on shear zones in the 1980's, these recent studies placed significant emphasis on the shear zones that are associated with most gold deposits. This led to a better understanding of their structural controls and of dynamic aspects of their formation, as well as the structural and crustal regimes under which they emplaced or were deformed. Recent work has also resulted in a better understanding of the *processes* involved in the formation of some lode gold deposits, and in a better appreciation of the importance of interaction between shear zones and fluid dynamics during mineralization (Sibson et al., 1988; Sibson, 1990; Cox et al., 1991; Peters, 1993).

Through these old and recent studies of lode gold deposits, we now better understanding some of the factors controling their geometry and are in a position to use this knowledge to place additional constraints on predictions of the shapes and orientations of deposits and orebodies. However, prediction the locations of these deposits, for example the site of orebodies along a given shear zone, is a far more

complex and will be a major challenge for the coming years. In this case, progress will come in part through continually improving our understanding of the structural processes involved.

The overall objective of this document is to examine structural factors controlling the geometry of deposits and orebodies and how they can be used in exploration and mining. Another important objective is to illustrate how to approach the structural analysis of lode gold deposits, what questions to ask and how to approach them. We cover a wide range of structural situations and problems commonly encountered in deformed terranes and we present their analysis in as global a perpective as possible. However, as indicated in the title, we restrict our discussion to deposits in deformed terranes, such as greenstone belts, which are typically dominated by compressional, strike-slip or transpressional tectonic regimes and which are most relevant to Canadian gold deposits.

Three main factors influence the geometry of gold deposits in deformed terranes (Table 1.1): (1) the *stress regimes* in which deposits were formed or deformed, (2) the presence of *strength anisotropies* (competency contrasts), which influence the localization, geometry and kinematics of shear zones, and veins, and (3) the *structural history* of the deposits, which dictates whether a deposit is relatively undeformed or has been structurally overprinted. These factors illustrate that, in analyzing the structure of a gold deposit, we are faced with the problem of understanding local structures in the context of regional deformation. Even though we emphasize the deposit-scale in this document, it is clear that full understanding of the structural controls of lode gold deposits, and prediction of their geometry, cannot be achieved without some knowledge of the regional structural evolution. It thus becomes imperative in any exploration program to gain structural knowledge outside the immediate target area and to collect and consider data at all scales.

Our experience also shows that a diversity of types of gold deposits occur in deformed terranes in Canada, and that not all deposits formed at the same time nor have they experienced a similar structural history. Deposits formed late in the structural evolution of their host terranes will be preserved in their *undeformed* state, whereas earlier ones will be *structurally overprinted* to varying degrees. It is also expected that the geometry of different types of gold deposits will be influenced be different sets of factors because of differences in origin, in structural setting or in timing of emplacement (Table 1.1).

For example, synvolcanic auriferous sulphide bodies will always be structurally overprinted to some degree: such sulphide bodies will be strained, folded, or overprinted by shear zones, as is the case for the Bousquet deposits in northwestern Quebec (Tourigny et al., 1993). In contrast, syn-tectonic auriferous vein deposits are commonly associated with shear zones which developed late in the local structural history: such deposits are likely to be relatively undeformed and their geometry will be controlled by the prevailing stress/strain regime at the time of

their formation and by local strength anisotropies. In other cases, auriferous shear zones may have developed during an early increment of deformation and may be folded or reactivated during subsequent increments (Brommecker et al., 1989). In such cases, the present-day configuration of the deposits will reflect the combined effects of factors controlling shear zone development and those of subsequent deformation. Clearly, one of the important challenges of the explorationist is to determine if a deposit is undeformed or structurally overprinted before making structural interpretations.

Table 1.1. Main factors influencing the geometry of lode gold deposits

FACTOR	EFFECTS
STRESS/STRAIN REGIME:	Controls orientation and kinematics of shear zones and veins Variations in stress ratio imposes deviations from 2D deformation
STRENGTH ANISOTROPY:	Influences localization of shear zones and veins, as well as their reactivation Induces local refraction of stress axes, causing deviations from regional patterns Influences complexity of shear zone and vein networks
HISTORY OF DEPOSIT:	Dictates the degree of structural overprinting and of modification of original shape and orientation Influences the complexity of vein networks

The organization of this document revolves around the main factors influencing the geometry of gold deposits. In Chapter 2, the recurring geological and structural characteristics of gold districts are examined, from the orogen-scale to that of the district. This chapter serves to place all the subsequent deposit-scale discussion into a more regional context. Chapter 3 focusses on the various structural features commonly associated with gold deposits on which is based structural analysis,

such as structural fabrics, shear zones and veins. These various structural elements are described and their significance and inter-relationships are also considered.

Chapters 4, 5 and 6 examine each of the three main factors identified above as being important in influencing the structure of gold deposits (Table 1.1). Each chapter begins with some theoretical considerations, followed by illustration of the different effects of these factors with several geological examples. Chapter 4 addresses the influence of stress/strain regimes under which syn-tectonic vein deposits are formed, whereas Chapter 5 focusses on the additional influence of strength anisotropies in such deposits. Both chapters apply to relatively undeformed syn-tectonic, shear zone-related gold deposits, particularly those of the vein-type. Chapter 6 deals with the structural history of the deposits: it emphasizes the effects, and the recognition, of deformation of deposits and of reactivations of shear zones and veins.

Throughout the document, we have tried to cover, through a large number of examples, a variety structural settings and problems that are commonly encountered by exploration and mining geologists. Accordingly, we restrict the discussions to the scales of the deposits and of the outcrops. These examples are drawn largely from our own work on gold deposits and that of numerous field assistants and graduate students with whom we have been associated over the last 10-12 years.

This document summarizes our present state of understanding of the structure of lode gold deposits. There is no doubt in our minds that this is only a progress report: many questions remain unanswered and many surprizes almost certainly lie ahead of us.

ACKNOWLEDGEMENTS

We would like to thank colleagues in universities and Provincial surveys and all exploration and mine geologists who have shared with us their knowledge of gold deposits, as well as numerous field assistants and graduate students who have assisted us in the course of our studies of gold deposits. Special thanks are also extended to K. Lauzière and K.K. Nguyen for their assistance with the preparation of many of the figures.

CHAPTER 2
STRUCTURAL CHARACTERISTICS OF GOLD DISTRICTS

INTRODUCTION

The deformed terranes that contain Canadian lode gold deposits include both Precambrian granite-greenstone belts and Phanerozoic belts composed of island arc/oceanic assemblages accreted to continental margins (Fig. 2.1). These two types of gold belts are distinguishable both in terms of age and in terms of the greater along-strike continuity of the younger terranes, but there is increasing acceptance of the notion that they have comparable origins and similar geological histories (Poulsen et al., 1992). Both types of belts are characterized by the presence of terranes of contrasting volcanic, plutonic and sedimentary composition, by polyphase deformational histories, by important crustal-scale faults and shear zones and by regional strain patterns that reflect a dominance of transpressional deformation. Considering the similarities of their composition and deformational history, it is not surprising that both the Phanerozoic and Precambrian terranes contain comparable ore deposit types, most notably lode gold and base metal massive sulphide deposits.

LITHOLOGICAL COMPOSITION

Most auriferous districts occur at or near major terrane boundaries. For example, the Val d'Or and Rice Lake districts in Superior Province occur at sub-province boundaries between northern volcano-plutonic domains and southern metasedimentary domains (Fig. 2.2, 2.3) and the Chibougamau district (Fig. 2.4) occupies the northern boundary of the Abitibi Subprovince. Likewise, the early Proterozoic La Ronge gold belt straddles the boundary between the Central metavolcanic belt and the McLean Lake metasedimentary belt within the Trans-Hudson Orogen (Fig. 2.5). The Paleozoic Baie-Verte gold belt in the Newfoundland Appalachians occupies the boundary between the allochthonous metavolcanic-plutonic rocks of the Dunnage Zone and the deformed metasedimentary rocks of the Fleur de Lys belt (Fig. 2.6). Likewise, the Cariboo gold district in British Columbia (Fig. 2.7) occurs in deformed continental margin metasedimentary rocks of the Barkerville terrane at their thrust contact with oceanic rocks of the Slide Mountain terrane.

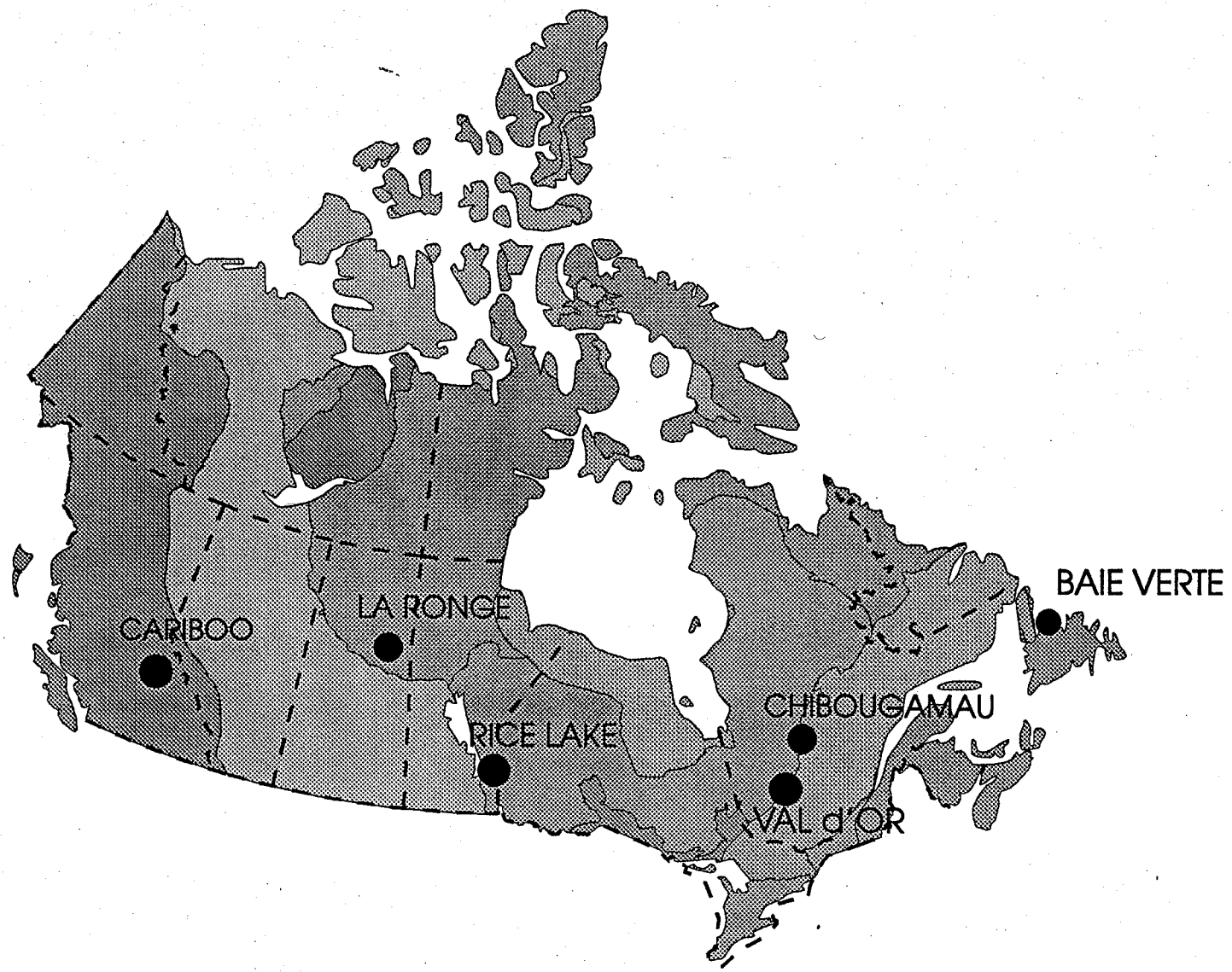

Figure 2.1. Location of Canadian gold districts from which most examples that are discussed in the text are drawn.

In most districts, the metasedimentary domains consist of thick sequences of metaturbidites in which the metamorphic grade ranges from greenschist to upper amphibolite and granulite facies. Examples include the Pontiac and English River sequences of Superior Province; the McLean Lake (Kisseynew-equivalent?) sequences of the La Ronge Domain; the Fleur de Lys sequence of western Newfoundland and the meta-sandstones and -pelites of the Snowshoe Group in the Cariboo District.

Volcano-plutonic domains in gold districts consist of elongate belts of predominantly metavolcanic supracrustal rocks metamorphosed at greenschist to lower amphibolite facies conditions. Most contain mainly mafic to felsic metavolcanic rocks, and locally significant volumes of ultramafic rocks. In the Phanerozoic terranes the ultramafic rocks are typically parts of ophiolite sequences whereas they are of komatiitic type in the Precambrian terranes. Narrow belts of metasedimentary rocks within these volcanic domains commonly comprise polymictic conglomerates, arenites, greywackes, mudstones, and locally significant amounts of oxide facies iron formation in the Archean examples. Typified by the Cadillac conglomerates of the Southern Abitibi, the Opemisca Group of the Northern Abitibi, the McLennan Lake Group meta-arkose of the La Ronge Domain, these narrow belts of metasedimentary rocks are considered to represent late-stage alluvial-fluvial accumulations that unconformably overly the metavolcanic rocks of the respective belts. The metavolcanic rocks of these belts are also intruded by a variety of gabbroic sills and subvolcanic, dioritic to tonalitic plutons. Both metavolcanic and metasedimentary rocks contain a suite of syn- to late-tectonic stocks, plutons, dykes and batholiths, ranging in composition from dioritic to tonalitic, monzonitic, syenitic, and granitic.

PROGRESSIVE DEFORMATION AND STRUCTURAL HISTORY

The structure of many greenstone gold districts is characterized by several recognizable increments of deformation, as indicated by the existence of multiple generations of overprinting metamorphic fabrics and folds. Structural analysis in these belts is complicated by the highly heterogeneous nature of the deformation which, in part, can be attributed to the complex competency contrasts that are inherent is such lithologically diverse terranes. It is difficult to correlate structures from one area to another in these terranes because of this heterogeneity and because of the local, domainal development of structural fabrics. Experience gained from several gold districts shows that one of the increments of deformation, most commonly identified as "D2", has resulted in the most penetrative planar and linear fabrics and these can be taken as a point of reference in the discussion of the other increments. Such foliations (planar fabric) and elongation lineations (linear fabric) correspond to the shape fabrics of geological objects and to the

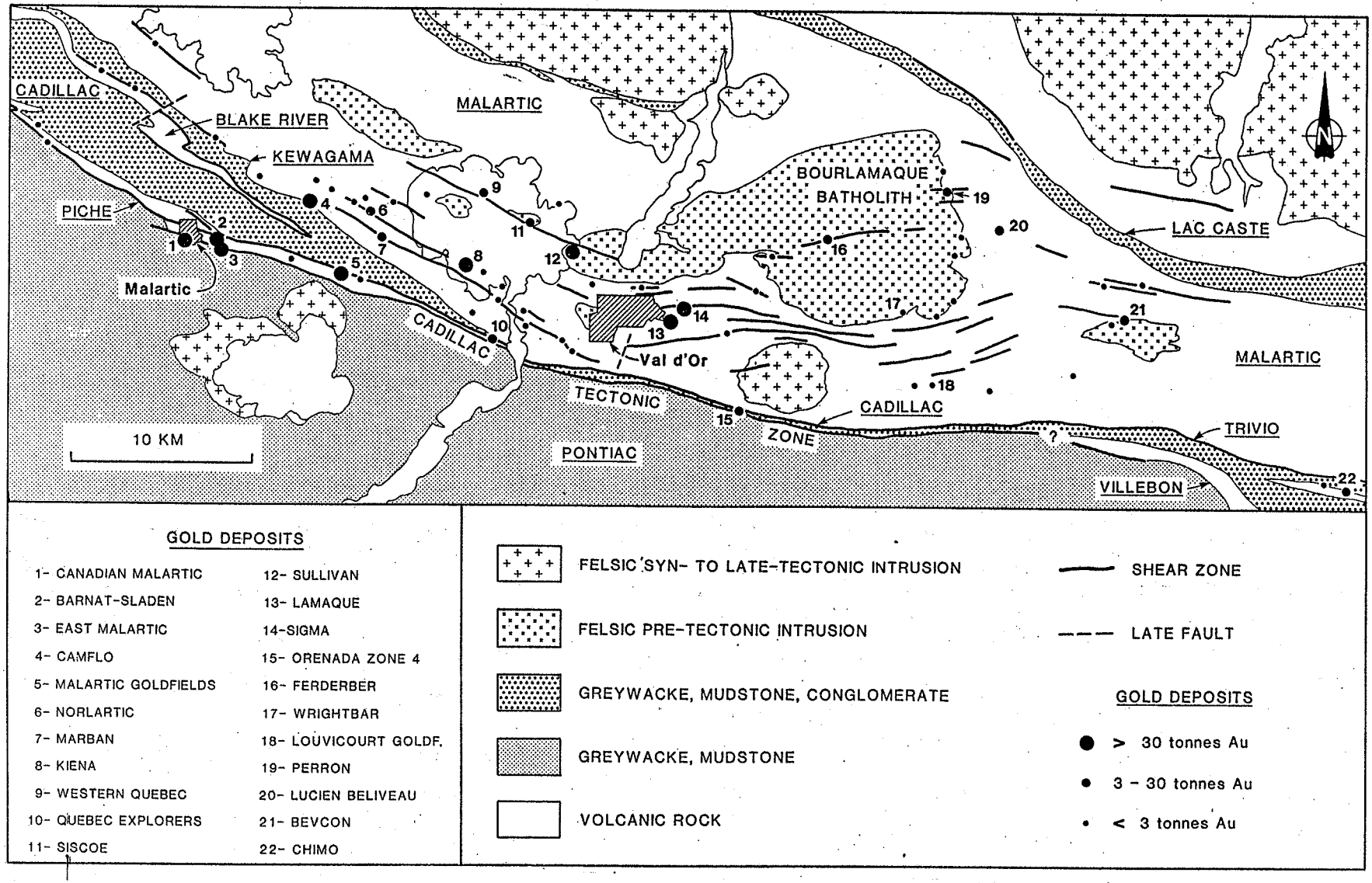

Figure 2.2. Geology and Gold Deposits of the Val d'Or district, Abitibi Subprovince, Quebec.

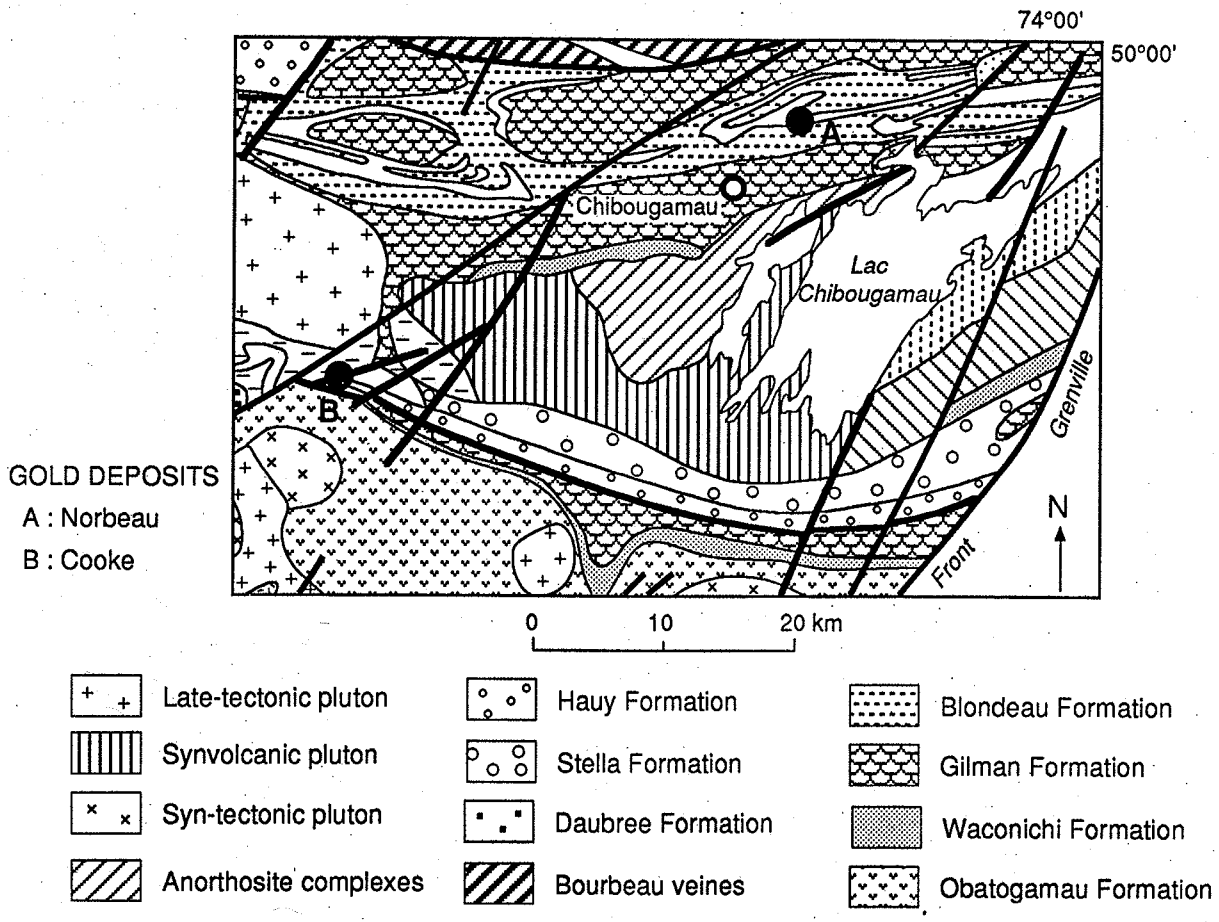

Figure 2.3. Geology and Gold Deposits of the Chibougamau district, Abitibi Subprovince, Quebec.

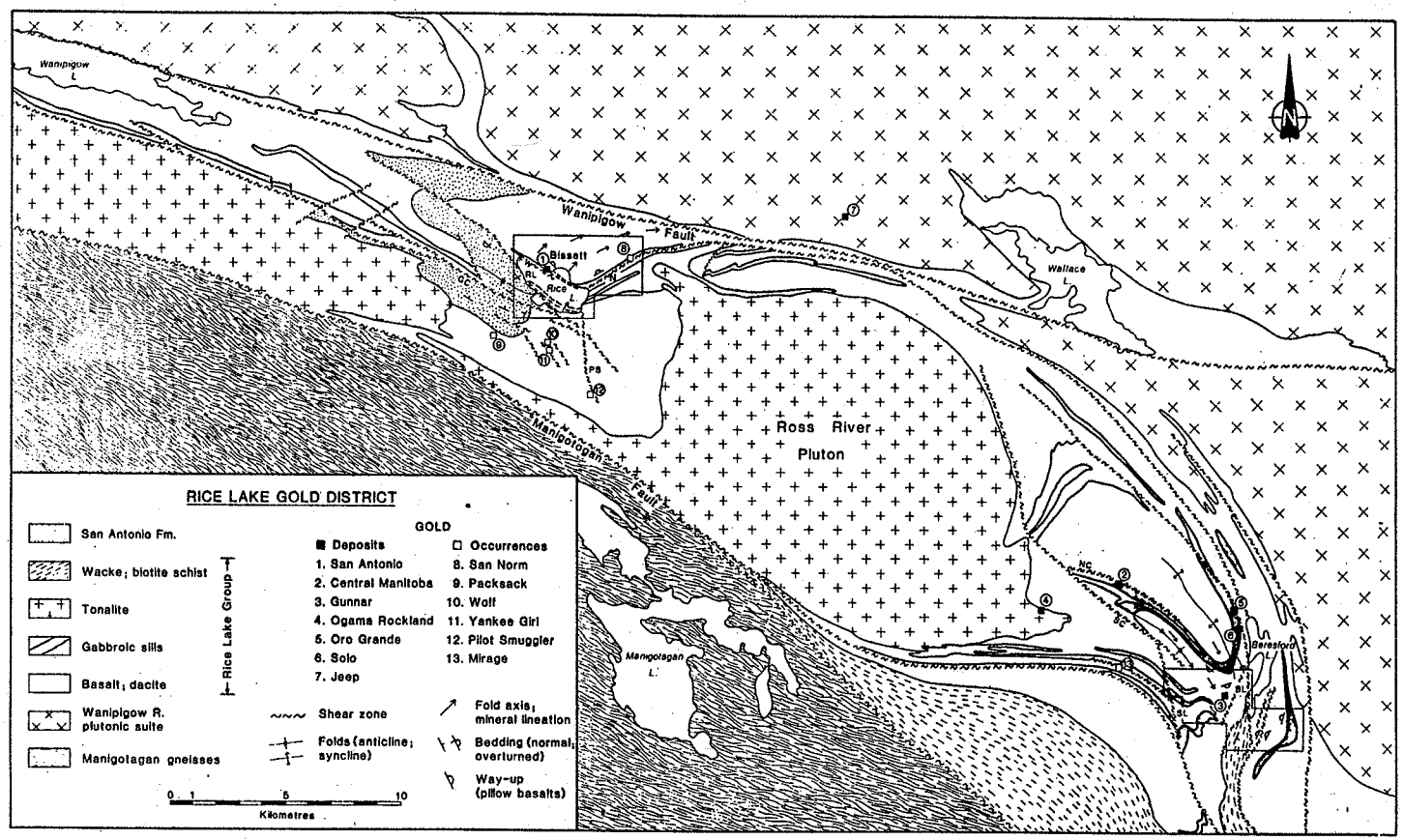

Figure 2.4. Geology and Gold Deposits of the Rice Lake district, Uchi Subprovince, Manitoba.

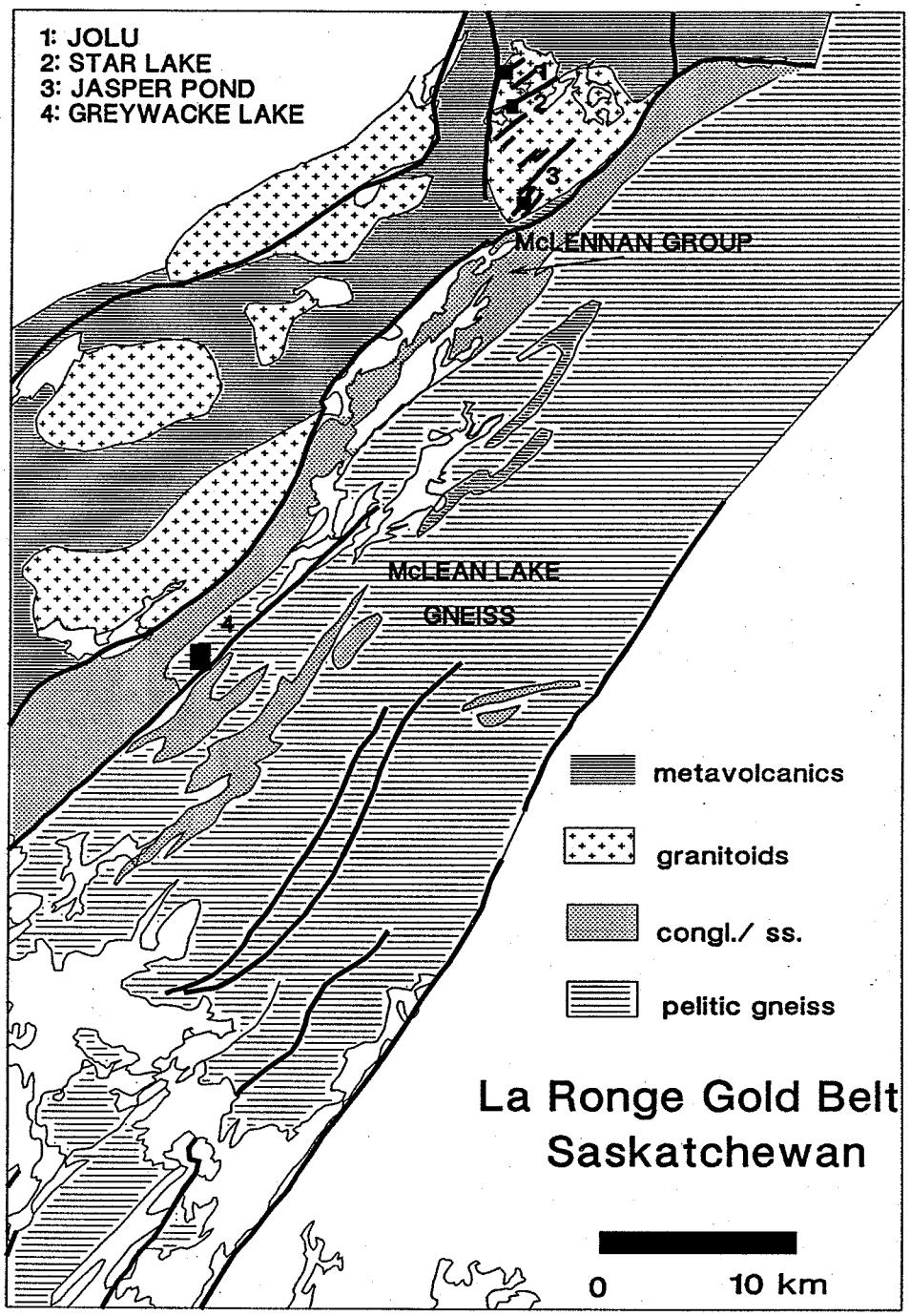

Figure 2.5. Geology and Gold Deposits of the central part of the La Ronge district, Saskatchewan

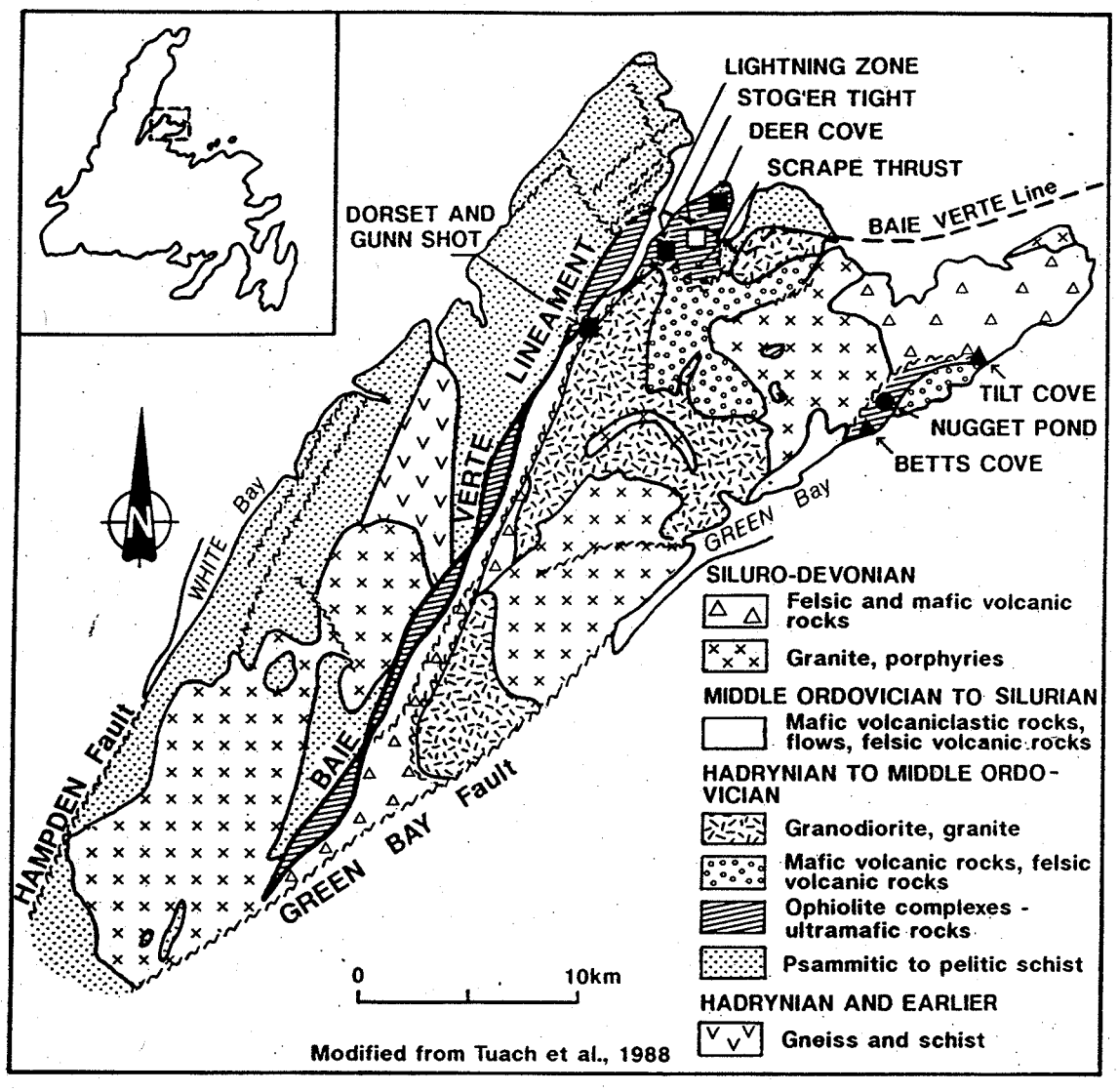

Figure 2.6. Geology and Gold deposits of the Baie Verte district, Newfoundland.

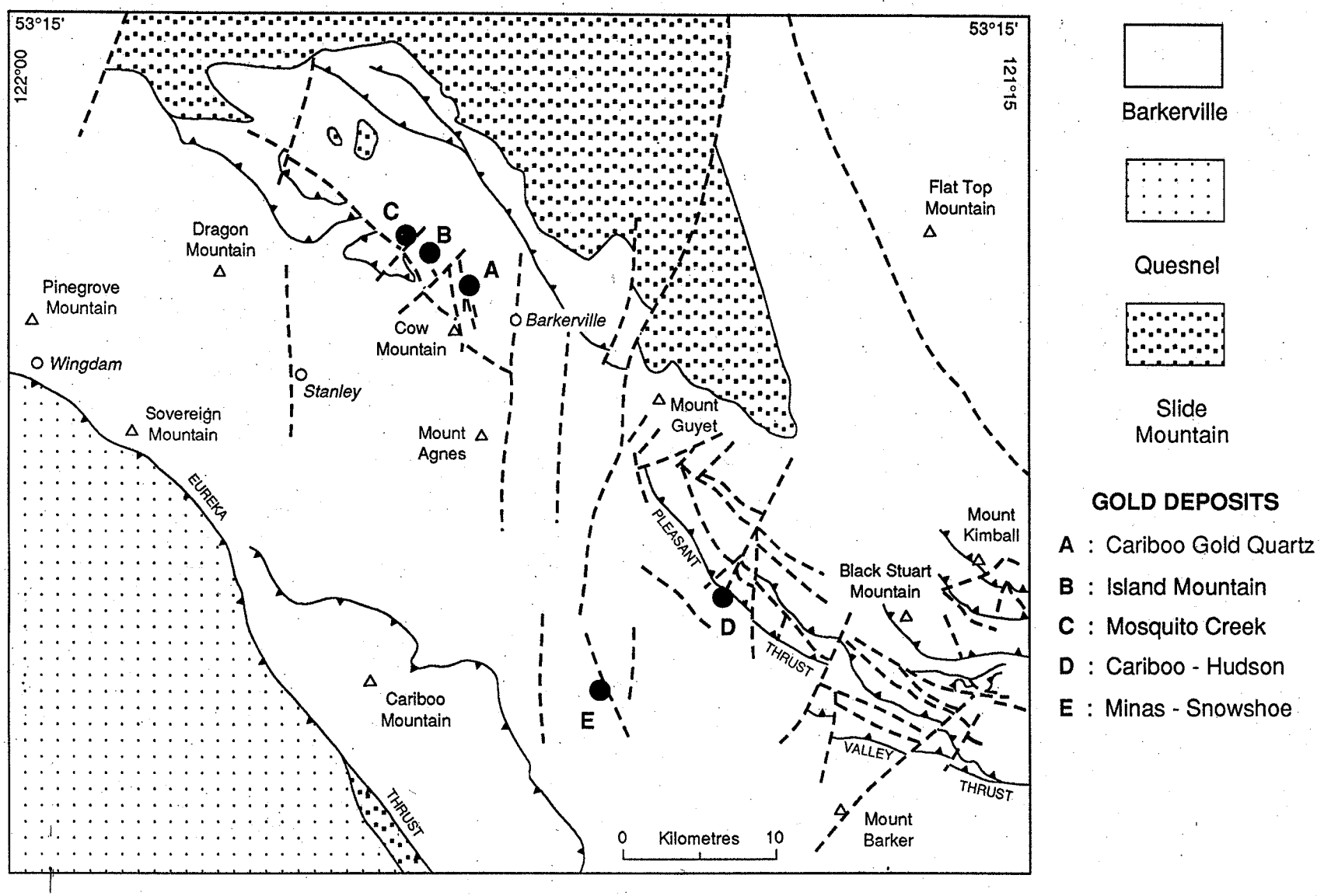

Figure 2.7. Geology and Gold deposits of the Cariboo district, British Columbia.

preferred orientation of metamorphic minerals. In many greenstone gold districts, the penetrative foliation is subvertical and subparallel to lithological units and contributes to the definition of the overall structural trend of a district.

At least three main increments of deformation can be identified in most gold districts (Table 2.1). In all districts, early folds and a layer-parallel penetrative foliation are ascribed to the D1 increment of deformation which most commonly corresponds to a period of "thin-skinned" thrusting and related isoclinal folding. As is commonly the case however, the full significance of the D1 increment of deformation is difficult to document owing to common overprinting by younger structures. Development of the strongest and most penetrative foliation in most districts corresponds to D2 deformation which represents an increment of "thick-skinned" shortening. S2 foliation is typically subvertical and axial planar to upright, tight to isoclinal, F2 folds. The penetrative S2 foliation also commonly contains an elongation lineation, defined by a mineral lineation and by the long axes of geological objects. Plunges of L2 most commonly are steep and down the dip of S2 (Val d'Or, Rice Lake, Chibougamau, La Ronge) but can also vary continuously within a district from steep to shallow attitudes. S2 generally records the horizontal shortening of a district with accompanying subvertical to subhorizontal elongation in the S2 plane. In most districts, the D3 increment of deformation is locally and best developed in the vicinity of major strike-slip shear zones. D3 is typically characterized by steeply plunging asymmetric folds and subvertical axial planar crenulation cleavage that overprints S2.

Most gold districts have therefore experienced a similar structural evolution, involving early thrusting, thick-skinned compressional deformation (D2), progressively evolving into transcurrent deformation (D3). The districts, however, and even subareas within districts, differ from one another by the relative importance of these three increments of deformation. For example, at Val d'Or, D2 accounts for the bulk of the structural trend and the finite strain pattern, which is best characterized by the steeply plunging elongation lineation. D3 has had overall minor effects, which are geographically restricted to the Cadillac fault and the western part of the district (Robert 1990).

FAULTS AND SHEAR ZONES

Gold districts are commonly associated with major crustal-scale shear zones which mark the boundaries between lithologically contrasting domains. They are generally regarded as the major channelways for upward migration of deep-seated fluids (Kerrich, 1989; Eisenlohr et al., 1989) but their genetic relationship to gold deposits is poorly established. Within districts, the deposits actually are preferentially associated with arrays of smaller subsidiary shear zones dispersed away from the major ones. Significant portions of shear zones of all scales show

TABLE 2.1 - Deformation History of Selected Canadian Gold Districts

DISTRICT	D1	D2	D3	REFERENCE
Val d'Or	NW-SE upright folds and steep shear zones; NE-SW shortening	E-W subvertical cleavage containing subvertical elongation lineations; steep N- and S- dipping reverse shear zones; N-S shortening	ENE crenulation cleavage and steep open folds; reactivations of shear zones in transcurrent mode	Hubert and Sansfacon, 1990; Hubert et al. 1984)
Chibougamau	N-S upright folds; no systematic foliation	E-W subvertical isoclinal folds and cleavage; steep elongation lineation; E-W steep reverse faults	N.E. crenulation cleavage; brittle-ductile N.E. faults	Daigneault et al., 1990
Rice Lake	NE-SW thrusting; NW shear zones	NE-SW shortening; NW-SE steep cleavage and steep elongation lineations; N-S and ENE-WSW oblique-reverse shear zones	ESE dextral shear zones; ENE crenulation cleavage	Brommecker et al. 1989
La Ronge	S1 foliation and transposed primary layering; F1 intrafolial fold axes, L1 rodding; mylonitic thrusts	S2 west-dipping, NE striking axial planes; NE-SW trending tight folds overturned to SE; doubly-plunging NE-SW fold axes, high strain shears on overturned F2 limbs	vertical N to NW axial planes; N to NW trending open folds; steep N and NW fold axes; dextral reactivation of D2 shears; new NE and NW shears	Lewry et al., 1990; Coombe et al., 1986
Baie Verte	tectonic slides; minor isoclinal folds and layer parallel schistosity	upright folds and penetrative cleaveage; prominent lineation	"strain-slip" and crenulation cleavages; dextral Green Bay Fault	Hibbard, 1983
Cariboo	layer parallel cleavage and rootless isoclinal folds; thrust deformation	asymmetric NW folds and penetrative cleavage; steep E-dipping reverse faults	open folds, warps kinks and crenulations; steeply dipping strike faults	Struik, 1986; 1988

similar hydrothermal alteration (carbonatization) typical of gold deposits, as well as at least some lode gold mineralization. This at least suggests that similar fluids infiltrated all shear zones, and that shear zones of all scales can be considered to have formed interconnected, district-scale arrays (Robert and Poulsen, 1991).

The identification of shear zones through mapping the distribution of high strain versus low strain rocks is relatively simple but their kinematic interpretation is more complex, due to the multitude and ambiguous nature of kinematic indicators, and due to the relatively common problem of shear zone reactivation during subsequent deformation. In many districts, shear zones can be grouped into first and higher orders, according to their dimensions (Kerrich, 1989; Eisenlohr et al., 1989; Robert, 1990a). First order shear zones are the crustal-scale longitudinal faults marking the boundaries between major lithologic domains, represented by the Cadillac fault at Val d'Or, the Kapunapotagan Fault at Chibougamau, the Moore Lake-Beresford Lake Fault at Rice Lake, the Mclennan Lake Tectonic Zone in the La Ronge Domain, the Baie Verte Lineament in western Newfoundland and the Eureka Thrust in the Cariboo district. These zones of high strain extend along strike in excess of 100 km, reach thickesses of 1 km, and dip at steep to moderate angles to depths in excess of 10 km, as has been shown for the Cadillac fault (Jackson et al., 1990). Smaller, second order shear zones extend for a few to several tens of kilometres, reach widths of several tens of metres, and are also subparallel to the regional structural trend. The more abundant third order shear zones, to which the bulk of gold mineralization in most districts is associated, are less than a few kilometres long and up to several metres wide. The first order and most of the second order shear zones are subparallel in strike and dip to the regional structural trend and penetrative foliation. In contrast, third order shear zones tend to be oblique to the structural trend. At the scale of the district or that of a deposit, the three orders of shear zones tend to intersect, merge and branch, at least locally, and to form a three-dimensional array. This network can be regarded as a district-scale plumbing system along which fluids infiltrated.

It is likely that faults and shear zones developed during all increments of progressive deformation in any district (Brommecker et al., 1989). First order shear zones are probably the longest-lived structures and have undergone complex deformation histories. However, their internal structure is commonly dominated by an intense foliation, subparallel to the shear zone boundary and to the regional penetrative foliation. This dominant foliation is commonly overprinted by crenulation cleavages and asymmetric folds. For example, the internal foliation of the major faults at Val d'Or, Chibougamau and Rice Lake are overprinted by asymmetric Z-shaped F3 folds. Elongation lineations within first order shear zones are in general subparallel to the regional ones. In the Cadillac fault, elongation lineations are steeply to moderately plunging and, together with the presence of local steeply plunging sheath folds (Robert, 1989), they indicate significant dip-slip

movements along that fault. The steeply plunging Z-shaped F3 folds observed within the fault represent dextral strike-slip reactivation during D3.

REGIONAL STRAIN

There is an overall progressive transition with time from compressional to transcurrent regimes in most gold belts. This has led to the concept that the overall regime is a "transpressional" one in which the compressional and transcurrent components of deformation may be separated in space and/or in time. It is important to note however that, in a strict theoretical sense, "transpression" refers to a simultaneous wrenching and shortening (i.e. the general non-coaxial deformation of Hanmer and Paschier, 1990). Whether accumulated by a single transpressive strain or by successive compressive and strike slip components, the resulting regional strains are typically complex and inhomogeneous, even in the absence of major competency contrasts.

CHAPTER 3: GEOLOGICAL STRUCTURES ASSOCIATED WITH GOLD DEPOSITS

INTRODUCTION

This chapter focusses on the nature and significance of a number of geological structures that are commonly associated with gold deposits. We review the nature of these geological structures and, more importantly, we examine how to analyse the and how to use them, alone or in combination with other structural elements, in order to place constraints on the structural settings and controls of gold deposits. The emphasis is placed on mesoscopic structural elements, as they can be observed on the scales of the outcrop and the hand specimen.

The emphasis is placed on shear zones and veins, the two most common types of geological structures of gold deposits. Despite the diversity of types of gold deposits, nearly all of them are associated with shear zones, in one way or another. Besides vein-type gold deposits, which are typically related to shear zones (Hodgson, 1989; Poulsen and Robert, 1989), auriferous semi-massive to massive sulphide orebodies, such as those of the Bousquet deposit (Marquis et al., 1990; Tourigny et al., 1993), and disseminated gold orebodies such as those at Hemlo (reference.) and Hope Brook (Stewart, 1992) also occur within wide, regional shear zones. Veins are also present in a majority of gold deposits: they may form the bulk of the ore, in which case they provide constraints on the structural controls of the mineralization, or they may overprint the ore, in which case they provide constraints on the post-ore deformation history. Thus, structural analysis of most gold deposits will combine information from both shear zones and veins present in the deposits.

This chapter begins with a brief review of planar and linear structural fabrics commonly observed in gold deposits. Such fabrics form the basic structural elements of shear zones, which are considered next. It is followed by a section on the different types of veins encountered in gold deposits; a final section examines common relationships observed among these various structural elements.

Where appropriate, we have tried to address problems with which geologists are commonly faced with in the field. The different geological structures discussed in this paper are illustrated with abundant field examples, which have been selected for their clarity and quality; as such, they may not all be entirely representative of what we normally see in the field. Finally, it is important to note

that this chapter only considers undeformed structural elements; the question of overprinted structures is addressed in Chapter 6.

STRUCTURAL FABRICS

Planar and linear structural fabrics within shear zones and adjacent rocks are particularly important in the context of structural analysis of lode gold deposits and are considered briefly below. For more information on the subject, the reader is referred to Turner and Weiss (1963), Hobbs et al. (1976), McClay (1987), and Twiss and Moores (1992), among others.

In general, planar structural fabrics, or foliations, are defined by the preferred planar orientation of minerals and mineral aggregates, which typically corresponds on outcrop to a schistosity (Fig. 3.1). Foliation is also defined by the shape of geological objects such as pebbles, pillows, varioles and lapilli. It is generally agreed that such planar structural fabrics correspond to the XY plane of the finite strain ellipsoid (Ramsay and Huber, 1983).

Two common types of lineations are also present: elongation and intersection lineations. Because they have different structural significance, it is very important to distinguish between these two types of lineations. Elongation lineations, also commonly referred to as stretching lineations, correspond to a mineral lineation (Fig. 3.1) and to the shape of geological objects within the rocks such as pebbles, pillows, varioles and lapilli (Fig. 3.2). Intersection lineations, including crenulation lineations, are linear elements corresponding to the intersection of two surfaces (bedding and foliation, two foliation planes). Elongation lineations correspond to the X axis of the finite strain ellipsoid (Ramsay and Huber, 1983). In contrast, intersection lineations do not necessarily bear any consistent relationships to finite strain axes, although one common observation in gold deposits and districts is that intersection lineations are parallel to elongation lineations, which are in turn commonly parallel to mesoscopic fold axes.

In general, rocks in gold districts display at least one set of penetrative foliation and elongation lineation. However, these fabrics are not uniformly developed and also vary in relative intensity; as a result, some rocks only contain a foliation (commonly referred to as S-tectonites; Fig. 3.1C) whereas others only display an elongation lineation (L-tectonites; Fig. 3.1A). However, most rocks display both types of penetrative fabrics. Additional foliations are also commonly present in the form of crenulation cleavages, as well as their related intersection lineations.

As pointed ou in Chapter 2 our experience shows that, in a number of gold districts, the orientation of penetrative foliations and elongation lineations is very coherent and varies rather smoothly across the districts; this suggests that penetrative fabrics reflect the dominant structural regime is which the rocks were

deformed. Thus, it is possible to use, with caution, the orientations of the regional penetrative foliations and elongation lineations as a first approximation of the structural regime in which gold deposits were formed or deformed.

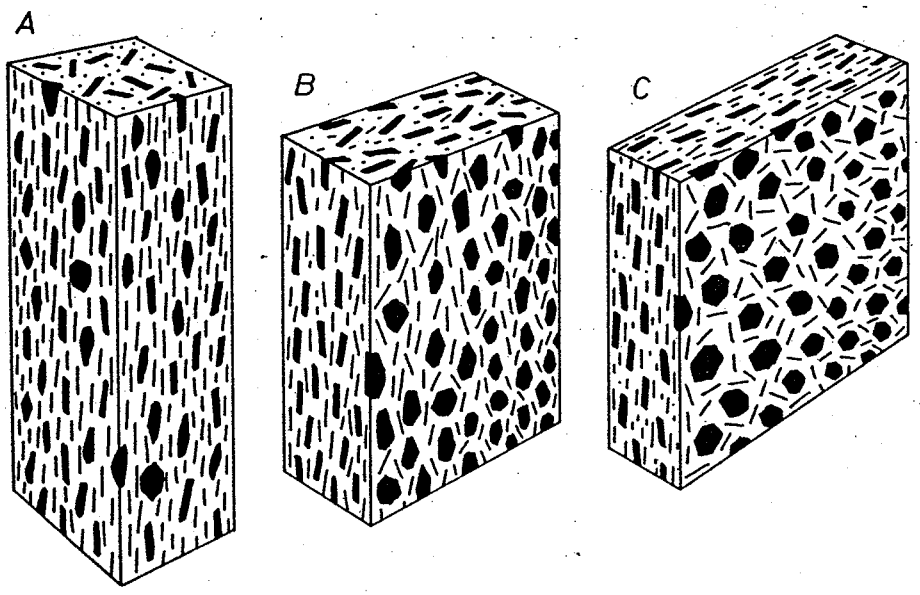

Figure 3.1. Planar and linear tectonic fabrics corresponding to the three main types of strain, as defined by the preferred orientation of minerals; from Ramsay and Huber (1983). (**A**) Prolate strain, resulting in L-tectonites. (**B**) Plane strain, resulting in L-S-tectonites. (**C**) Oblate strain, resulting in S-tectonites.

SHEAR ZONES

As indicated above, shear zones are an important component of most gold deposits and they provide essential information on the structural setting and controls of gold deposits. The orientation of shear zones is controled by two main factors: the orientation of stress axes and the presence of strength anisotropies in the rocks. Shear zones within a homogeneous rock mass will form at predictable angles to the maximum compressive stress and will have predictable senses of shear. In heterogeneous rock masses, however, shear zones will tend to develop at sites of strength anisotropies such as contacts between lithological units and the angular relationships of shear zones to stress axes may deviate from those predicted. Chapters 4 and 5 consider in detail the effects of these two important factors of shear zone development. After identification of shear zones and their boundaries, the other critical aspect of shear zone analysis is the determination of the direction and sense of movement along them. Kinematic interpretation of shear zones is particularly important because it allows reconstruction of tectonic forces responsible for development of mineralized veins or for the deformation of a

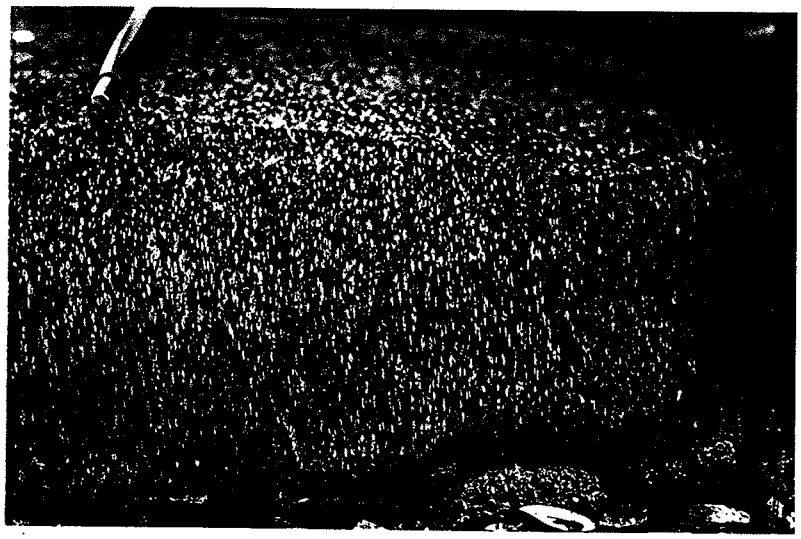

Figure 3.2. Examples of vertically elongated varioles from the Val d'Or district.

deposit. In addition, in a large number of cases, vein orientations and the plunges of orebodies have predictable geometric relationships to the direction of shear.

There is a voluminous body of recent literature on shear zones, their geometry and their kinematic analysis. For more information on these topics, the reader is referred to Ramsay (1980), Bell and Hammond (1984), Ramsay and Huber (1983, 1987), Hanmer and Passchier (1991), among many others. Many documents on shear zones emphasize those that developed in medium to coarse grained crystalline rocks at amphibolite grade or higher, in which a variety of kinematic indicators are well developed. This contrasts with the greenschist grade shear zones typically encountered in gold districts, which commonly consist of schist and phyllonite containing scarce reliable shear sense indicators, if any.

In this section, we focus on some common characteristics of shear zones in gold deposits and gold districts and common difficulties and problems of shear zone analysis encountered in the field. We first consider the nature and composition of auriferous shear zones, which is important for their identification in the field, followed by examination of their geomety and internal structures and their kinematic analysis.

Nature and composition of shear zones

Ramsay (1980) classified shear zones as brittle, brittle-ductile and ductile (Fig. 3.3). Brittle shear zones are those across which markers are abruptly offset along discontinuities; brittle shear zones will here be referred to as faults. Ductile shear zones are those along which deformation state varies continuously across the zone

and markers are progressively offset without discontinuities. Brittle-ductile shear zones are those along which there are both continuous and discountinuous deformation and offset of markers. A large number of auriferous shear zones display evidence of both continuous deformation, as indicated by the presence of intense penetrative foliation, and discontinuous deformation, as indicated by the presence of veins, slip surfaces and breccias. This is the case of the shear zone presented in Figure 3.4A, which contains a discrete slip surface in its center. It is important to note that the continuous or discontinuous character of a given shear zone is in part dependant on the rheological properties of the deformed rocks. It is therefore expected that the character of a particular shear zone will change as different host rocks are intersected. Brittle shear zones are also common in gold deposits in the form of late, post-ore faults.

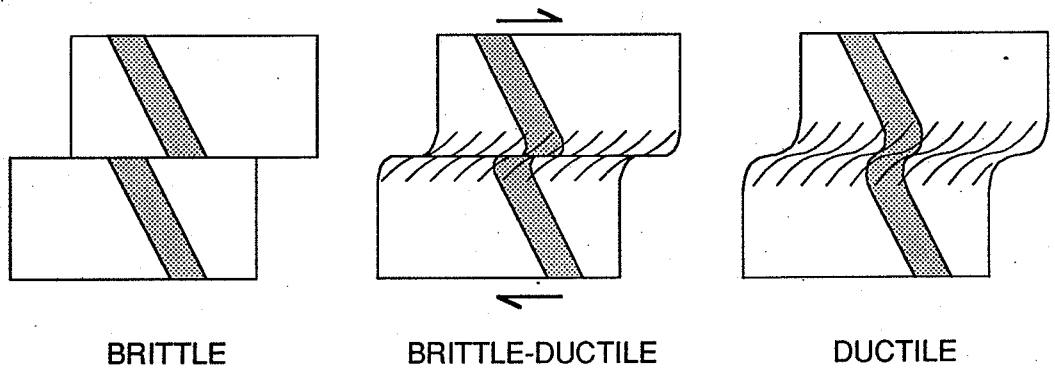

Figure 3.3. Classification of shear zones; adapted from Ramsay (1980).

As emphasized in Chapter 2, shear zones in gold districts occur over a wide range of scales: they range from outcrop-scale, to deposit-scale such as those intimately associated with vein-type gold deposits, to regional-scale, such as the shear zones hosting and overprinting entire gold deposits such as the Hemlo (reference) and Bousquet (Tourigny et al., 1988, 1989) deposits. Shear zones are planar to curviplanar zones of strongly foliated rocks, most commonly in marked contrast with surrounding, less deformed rocks. They are also commonly, but not always, characterized by an increased abundance of veins and veinlets. A common geometric attribute of outcrop- and deposit-scale shear zones is their anastomosed character, as defined by merging and bifurcating shear zone splays separated by lenticular domains of less foliated rocks. Such complex shear zone patterns reflect particular ways in which shear zone segments developed, as well as the heterogeneous nature of the strain in gold districts.

Shear zone boundaries can be locally sharp but they are generally gradational. The identification of shear zone boundaries and orientations is important because it provides the essential framework for their kinematic analysis. Boundaries are

generally easy to define in the case of outcrop- and deposit-scale shear zones, where the contrast in intensity of foliation is readily observed and mappable (Figs. 3.4A and B). However, in the case of large, regional shear zones with widths on the order of hundreds of metres or more, the identification of the boundaries is complicated by the fact that strain gradients may be spread over a wide area and that different protoliths, responding to deformation in different ways, are likely to be involved. Another common difficulty in identifyinging shear zones is to decide if we are dealing with a true shear zone, i.e. a zone along which there is displacement, or with a zone of high strain but without displacement.

A wide range of types fault rocks are present within shear zones, depending largely on the nature of the protolith and the presence or absence of hydrothermal alteration during deformation. Three types of fault rocks are commonly observed in auriferous shear zones: *mylonite*, *phyllonite* and *schist*. It is important to realize that all three types of fault rocks may be present within single shear zones, especially larger ones, because they are likely to overprint a variety of rock types and because only selective portions of shear zones are altered. However, the most important point is not so much the term used to designate shear zone rocks but the recognition that they are anomalous in their regional context.

In coarse to medium grained rocks such as granitoids and gabbros, shear zone development may be accompanied by progressive grain size reduction, producing rocks of the *mylonite* series (Sibson, 1977). However, in the more common cases where deformation was accompanied by metasomatism, such coarse to medium grained rocks have been converted to foliated, phyllosilicate-rich rocks for which the mylonite terminology in not appropriate. The alternate term used by a number of geologists is *phyllonite* (Sibson, 1977; Poulsen, 1986).

In the most common situation where shear zone protoliths are fine grained volcanic or sedimentary rocks, progressive shear zone deformation produces typically phyllosilicate-rich rocks (chlorite, sericite) which are best referred to as *schists*. However, other than their restriction to discrete zones, schists produced within shear zones cannot be distinguished form schists that are regionally developed. Compositional layering is a common characteristic of shear zones in which deformation was accompanied by hydrothermal alteration. For example, chlorite-carbonate schists derived from the deformation and alteration of mafic volcanic flows will consist of alternating carbonate-rich, chlorite-rich and quartz and feldspar-rich layers.

Internal structure of shear zones

As pointed out above, a major objective of shear zone analysis is to determine the direction and sense of movement along it. This is relatively easy where geological markers (lithological contacts, dykes, veins, etc) are offset by the shear zone, as is

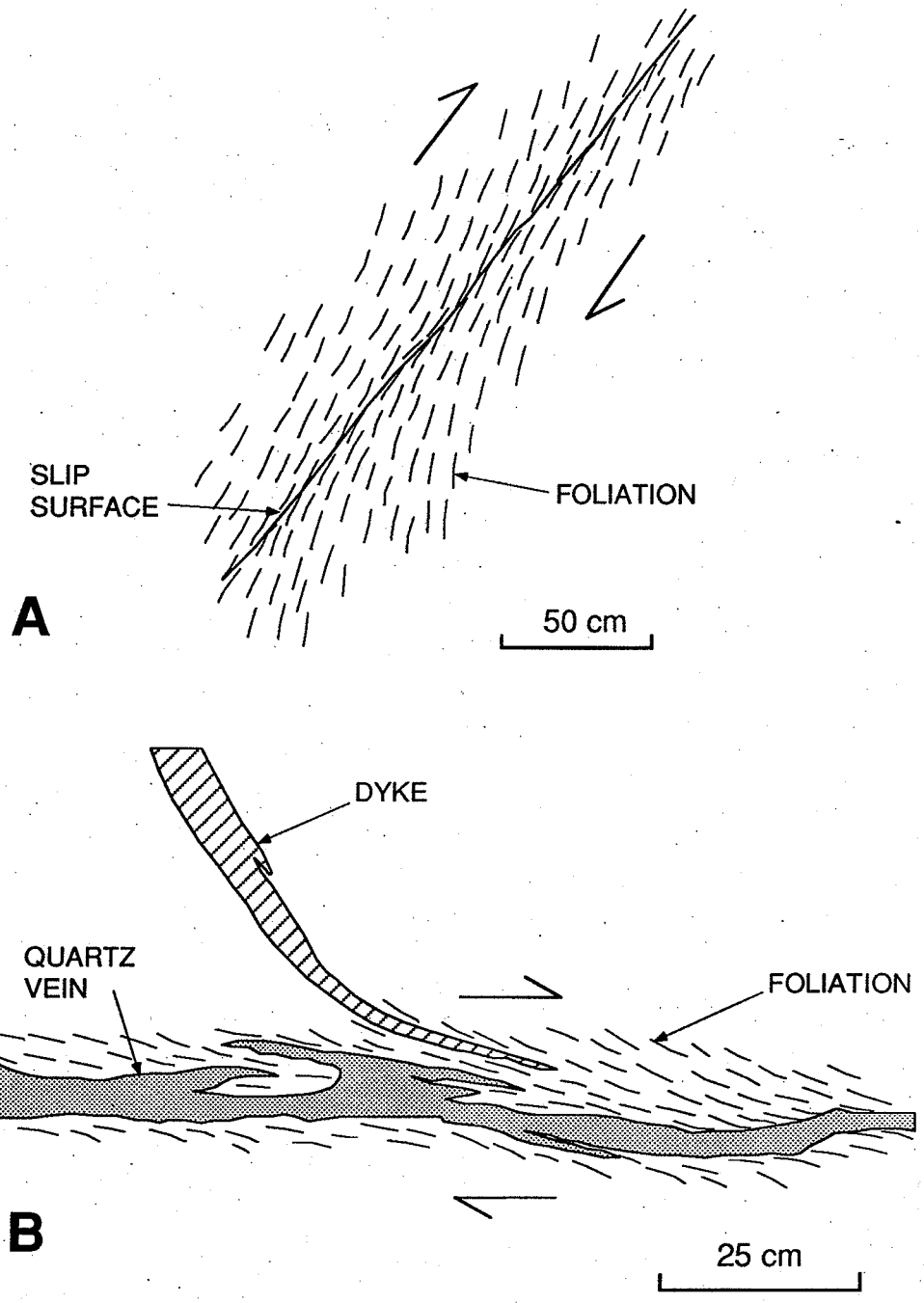

Figure 3.4. Examples of small scale shear zones illustrating the sigmoidal shape of their internal foliation; Val d'Or district. (**A**) Vertical cross-section of a reverse shear zone in mafic volcanic rocks; note the central slip surface within the shear zone. (**B**) Outcrop view of a sinistral shear zone within fine grained diorite containing a central quartz vein and offsetting a granodiorite dyke. In both cases, the shear zones are viewed in a plane perpendicular to the foliation and containing the elongation lineation.

the case in Figure 3.4B. However, in a large number of cases, such offset markers are absent and shear zone analysis must rely on their internal features.

Idealized shear zone models based on simple shear predict the foliation (also commonly termed S-surface) to lie oblique to the shear zone boundaries (Fig. 3.5). It is generally agreed that the foliation and the elongation lineation within shear zones corresponds to the XY plane and to the X axis of the finite strain ellipsoid, respectively. Thus, variations in orientation and intensity of foliation within a shear zone tracks variations in intensity and orientation of finite strain across the zone (Ramsay, 1980).

The resulting asymmetry of foliation relative to shear zone boundaries is one of the most reliable indication of the *sense of shear* (Fig. 3.5), which is easily determined for the two natural shear zones illustrated in Figure 3.4. The *direction of movement* along a shear zone is obtained by projecting the elongation lineation onto the plane containing the shear zone. It is also given by a line perpendicular to the intersection between the shear zone boundaries and the internal foliation, projected onto the plane of the shear zone as illustrated in Figure 3.5. This intersection corresponds to the Y-axis of the finite strain ellipsoid, and to the *B-axis* of the shear zone, which is defined as the line perpendicular to the movement direction within the plane of the shear zone. The B-axis is a convenient way of representing the movement direction of shear zones as it is not sensitive to common undulations of shear zones about their Y-axis (Fig. 3.5). Intersections between shear zones and related splays are in many cases parallel to the B-axis of the main shear zone.

A final important point is that, in order to see any obliquity of foliation, the shear zone should be observed in the proper plane: perpendicular to foliation but containing the elongation lineation (Fig. 3.5). In the case of reverse shear zones for example, the asymmetry of foliation would be best observed in cross-section (Fig. 3.4A), whereas for strike-slip shear zones, it would be best observed in plan view (Fig. 3.4B).

As pointed out by Hanmer and Passchier (1991), *natural shear zones* are likely to form by a combination of simple shear and shortening across the zone (pure shear), which reduces the expected obliquity of foliation to shear zone boundaries. The same will hold for shear zones experiencing a volume decrease, as would be reflected by the presence of pressure solution cleavages (Ramsay and Huber, 1987). However, as illustrated below, a significant number of auriferous shear zones approximately conform to the theoretical model of simple shear without significant across-shear shortening or volume change.

At the Paramaque showing of the Val d'Or district, auriferous quartz veins are hosted by a shear zone oriented at 105-60° within a gabbro sill (Fig. 3.6A). The gabbro is cut by a tonalitic feldspar porphyry dyke, which is offset by the shear

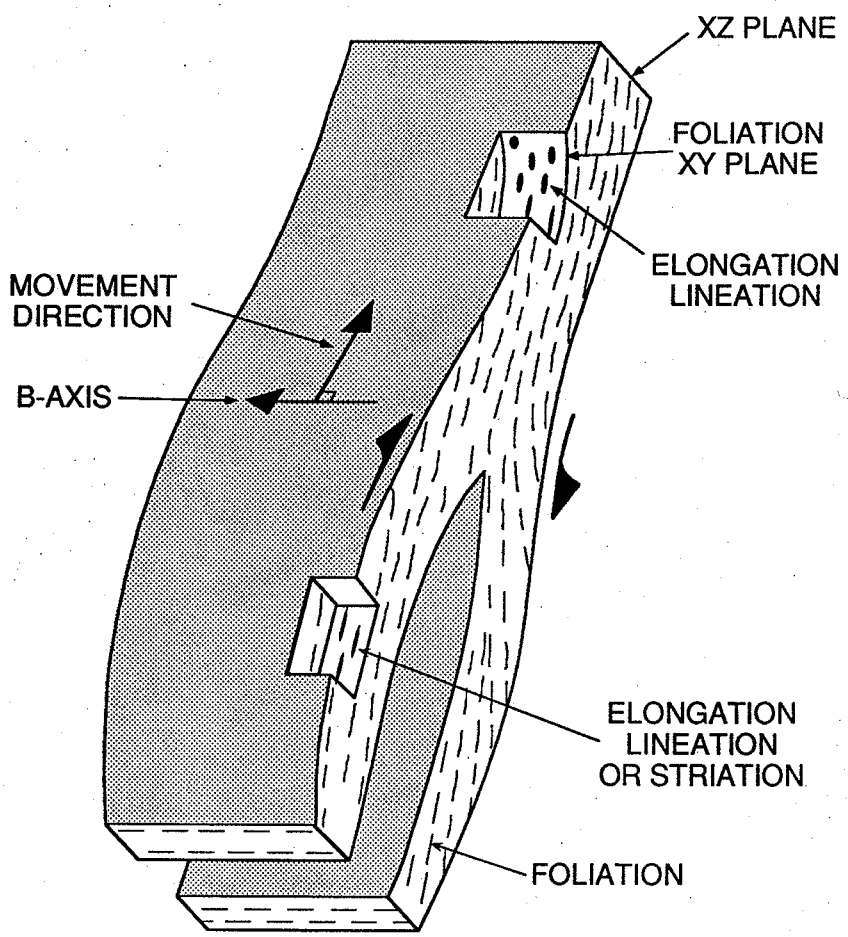

Figure 3.5. Diagram representing an idealized shear zone in three dimensions, showing geometric relationships among the structural elements of the shear zone, its movement direction and its B-axis; adapted from Poulsen and Robert (1989).

zone. The foliation within the shear zone has an average orientation of 092-75°, and is oblique to the boundaries of the shear zone: it strikes more easterly and dips more steeply than the shear zone. This angular relationship readily indicate a reverse-dextral sense of movement along the shear zone. The dextral component of movement can be determined on outcrop from the angular relationship between the trace of the foliation and that of the shear zone and from the sense of dragging of the feldspar porphyry dyke along the shear zone (Fig. 3.6A). The shear zone foliation contains an elongation lineation raking 60° to the west, and defined by the alignment of plagioclase grains within the foliation plane. The movement direction along the shear zone is obtained by projecting this lineation onto the plane of the shear zone (Fig. 3.6B). The intersection between the foliation and the shear zone, which corresponds to the shear zone's B-axis, lie at 90° to the movement direction. If no well-developed elongation lineation were present (as is commonly the case),

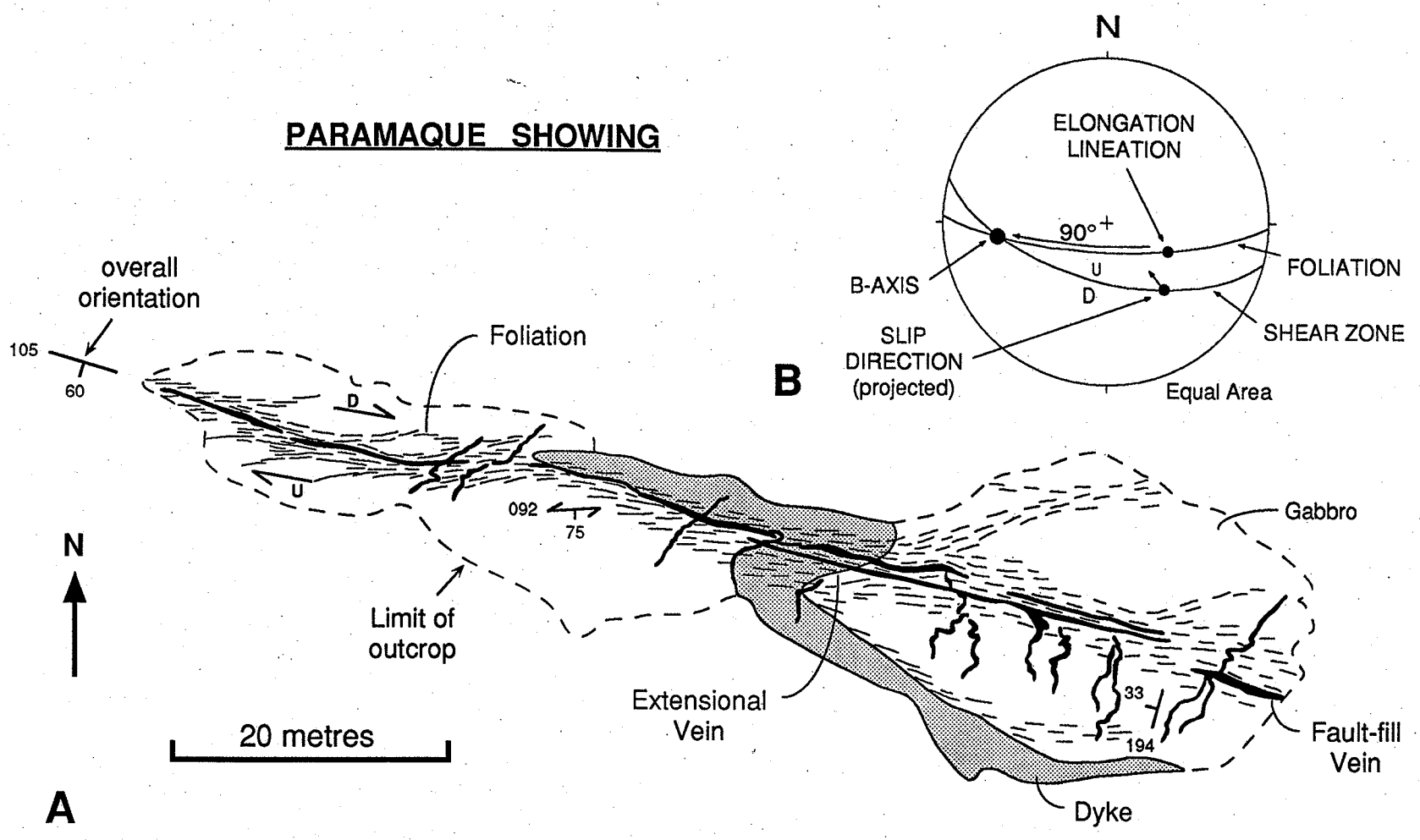

Figure 3.6. Paramaque showing, Val d'Or. (**A**) Simplified outcrop map showing the shear zone and the related veins. Note the dextral dragging of the dyke; modified from Mannard (1990). (**B**) Stereographic projection of the structural elements of the shear zone.

the movement direction could have been determined from the intersection between the shear zone and the foliation (Fig. 3.6B).

However, many other auriferous shear zones do not conform to such model: in a number of cases, elongation lineations are poorly developed or even absent, and in a number of others, foliation is parallel to shear zone boundaries. Such shear zones tend to be those of larger dimensions, for which kinematic interpretations are particularly difficult.

Secondary foliations such as crenulation cleavages and shear bands are also commonly present within shear zones in addition to the main foliation. These additional foliations may represent overprinting deformation, either related to shear zone reactivation or to development of regional cleavages, which best develop in layered rocks such as those within shear zones; they may also represent cleavages resulting from progressive deformation within the shear zone, in which case they can be used to determine the sense of shear as discussed in detail by Hanmer and Passchier (1991). Common secondary foliations related to progressive shear zone development include shear bands and C planes (for the french word cisaillement), parallel to shear zone boundaries, which combine with the main shear zone foliation to form "C-S" fabrics (Berthé et al., 1979)

It is generally difficult to determine if a secondary foliation within a shear zone is related to shear zone development or if it is due to overprinting deformation. However, a necessary condition for the use of secondary cleavages as shear sense indicators is that their intersections with the main shear zone foliation must be perpendicular to the elongation lineation. Another general rule is that cleavages related to shear zone development form at and angle of 45° or less to the boundaries. In practice, many secondary foliations within shear zones do not meet these criteria and have no kinematic significance. In fact, in many auriferous shear zones such intersection lineations are parallel, rather than perpendicular, to the elongation lineation. It should be noted that intersection lineations within shear zones have, in general, no kinematic significance.

Finally, a significant number of shear zones display *internal folding of their foliation*. These folds are typically intrafolial, asymmetrical (Fig. 3.7A; Bell and Hammond, 1984) and may result either from continued displacement along the shear zone or later reactivation along a different slip direction. In the first case, asymmetric folds are generated with their axes perpendicular to the slip direction, i.e. parallel to the shear zone's B-axis. The asymmetry of such folds is considered to be indicative of the sense of shear (Platt, 1983). With increasing shear strain, the axial surfaces of these folds progressively rotates toward parallelism with the shear plane, and these folds may evolve into non-cylindrical to sheath folds, the axis of the sheath being parallel to the slip direction (Fig. 3.7B). At high shear strains, fold axes become sub-parallel to the elongation lineation.

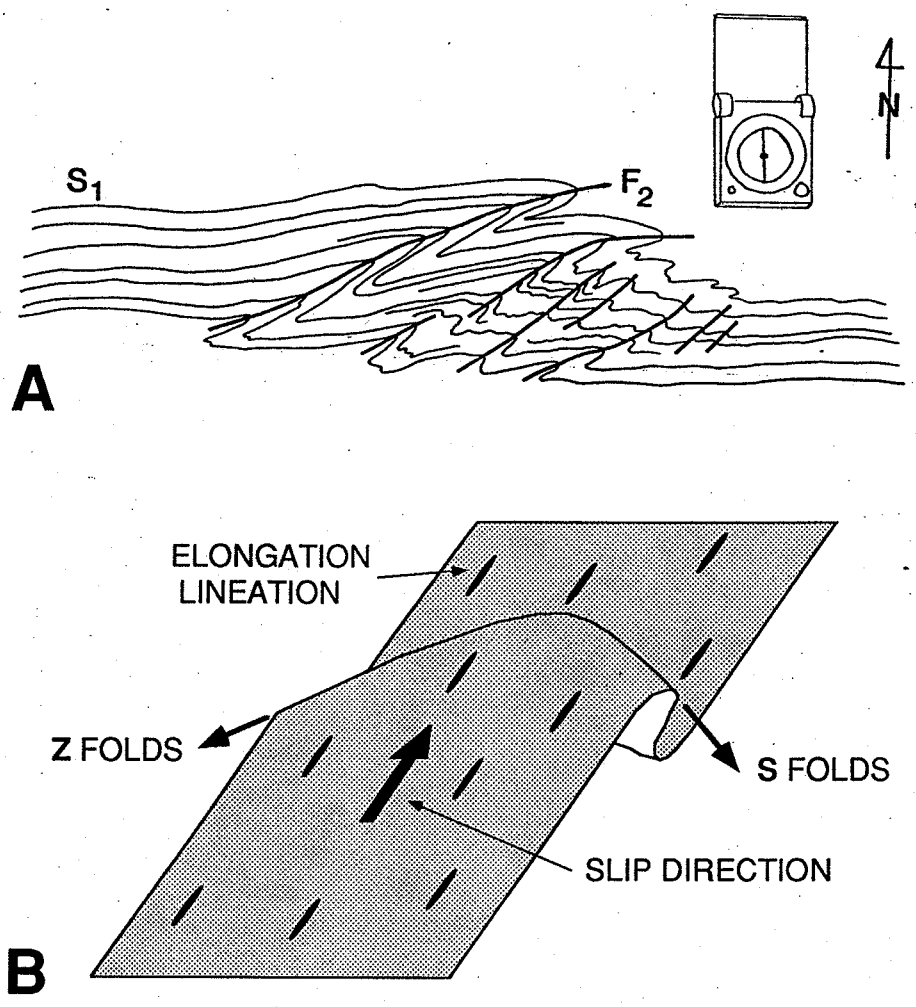

Figure 3.7. Folds within shear zones. (**A**) Field example of an intrafolial fold within the Cadillac tectonic zone, Val d'Or district. This fold has a subvertical plunge, parallel to the local elongation lineation, and results from the dextral strike-slip reactivation of the Cadillac tectonic zone. (**B**) Diagram illustrating the progressive rotation of fold hinges towards the elongation lineation as a result of continued simple shear along a shear zone. Folds with opposing plunges relative to the elongation lineation have opposing asymmetries.

It is important to note that in such cases, the asymmetry of the folds will change depending on which side of the elongation lineation the axes are plunging (Fig. 3.7B). The hinges of folds produced during subsequent reactivation of shear zones should not bear any specific angular relationship to the elongation lineation in the folded foliation plane. If, by coincidence, these folds plunge subparallel to the elongation lineation, their asymmetry will remain constant irrespective of their plunges relative to the elongation lineation. For example, in the Larder Lake-Cadillac tectonic zone, where the main foliation contains a down-dip elongation lineation, Z-shaped folds of the main foliation like that shown in Figure 3.7A range

in plunge from moderate to the west to moderate to the east. If these folds had been generated with their axes perpendicular to the movement direction and progressively reoriented toward this direction due to high shear strains, folds plunging to the west should have asymmetries opposite to those plunging to the east. However, as these folds have consistent asymmetries, they have been interpreted to result from dextral strike-slip reactivation of this tectonic zone (see Robert, 1989).

VEINS

Several different types of veins are associated with gold deposits (Hodgson, 1989). Different types of veins form by different mechanisms and have different structural significance. As a result, it is very important in structural analysis to properly identify the types of veins present in a given deposit. This can generally be achieved by combining different characteristics of veins such as their structural sites, their geometric arrangement and relationships to other structures such as shear zones, and their internal structures and textures. We use the term "vein" in its strict sense, i.e. to designate fissure-filling hydrothermal material. We do not consider the so-called "replacement veins" because they do not convey any additional structural information. The reader is referred to Hodgson (1989) for a discussion of replacement veins.

This section begins with a consideration of theoretical aspects of fracturing of rocks and vein formation, which provides a framework for classification of veins. It is followed by detailed examination of structural and textural features of the main types of veins.

Theoretical considerations

Veins form in response to deformation of a rock mass by the infilling of progressively opening fractures with hydrothermal material. In most cases, fracture generation, opening and infilling are part of a continuous process. This is well established in the case of fibre veins (Ramsay and Huber, 1983) and can be demonstrated for a number of auriferous veins (see below). However, in other cases an existing fracture may be opened and filled at a later time, possibly under different stress condition: in this case, the fracture can be regarded as reactivated.

Considering that in most cases fracture and vein development are parts of a continuous process, the principles governing fracturing in intact rocks provide an appropriate framework for discussing mechanisms of vein formation. As shown in Figure 3.8, there are three modes of failure in intact rocks producing three types of fractures: *shear*, *extensional-shear*, and *extensional* fractures (Sibson, 1990) The

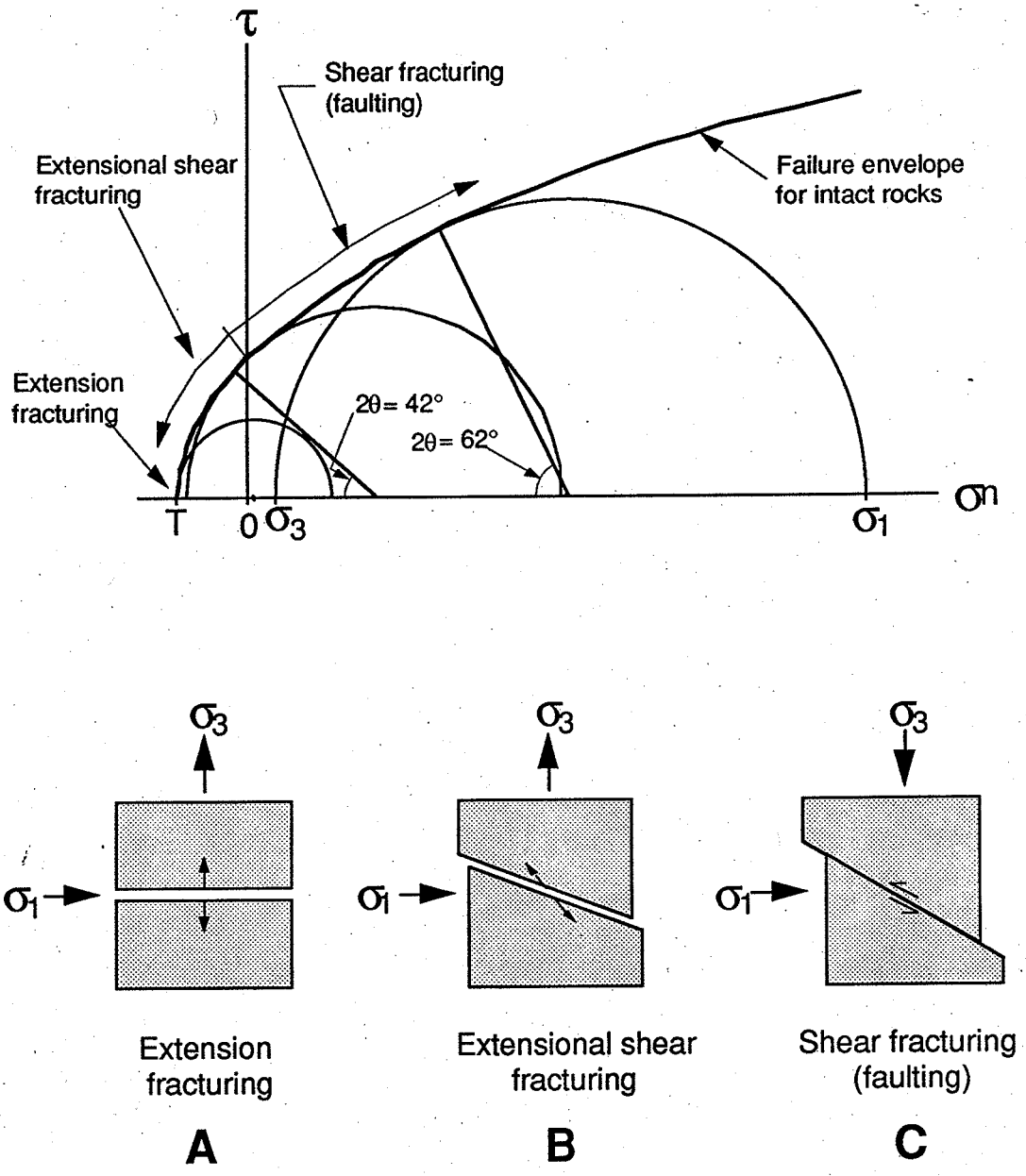

Figure 3.8. Mohr diagram illustrating the three different types of fracturing of an intact rock mass and the corresponding stress states. Three block diagrams represent these three modes of fracturing and show the expected relative displacements of the fracture walls as well as the angle between the fracture and σ1.

type of fracture produced is determined by the position of the intersection of the Mohr circle, representing the stress state ($\sigma 1$-$\sigma 3$), with the failure envelope. Extensional and extensional-shear fractures will only be produced in situations where $\sigma 3$ has a negative value; extensional fractures will be produced if $\sigma 3$ exceeds the tensile strength of the rock, T,and extensional-shear fractures will form at values of $\sigma 3$ between 0 and T.

As further illustrated in Figure 3.8, the angle of the fracture with respect to the three principal stress axes also varies depending on where the Mohr circle intersects the failure envelope. In fact, there is a continuum between extensional fractures, which develop at an angle $\theta = 0°$ to $\sigma 1$, corresponding to case A in Figure 3.8, and shear fractures produced at an angle $\theta \sim 22°$ to $31°$ to $\sigma 1$, the latter angle corresponding to case C. In the case of extensional-shear fractures, corresponding to case B in Figure 3.8, fracture angles will be anywhere between $0°>\theta>\sim 22°$.

It is therefore expected that three types of veins can be produced, corresponding the three modes of fracturing presented above (Fig. 3.9): *shear veins*, *extensional veins*, and *extensional-shear veins*. Examples of these three types of veins have been observed in nature, as well as in gold deposits (Ramsay and Huber, 1987; Poulsen and Robert, 1989; Robert, 1990). As for their host fractures, these three types of veins define a continuous spectrum of vein types in which the opening or displacement vector ranges from perpendicular to vein walls in the case of extensional veins, to subparallel to vein walls in the case of shear veins (Fig. 3.9). By definition, the opening vector of extensional veins is perpendicular to the walls of the veins, whereas in the case of extensional-shear veins, the opening vector is oblique to the walls. In shear veins, the opening vector corresponds to the relative displacement of both walls and is subparallel to the vein.

In deformed terranes at greenschist of higher metamorphic grades, it is generally accepted that extensional veins can only form if the fluid pressure exceeds the least principal stress by an amount corresponding to the tensile strength of the rock i.e., $P_{fluid} > \sigma 3 + T$ (Etheridge, 1983). In compressional regimes under which a large number of auriferous quartz veins formed, $\sigma 3$ is vertical and corresponds to the weight of the overlying column of rocks, also referred to as the lithostatic load. In order for extensional veins to form under such regimes, the fluid pressure must therefore exceed the lithostatic load, hence the common reference to lithostatic of supra-lithostatic fluid pressures in discussions of auriferous quartz veins (see for example Sibson et al.,1988).

As pointed out above, using veins to decipher the structural controls and history of gold deposits hinges on knowledge of their mechamism of formation, which essentially consists in determining if a vein is a shear or an extensional (including extensional-shear) vein. In the field, it is generally possible to identify extensional

or extensional-shear veins because of the common presence of diagnostic features such as external markers of opening vector (earlier veinlets, lithological contacts, etc), matching walls and mineral fibres, which clearly indicate the direction of opening of the veins. For the numerous veins hosted by shear fractures in faults and shear zones, it is commonly not possible to determine if the vein formed during movement along the fracture or if it formed as a result of extensional opening of a pre-existing shear fracture. To overcome this problem, Cox (1991) has used the term non-genetic term fault-fill vein, which we have adopted in our classification (see below), for those veins occurring in, and parallel to, shear zones and faults.

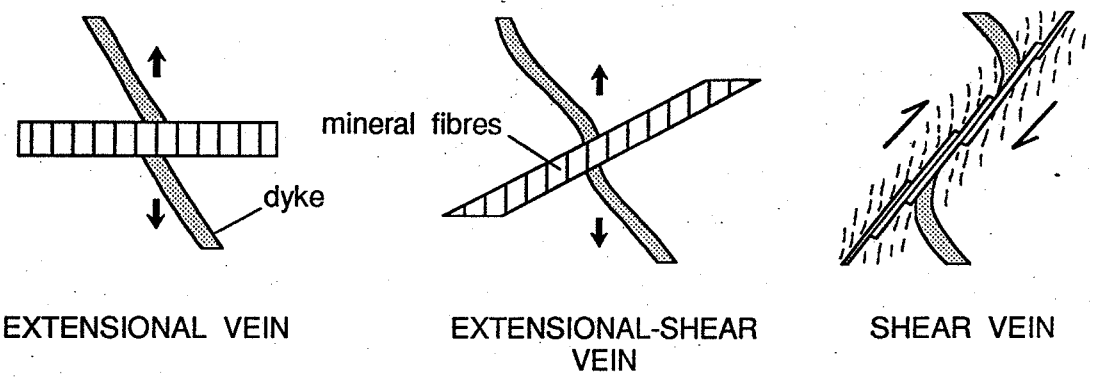

Figure 3.9. Schematic representation of the types of veins corresponding to the three modes of fracturing illustrated in Figure 3.8.

Classification of veins

Any ideal classification of veins should be based on characteristics that are observable in the field and should also reflect, at least in some ways, their formation mechanisms, as interpreted from a combination of characteristics. However, such an approach is complicated by the fact that features diagnostic of the vein formation mechanisms are not always present, that veins in similar structural sites may have formed by different mechanisms, and that some veins have formed by a combination of mechanisms. The classification of veins adopted here is presented in Table 3.1; it follows in many respects the approach of Hodgson (1989), Poulsen and Robert (1989), Sibson (1990), and Cox (1991). It is based on a combination of structural sites and special character of the veins; it also reflects differences in geometric relationships of the veins to shear zones and differences in internal structures and textures of the veins.

Three main categories of veins are distinguished: *fault-fill veins*, *extensional veins*, and *stockwork* and *breccia veins*. Fault-fill veins, as their name indicates, typically occupy faults and the central parts of shear zones. They are parallel or subparallel to their host structure and to the shear zone foliation. They contrast with extensional veins which either occur as planar veins in low strain rocks outside and

Table 3.1. Vein classification and main characteristics

VEIN TYPE	INTERNAL FEATURES	STRUCTURAL SITE	GEOMETRY	FORMATION MECHANISMS
FAULT-FILL VEINS	- laminated structure - foliated wallrock slivers - slip surfaces - fibres at low angle to vein walls	- shear zone or fault - fold limbs	- parallel to host structure	- shear fracturing - extensional opening of existing fractures
EXTENSIONAL VEINS	- open-space filling - mineral fibres at high angle to vein walls	- outside shear zones	- planar veins at moderate angle to shear zone	- extensional fracturing - extensional-shear fracturing
		- AC joints in folds	- perpend. to fold hinge	
EXTENSIONAL VEIN ARRAYS	- internal layering: multiple openings	- within shear zones	- arrays of planar to sigmoidal veins at high angle to foliation	
STOCKWORKS	- 2 or more oblique to orthogonal vein sets	- non specific	- tabular to cigar shaped zones	
BRECCIA VEINS				
- jigsaw puzzle	- angular clasts, no rotation	- along faults	- parallel to host structure	- implosion (?)
- fault breccia	- vein and wallrock clasts - rotation and abrasion	- fault or shear zone	- parallel to host structure	- fault slip

between shear zones, or as arrays of sigmoidal veins within and fringing shear zones. Extensional veins typically lie at high angle to the local foliation. Finally, stockwork and breccia veins (i.e. breccias with a hydrothermal matrix) form a special group of veins which consist of superimposed multiple sets of veins and fractures. They contrast with fault-fill and extensional veins, which normally consist of single sets of fractures. As listed in Table 3.1 and discussed in detail below, a number of internal features of veins, if present, are diagnostic of these types of veins and how they form.

Fault-fill veins

Fault-fill veins are by far the most common type of veins in gold deposits and are the source of most of the vein-type ore extracted from these deposits. Most fault-fill veins form mineralized lenticular bodies either in discrete faults or in the central part of shear zones. Within shear zones, fault-fill veins are either parallel, or a low angle, to the shear zone boundaries and are also sub-parallel to the shear zone foliation (Fig. 3.10A; Hodgson, 1989). These geometric relationships are well illustrated by the Paramaque gold showing described above (Fig. 3.7). In some districts, or in competent host rocks in other districts, fault-fill veins rather occur along discrete faults with minimal or no development of wallrock foliation. Fault-fill veins are also associated with folds: they may occur in dilational jogs at bedding-discordant faults segments crossing fold hinges along otherwise bedding-parallel faults (Fig. 3.10B). They may also occur as saddle reefs as a result of flexural slip along fold limbs (Fig. 3.10 C; Hodgson, 1989; Cox et al., 1991).

Fault-fill veins commonly reach a few metres in thickness and range from tens to hundreds of metres in their longest dimensions. Several fault-fill veins, separated by barren fault or shear zone segments, may occur along strike or down dip within a single structure. In most cases, fault-fill veins form elongate lenses within their host structures and thus define oreshoots with plunges corresponding to their long axis. As discussed at the end of this chapter, the plunges of oreshoots within shear zones and faults commonly bear simple geometric relationships to the slip direction along the host shear zone and is predictable.

Internal characteristics

Fault-fill veins are typically laminated, as illustrated by the examples shown in Figures 3.11, 3.12 and 3.13. Individual quartz bands or laminae are commonly separated by slivers of foliated wallrocks or by millimetre-thick septa probably derived from wallrocks. They can also be separated by slip surfaces enhanced by the presence of hydrothermal minerals such as tourmaline and chlorite (see below). In other cases, the laminated character of the veins is only defined by

subtle differences in the color and texture of quartz. The individual quartz laminae comprizing the veins range in thickness from a few millimetres to tens of centimetres. They may differ from one another in their internal textures, mineral proportions and degree of deformation. Individual laminae within fault-fill veins are generally parallel to subparallel to the vein margins.

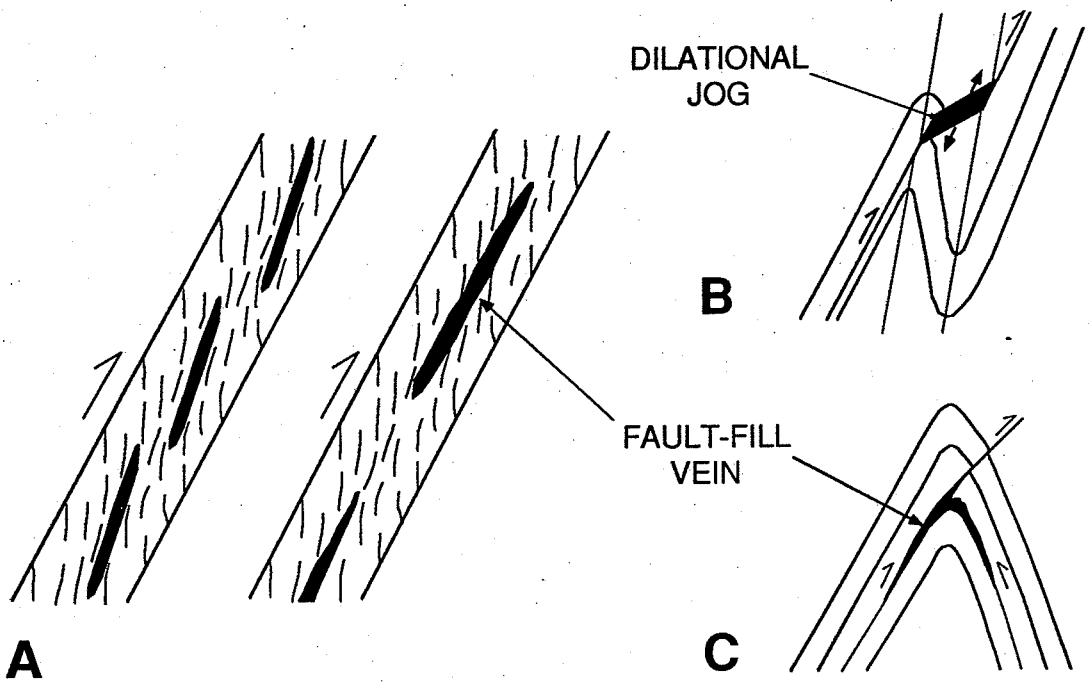

Figure 3.10. Common geometric arrangements of fault-fill veins in shear zones and folds. (**A**) Fault-fill veins in central portions of shear zones, oblique and parallel to shear zone boundaries. (**B**) Fault-fill vein in a dilational jog developed along a bedding-discordant segment of an otherwise bedding-parallel fault where it crosses the hinge of a fold; adapted from Cox et al. (1991). (**C**) Fault-fill vein forming a saddle reef due to flexural slip along fold limbs; adapted from Cox et al. (1991).

As pointed out by Hodgson (1989), the entire spectrum exists among laminated fault-fill veins from sheeted veinlet zones, in which the proportion of wallrock component is approximately equal to, or greater, than that of vein component, to ribbon-textured veins in which the vein component dominates. In a number of fault-fill veins hosted by shear zones, observed variations in vein to wallrock ratio and in vein morphology define a crude lateral or vertical zoning, as illustrated in Figures 3.11A and B. Near their lateral and vertical terminations, fault-fill veins consist of isolated veinlets separated from each other by signficant thickness of wallrocks. Such isolated veinlets are relatively common in "barren" segments of shear zones between fully developed fault-fill veins. Moving laterally towards the central part of the fault-fill veins, individual veinlets increase in abundance and are more closely

spaced, defining what can be regarded as a sheeted veinlet zone (Fig. 3.11A). These veinlets are parallel to sub-parallel to the foliation in the host shear zone, and their dimensions are similar to those of individual laminae comprising fault-fill veins. The central part of fault-fill veins is dominated by quartz laminae with subordinate proportions of wallrocks slivers, which commonly become thoroughly altered and completely replaced by hydrothermal minerals, to the extent that they may be difficult to distinguish from true fissure-filling material (see Robert and Brown, 1986). Such "lateral" zoning in the character of fault-fill veins may be important to recognize in a drilling program because the presence of relatively abundant foliation-parallel veinlets may indicate the proximity of thicker fault-fill veins.

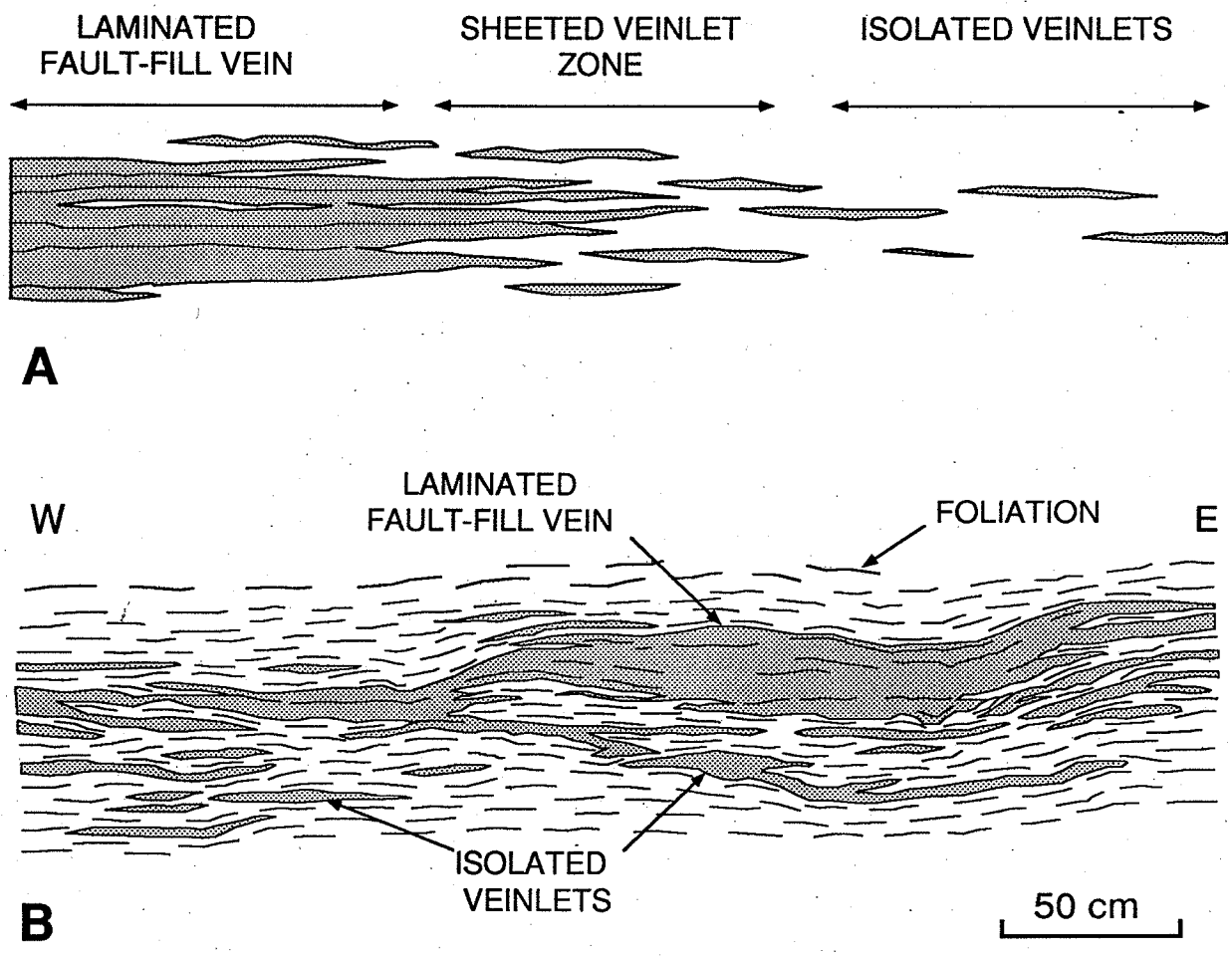

Figure 3.11. Characteristics of fault-fill veins in shear zones. (**A**) Schematic representation of commonly observed lateral zoning in proportion of vein to wallrock. (**B**) Plan view of a fault-fill vein illustrating how individual veinlets amalgamate to form larger laminated quartz lenses; Sigma deposit, Val d'Or.

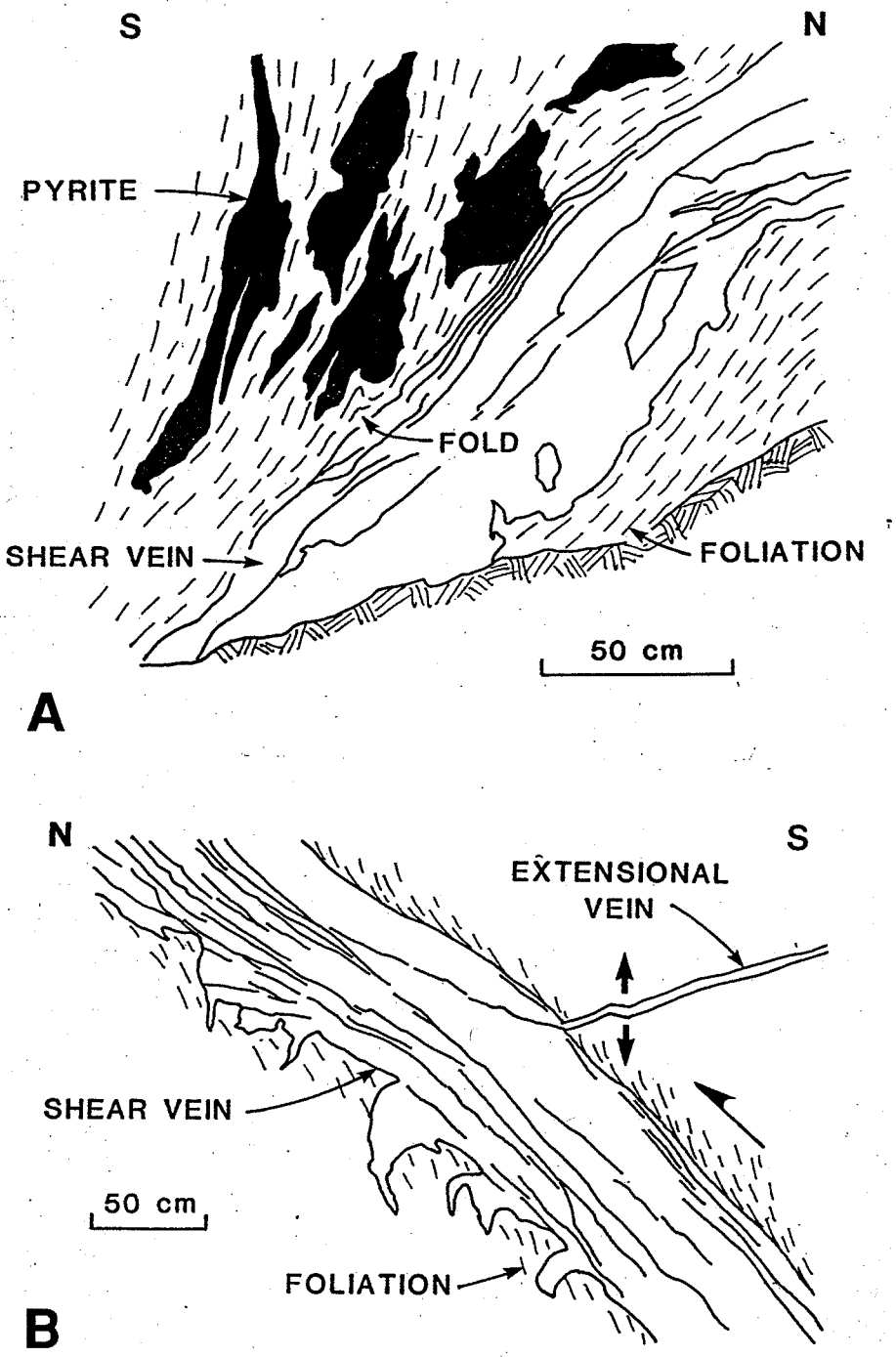

Figure 3.12. Characteristics of fault-fill veins. (**A**) Cross-section of a fault-fill vein in a well-developed shear zone showing the internal laminated character of the vein. Note the obliquity of foliation to the central vein and to the shear zone boundaries indicating reverse sense of movement; Dumont deposit, Val d'Or. (**B**) Cross-section of a typical laminated fault-fill vein containing multiple internal slip-surfaces. Note the planar extensional vein in the hangingwall cutting across the external part of the fault-fill veins and merging with a central slip surface; Lucien Béliveau deposit, Val d'Or.

In many cases, as in the examples shown in Figure 3.11B and 3.13A, it is clear that the central or thicker parts of fault-fill veins result from the merging and juxtaposition of numerous quartz veinlets due reopening of existing veins or due to the formation of new veinlets immediately adjacent to, or overlapping with, existing ones. Accordingly, the incorporation of wallrock slivers within the veins is generally considered as a natural consequence of their incremental growth (see Robert and Brown, 1986a).

Striated fault surfaces, or *slickensides*, are also commonly observed along wallrock slivers or along the interfaces between individual quartz laminae within fault-fill veins (Figs. 3.12A, 3.12B and 3.13A). In some cases, the striae, or *slickenlines*, are defined by hydrothermal minerals such as quartz and tourmaline; such striae are termed *slickenfibres* and they clearly indicate that vein development was accompanied by slip along the veins. In some other instances, steps defined by the slickenfibres further indicate the sense of movement (Fig. 3.13B). Such vein structures are exactly those expected to form in shear veins as defined above and illustrated in Figure 3.9. Finally, in other relatively rare instances, dilational jogs are observed along fault-fill veins (Figs. 3.13C, D). Such dilational jogs not only indicate that vein development is accompanied by slip, but they also indicate the sense of movement. It is not clear at present if such dilational jogs along fault-fill veins are truly rare features or if they are common but not recognized because they occur at scales that exceed those of vein exposures on outcrop or within stopes.

Where present within fault-fill veins, slickenlines or slickenfibres show consistent rakes within single veins or among sets of veins within a deposit (see Robert and Brown, 1986a). Furthermore, where the complete data sets exist such as for many of the Val d'Or deposits (Robert, 1990a), slickenlines indicate the same direction of movement as the elongation lineation in the host shear zone, and where steeped slickenfibres or dilational jogs are observed, they indicate the same sense of movement as that deduced for the host shear zones. There seems to be good compatibility in direction and sense of shear between discrete slip events within the veins and ductile flow in the host shear zone, indicating that both are part of the same progressive deformation event.

In a number of cases, multiple sets of striations are observed on vein surfaces, clearly indicating reactivation. Only those striations produced during vein development should be considered in structural analysis of deposits. This is the case if striations correspond to fibres of minerals present in the veins or if their rake is compatible with that of the lineation in the host shear zone or with observable dilational jogs.

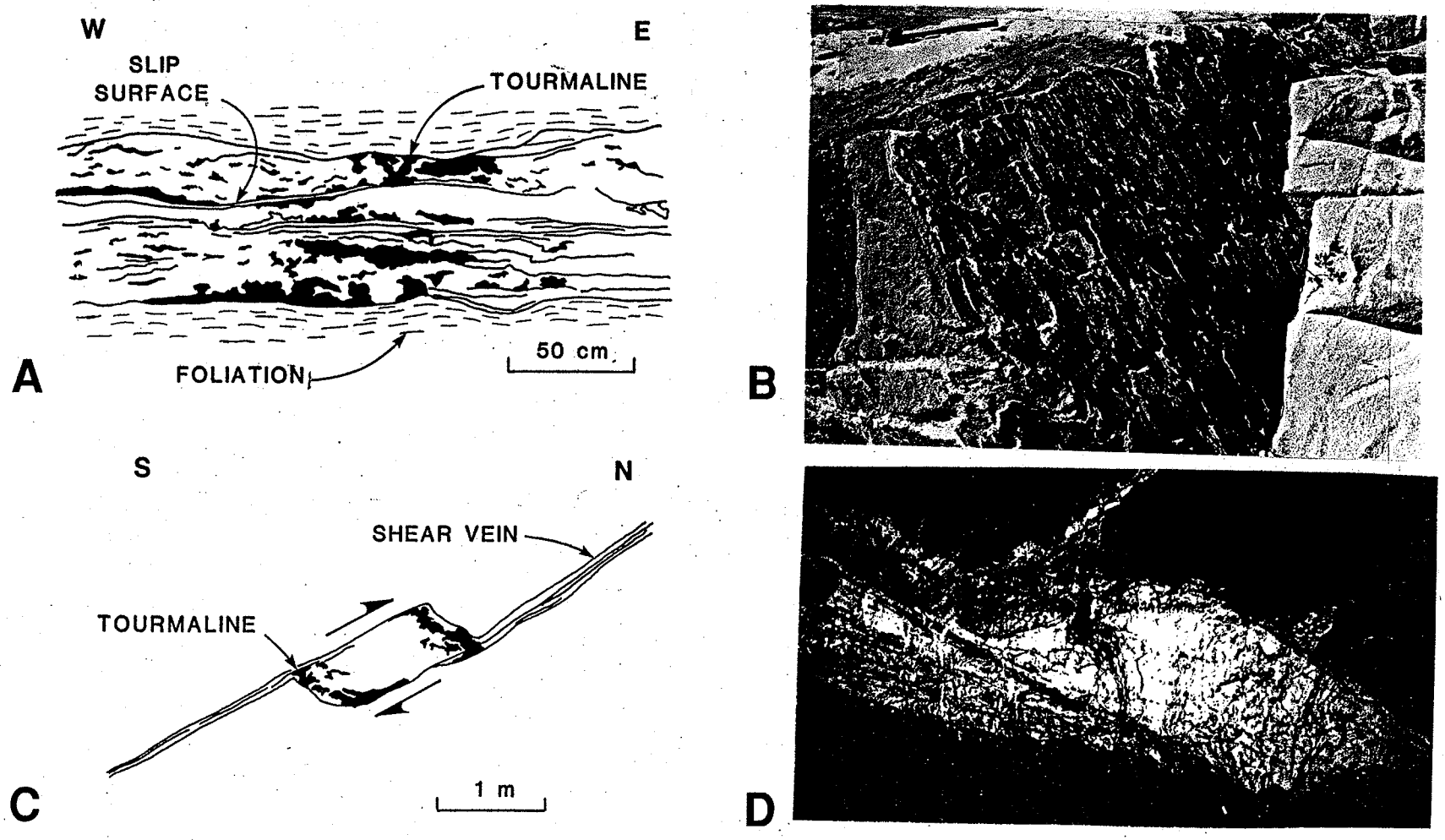

Figure 3.13. Characteristics of fault-fill veins. (**A**) Plan view of a laminated fault-fill vein containing abundant slip surfaces bounding quartz laminae with aggregates of tourmaline. The relatively "clean" thick laminae in the center records a late increment of opening of the fault-fill vein; Sigma deposit, Val d'Or. (**B**) Quartz-tourmaline slickenfibres within a fault-fill vein indicating reverse movement along the vein; Val d'Or. (**C**) Cross-section of a small dilational jog along a shallow-dipping fault-fill vein indicating reverse movement; Lamaque deposit, Val d'Or. (**D**) Cross-section of the upper termination of a dilational jog along a fault-fill vein; Louvicourt Goldfield deposit, Val d'Or.

Structural significance

An important point concerning the fault-fill veins described above is that they have developed in existing and still active shear zones or faults, rather than having been overprinted by shear zones. This is indicated by the fact that wallrock slivers within the veins are as strongly foliated and lineated as the shear zone rocks outside the veins. If the shear zones were overprinting existing quartz veins, which in general show evidence of greater competency than their altered hosts, wallrock slivers within the veins would not be as strongly foliated as the shear zone rocks themselves because they would be preserved from the overprinting strain by the more competent quartz. This interpretation is further supported by the observation that different quartz laminae within a fault-fill vein display contrasting states of strain, including some showing little or no strain (Boullier and Robert, 1992). However, this is not necessarily the case for all fault-fill veins: as discussed in Chapter 6, there are also clear cases where shear zone deformation overprints veins. In the present section, we are only concerned with undeformed veins.

If there is in general good evidence for incremental development of fault-fill veins within existing but still active shear zones, it is much more difficult to ascertain the way in which openings related to individual increments took place. Two different cases have been documented. Cox (1991) has shown that some fault-fill veins in the Lachlan fold belt in Australia have internal features, such as crack-seal textures, indicating that the veins are in fact extensional veins formed by opening perpendicular to existing fault planes. In the other case, which is particularly well illustrated at Val d'Or (Robert, 1990a), the presence of hydrothermal slickenfibres and dilational jogs indicate that these fault-fill veins are true shear veins. Unfortunately, in the majority of situations it is not possible to determine the opening mechanism of fault-fill veins because of the absence of diagnostic internal textures and structures, or because such textures and structures have been destroyed during deformation accompanying subsequent growth increments of the veins (Boullier and Robert, 1992).

Fault-fill veins, in cases where the direction and sense of movement along them can be documented, provide important structural information used to reconstruct the stress field responsible to their development, much like shear zones.

Extensional veins and vein arrays

Extensional veins and vein arrays are relatively common in gold deposits. In a large number of deposits, they are auriferous and can be shown to be of the same age as the more significant fault-fill veins. Extensional veins have limited economic significance: they form orebodies only in rare cases where their grades and abundances justify bulk mining or where their grade and dimensions justify selective mining, such as at the Sigma deposit at Val d'Or (Robert and Brown,

1986). In other deposits, extensional veins commonly overprint the ore and are typically barren. From a structural point of view, however, these veins provide very important information, as will be further discussed below.

Extensional veins considered here are those veins formed by extensional or extensional-shear opening of fractures at moderate to high angle to fault planes and to shear zone foliation. As indicated in Table 3.1 and illustrated in Figure 3.14, these veins are generally spatially associated to shear zones and faults: they may occur within shear zones, where they form arrays of sigmoidal or planar sigmoidal (Fig. 3.15A, B), commonly fringing fault-fill veins, or they may also occur in low strain rocks outside shear zones, where they are planar and more extensive (Fig. 3.15C).

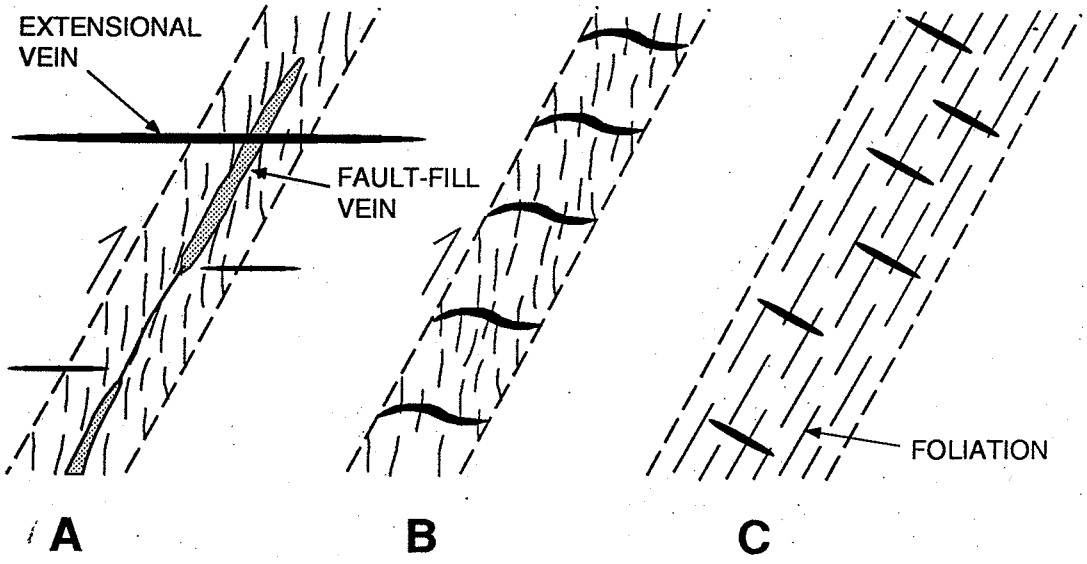

Figure 3.14. Common geometric arrangements of extensional veins. (**A**) Planar extensional veins outside faults and shear zones. (**B**) Arrays of sigmoidal extensional veins within shear zones. (**C**) Arrays of planar extensional veins within shear zones.

Internal characteristics

Extensional veins are relatively easy to identify because these have many diagnostic attributes, including internal structures and textures, indicating their opening vector. In general, extensional veins have parallel and planar walls, at least at the mesoscopic scale (Figs. 3.15C, 3.16A), in contrast with the irregular outlines of fault-fill veins (Figs. 3.11B and 3.12B). Irregularities or deflections of the vein walls are relatively common and can be matched across the vein, giving a good indication of the opening vector. This is well illustrated in Figures 3.16A and B, where matching walls of two extensional veins give clearly the opening vectors

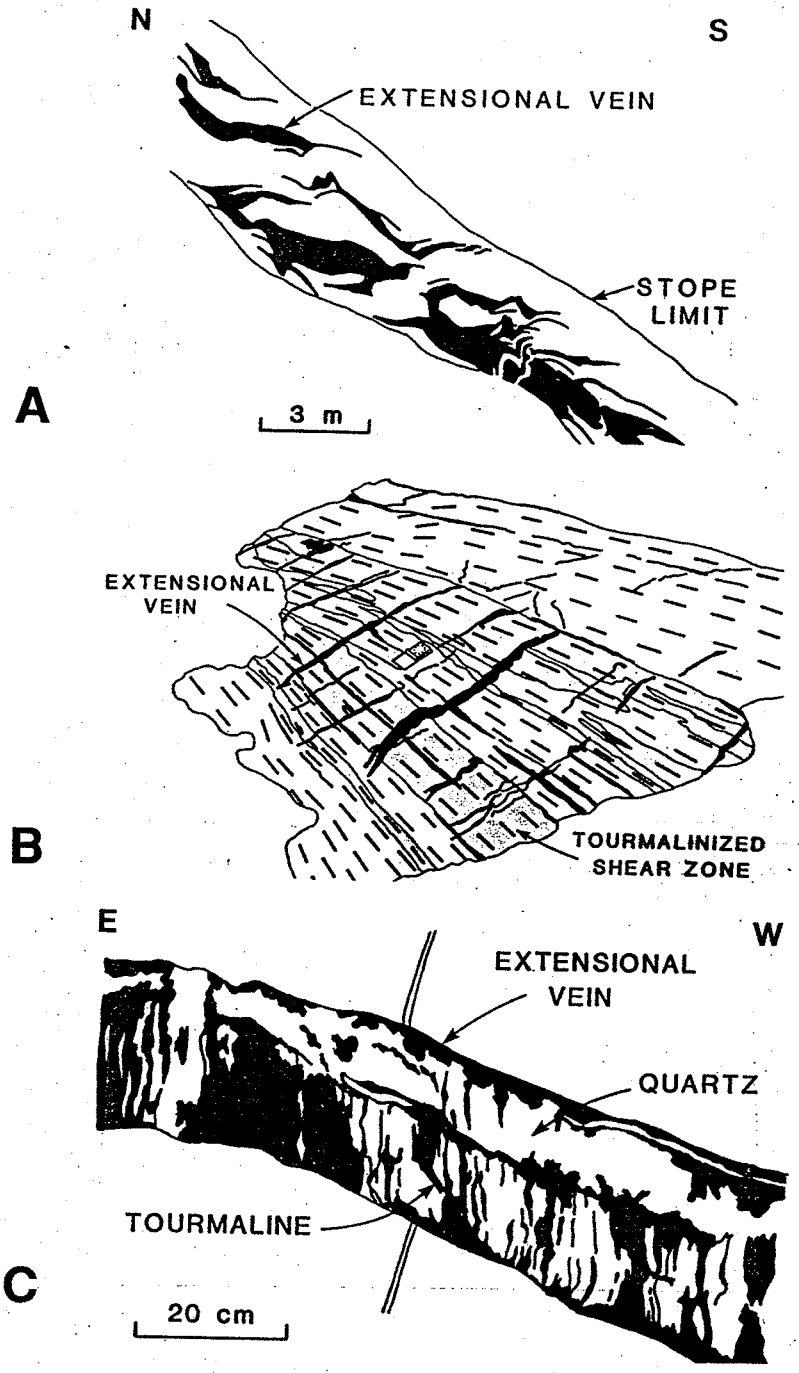

Figure 3.15. Examples of the three arrangements of extensional veins. (**A**) Cross-section of a large array of sigmoidal extensional veins in a reverse brittle-ductile shear zone; Perron deposit, Val d'Or. (**B**) Outcrop view of arrays of planar extensional veins perpendicular to the foliation within a tourmalinized shear zone. Note that the extensional veins are best developed in the more competent tourmalinized parts of the shear zone; Val d'Or. (**C**) Cross-section of a planar extensional vein external to shear zones in low strain rocks. Note the internal layering of the vein indicating multiple growth episodes, as well as the vertical tourmaline fibres indicating vertical opening of the vein, coincident with the matching segments of an earlier veinlet; Sigma deposit, Val d'Or.

and indicate that they correspond to extensional and extsensional-shear veins, respectively, as defined in Figure 3.9. In addition, the opening vector of extensional veins is also indicated by offset of geological markers such as lithological contacts or pre-existing veinlets, as in Figure 3.15C.

A number of internal structures and textures are common in extensional veins, many of which are diagnostic of such type of vein and also indicative of their opening vector. Extensional veins commonly display internal layering parallel to their walls indicating that, as fault-fill veins, they result from multiple episodes of opening and mineral precipitation (Fig. 3.15C). Individual layers comprizing a vein may differ in mineral proportions and in textures and structures.

Mesoscopic internal textures and structures observed within individual layers include, besides massive homogeneous filling (typically quartz), open-space filling textures, mineral fibres and rock bridges. *Open-space filling textures* have been described in a number of textbooks, including those of Lindgren (1933), and Craig and Vaughan (1981), among many others. In auriferous extensional veins, such textures are characterized by well developed crystals and radiating aggregates of crystals of hydrothermal minerals such as carbonate, pyrite, tourmaline, scheelite, attached to the walls of the veins or of the layers, as shown in Figure 3.16A. Such textures are described in detail by Robert and Brown (1986b) for the Sigma deposit at Val d'Or.

Mineral fibres are not uncommon in extensional veins; they consist of highly elongate minerals showing a constant preferred orientation within a vein or within a layer, as illustrated in Figures 3.15C and 3.16B. Veins dominated by such internal structures are termed fibrous veins by structural geologists; detailed descriptions of such veins can be found in Ramsay and Huber (1983) and in Boullier and Robert (1992). Fibrous veins form in cases where the rate of mineral precipitation is equal or greater than that of separation of fracture walls, and minerals fibres represent crystals that grew progressively as the fracture opened. Therefore, mineral fibres track the direction of opening of the veins. The vein illustrated in Figure 3.15C provides a good example of mineral fibres in extensional veins: they indicate vertical opening of the vein, compatible with that indicated by the separation of an earlier veinlet.

Rocks bridges, illustrated in Figure 3.17, are a peculiar feature of extensional veins. They consist of planar to sigmoidal slabs of wallrocks partially or completely enclosed within extensional veins, generally oriented at low to moderate angle to the walls, or separating individual overlapping echelon extensional veins. As documented by Pollard et al. (1982) and Nicholson and Pollard (1985), development of rock bridges, and echelon extensional veins are natural consequences of the propagation and dilation of extensional fractures and can be regarded as diagnostic of extensional veins. Propagation of the main fracture

induces rotation of the local principal stress axes at the fracture edges, which results in the development of smaller echelon extensional veins (Figs. 3.17A and B). As the echelon extensional veins dilate, the rock segments separating them, or rock bridges, will break and become slabs of wallrocks partially enclosed within the veins (Fig. 3.17C).

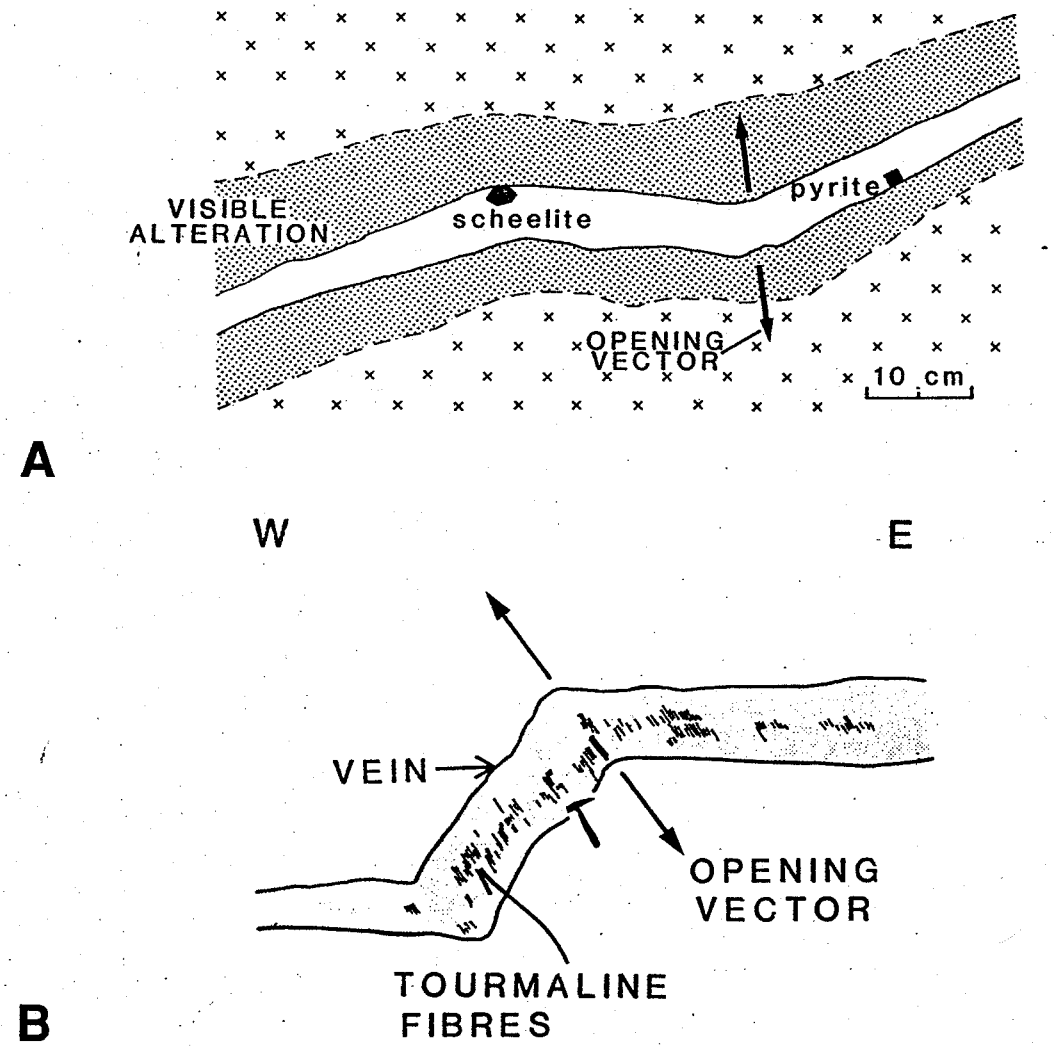

Figure 3.16. Characteristics of extensional veins. (**A**) Cross-section of an extensional vein with an opening vector perpendicular to the walls, as defined by the matching deflections of the vein walls; Sigma deposit, Val d'Or. (**B**) Cross-section of an extensional-shear vein with an oblique opening vector defined by tourmaline fibres and matching deflections of the vein walls; Sigma deposit, Val d'Or.

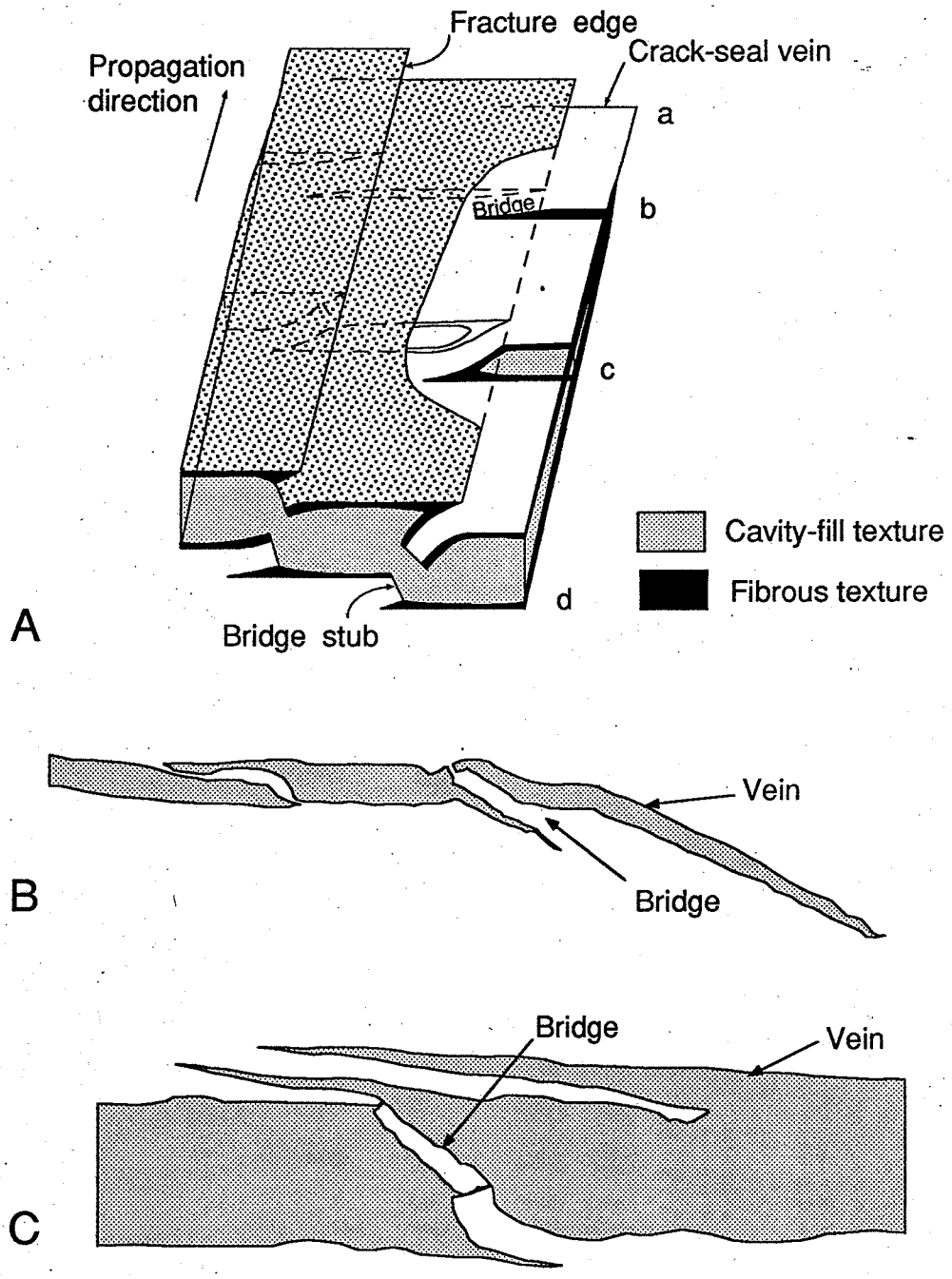

Figure 3.17. Rock Bridges in extensional veins. (**A**) Block diagram showing how rock bridges between en-echelon segments of an extensional vein become incorporated within the vein as a result of growth of the en-echelon segments; from Foxford et al. (1991). (**B**) Cross-section of en-echelon extensional veins separated by rock bridges; Sigma deposit, Val d'Or. (**C**) Cross-section of a large extensional vein containing broken rock bridges; Perron deposit, Val d'Or.

Spatial relationships

Extensional veins can be *internal* to shear zones and commonly form en echelon arrays (Figs. 3.14B and C), or *external* to shear zones and extend for considerable distance outside shear zones in less deformed rocks (Fig. 3.14A). Extensional veins *internal* to shear zones are generally small, less than 10 cm thick, and form at high angle to the foliation and lineation in the host shear zone. They commonly display sigmoidal shapes (Fig. 3.15A) but, in the more ductile shear zones, they may also be folded and boudinaged (Robert and Brown, 1986a). Arrays of sigmoidal extensional veins are better developed in more competent lithologies and the shape and orientation of the veins within the array are indicative of the sense of shear (Figs. 3.14B and 3.15A). In addition, small extensional veins, commonly termed ladder veins, are also commonly present in the most competent parts of shear zones and fault-fill veins (Fig. 3.15B). They are typically orthogonal to the shear zone foliation and represent late stage extension of competent vein material (Fig. 3.14C; Poulsen and Robert, 1989).

Extensional veins *external* to shear zones are well developed only in a few districts around the world, such as Val d'Or. These tabular veins are spatially associated with shear zones and fault-fill veins; they range in thickness from a few centimetres up to one metre and extend away from fault-fill veins in low strain rocks for distances up to several tens of metres (Fig. 3.14A).

Structural significance

Extensional veins are very important from a structural points of view: their opening vector corresponds to the local direction of elongation of the rocks. In the case of planar extensional veins occurring in low strain rocks outside shear zones, the opening vector of these veins give the axis of the bulk elongation of the rocks, in a way analogous to elongation lineations. Similarly, in the case of arrays of planar extensional veins within a shear zone or within any lithologic unit, such as those illustrated in Figure 3.15B, the opening vector of the veins indicate the direction of elongation of the rocks (within the shear zone or the unit) at the time of their formation.

Arrays of sigmoidal extensional veins, such as that illustrated in Figures 3.14B and 3.15A, define shear zones (see Ramsay and Huber, 1987). The veins initiate at an angle of ~45° to the boundaries of the array; with increasing shear strain, the veins will progressively rotate towards a higher angle to the boundaries, whereas new vein segments resulting from their propagation will be at a moderate angle to the boundaries, resulting in their overall sigmoidal shapes (Fig. 3.5). The sense of movement along such shear zones can be deduced in some cases from the

sigmoidal shape of the vein, or more reliably from the angle between the vein tips and the boundaries of the arrays.

Stockworks and breccia veins

Stockwork and breccia veins are a relatively common but in general volumetrically minor type of orebodies in gold deposits. Both types of orebodies can be regarded as composite structures, because they result from the combination of multiple sets of veins and fractures; in fact, as described below, the two commonly grade into one another.

Stockworks

Stockworks consist of two or more sets of veins and range in internal geometry and complexity from "organized" stockworks consisting of two or three well-defined oblique to orthogonal sets of veins, to complex networks of variably oriented veins and veinlets (Fig. 3.18). Two examples will be described to illustrate the range of geometries stockworks. The first example, from the Louvicourt Goldfield deposit at Val d'Or, represents a relatively simple, or incipient (?), stockwork whereas the second example, from the San Antonio deposit at Rice Lake, is a well-developed complex one. In both cases, the stockworks formed economic orebodies.

At the Louvicourt Goldfield deposit, cigar-shaped stockwork orebodies, known as the A and B ore zones, are hosted in a gabbro sill within which they plunge 25-30° to the west (Sauvé et al., 1993). Stockwork orebodies reach down-plunge extensions of 200 m, and their horizontal and vertical dimensions in cross-section are ~10 m and 15-20 m, respectively. As illustrated in Figure 3.18A, the stockworks consist of two oblique sets of extensional-shear veins, which intersect along a line parallel to the plunge of the entire orebodies. The two sets of veins commonly merge and show conflicting cross-cutting relationships, attesting to their broadly contemporaneous development. Fibres within these veins, as well as matching walls and markers indicate a steeply east-plunging opening vector for both sets of veins (Robert, 1990a), perpendicular to the plunge of the orebodies.

In contrast, the stockwork zones at the San Antonio deposit are internally complex, as illustrated schematically in Figure 3.19A and described by Poulsen et al. (1987) and Lau (1988). They are composed of stacked, moderately dipping extensional veins, referred to as ladder veins, linked by subvertical veins on the fringes of the zones (Fig. 3.18B). Due to increase in vein abundance, stockwork zones progressively grade into central breccias (Fig. 3.19A) composed of angular wallrock fragments enclosed within a hydrothermal matrix occupying up to 50% of the volume of the rock (Fig. 3.18C). The breccias are in turn cut by central fault-fill

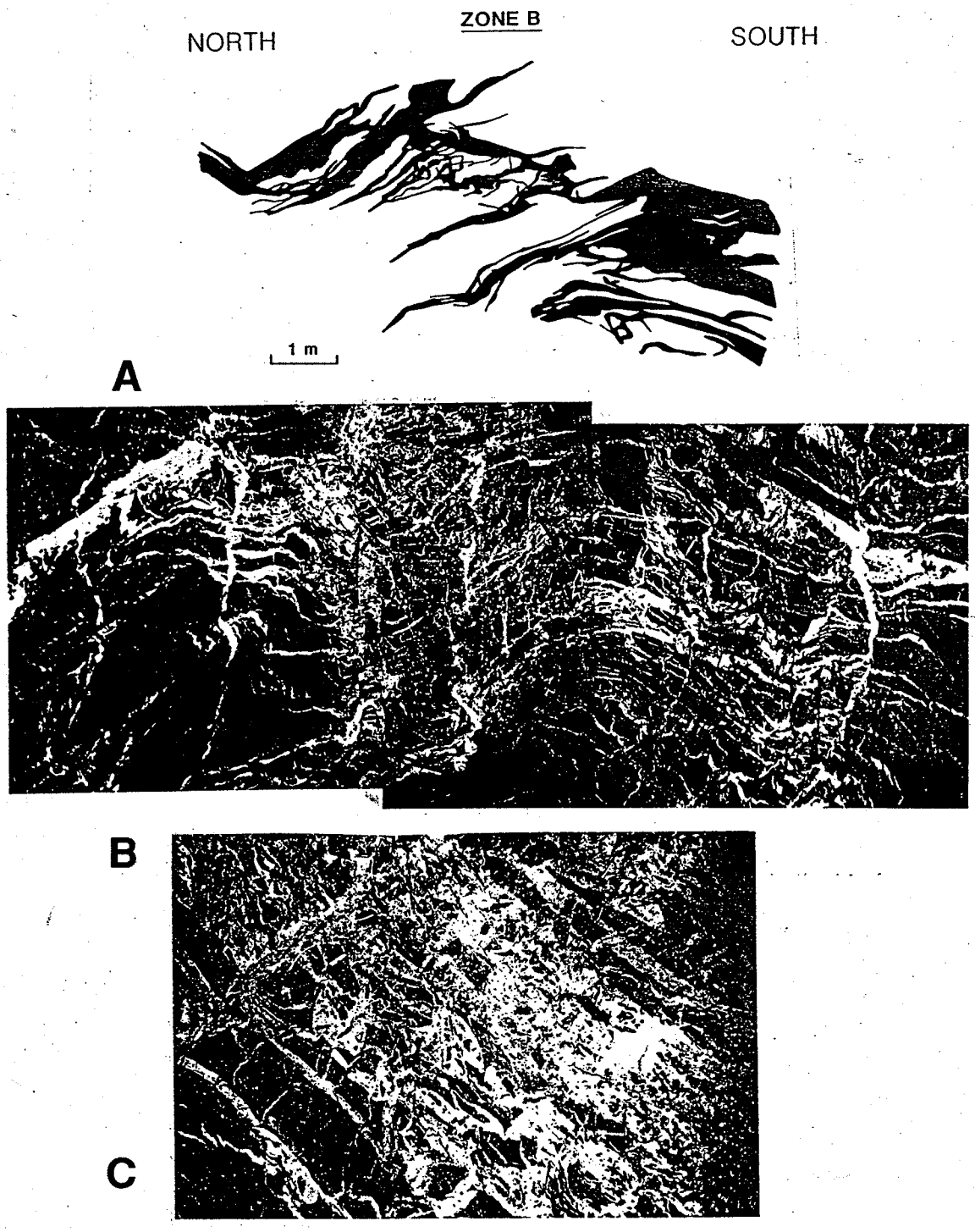

Figure 3.18. Examples of stockworks. (**A**) Cross-section of a stockwork consisting of two oblique sets of extensional-shear veins; Louvicourt Goldfield deposit, Val d'Or. (**B**) Longitudinal section of a stockwork composed shallow-dipping "ladder" veins cut by vertical veins. Note the local development of incipient central breccia due to intense veining; San Antonio deposit, Rice Lake; from Lau (1988). (**C**) Cross-section of central breccia zone developed within the same stockwork as in (B) as a result of intense veining; San Antonio deposit, Rice Lake; from Lau (1988).

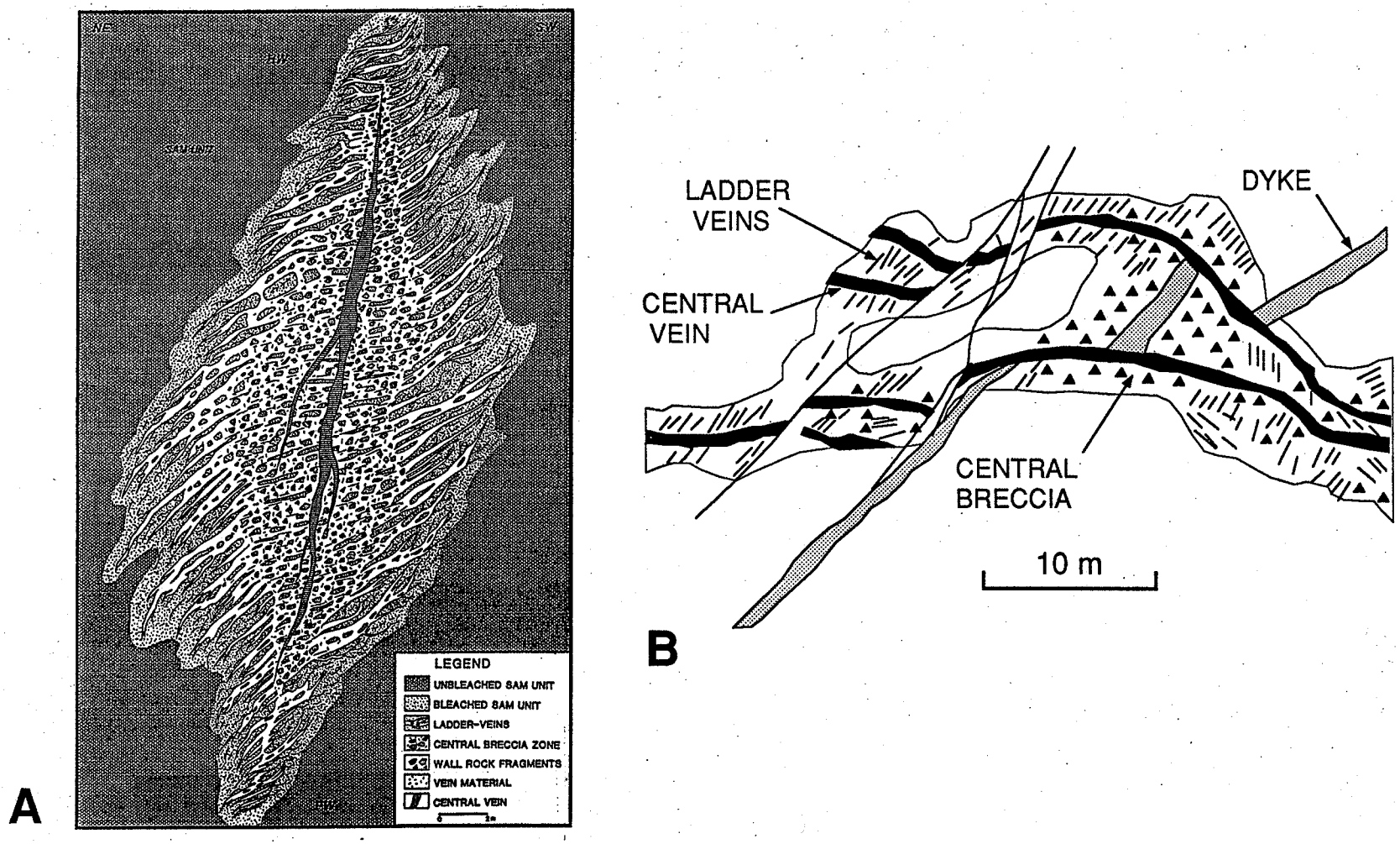

Figure 3.19. Stockwork zones at the San Antonio deposit, Rice Lake. (**A**) Schematic cross-section of stockwork zones showing shallowly-dipping ladder veins progreesing into central breccia zones which are cut by a central fault-fill vein; from Lau (1988). (**B**) detailed geologic map showing the distribution of ladder veins, central breccia zones and central fault-fill veins within the stockwork. Note that all the offset of pre-ore dykes on both sides of the stockwork is taking place along the central fault-fill veins; from Lau (1988).

veins which offset earlier dykes and along which all of the displacement along the stockwork zones has taken place (Figs. 3.19A and B). Movements along the central fault-fill veins may also account for the observed sigmoidal shape of the ladder veins (Fig. 3.18B). It is possible that the development of the central fault-fill veins represents reactivation of the stockwork zones during subsequent deformation (Lau, 1988).

Breccia veins

Several types of breccias are observed in gold deposits, and the term breccia vein is used here to designate any type of breccia with a hydrothermal matrix. Some breccia veins occur along mineralized shear zones or faults, preferentially but not exclusively where shear zones transect competent lithologies. Others rather occupy essentially extensional features along which there is very little if any offset.

A common type of breccia vein, referred to as "jigsaw puzzle breccia", consists of angular wallrock fragments set in a hydrothermal matrix of quartz or commonly tourmaline (Fig. 3.20A). Fragments are of a single compositional type and show no evidence of rotation; they could be fit back together by removal of the hydrothermal matrix. Such breccias have been referred to as *implosion breccias* by Sibson (1986) and interpreted to have formed as a result dilation related to discrete slip events at specific locations along shear zones. Alternatively, breccia veins with similar textures can also develop as a result of intense stockwork development, as illustrated above for the San Antonio deposit (Fig. 3.18C). The Chadbourne deposit, in the Noranda district, may in fact be a unique case of an entire deposit made up of a breccia similar to jigsaw puzzle breccias described here (Walker and Cregheur, 1982).

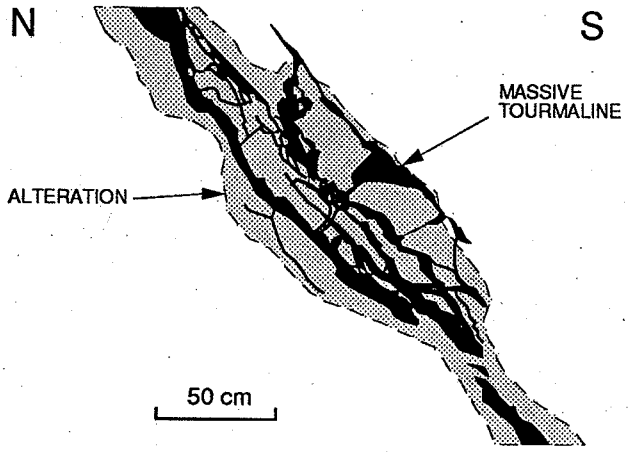

Figure 3.20. Jigsaw-puzzle breccia consisting of bleached wallrock fragments in a fine grained tourmaline matrix. Note the absence of rotation and mechanical abrasion of the fragments; Sigma deposit; Val d'Or.

Another common type of breccia veins consists of rounded to angular clasts of altered wallrocks and vein material set in a hydrothermal matrix. In such breccias, there is common evidence for rotation and communition of fragments, as well as re-brecciation. These breccias typically occur in association with, or as components of, fault-fill veins, and they share many characteristics with *fault breccias* (Sibson, 1986). Such breccia veins likely result from multiple faulting events of wallrocks and existing vein material. The hydrothermal nature of the matrix of these breccias further indicates that faulting was an integral part of the mineralization process.

RELATIONSHIPS AMONG VEINS AND SHEAR ZONES

As previously indicated, fault-fill and extensional veins are commonly spatially associated with shear zones, and recurring geometric patterns are observed among these three components of gold deposits. These patterns reflect key structural relations which can be used to place constraints on shear zone's B-axes and on the plunge of ore shoots, as defined by the long axes of veins or vein arrays within shear zones or by high grade intersections of different types of veins.

However, such geometric relations can only be used in cases where it can be demonstrated that the shear zones and the spatially associated sets of veins are contemporaneous. Thus, before we examine such geometric relationships, it is important to address the question of age relationships among shear zones and associated veins.

Age relationships

There are two aspects of the question of age relations among veins and shear zones which are usefull to address separately: the age relations among the veins themselves, and age relations between vein development and activity along the host shear zone.

Age relationships among veins

Most commonly observed at intersections of different veins are cross-cutting relationships (Fig. 3.21A). In some deposits, systematic cross-cutting relationships are observed between two types of veins, for example planar arrays of extensional veins cross-cutting at high angle existing shear zones and fault-fill veins (Fig. 3.15B). In some other deposits, conflicting cross-cutting relationships between two vein types are observed, either along the same structure or along parallel ones within the same deposit (Robert and Brown, 1986a; Robert 1990). Such conflicting cross-cutting relationships are illustrated in Figure 3.21B, where a shallow-dipping

extensional vein cuts across part of a subvertical fault-fill vein but is in turn offset by later movement along a slip surface within the fault-fill vein. Similarly, a small extensional vein shown in Figure 3.12B cuts across the external portion of a fault-fill vein and merges with a slip surface in its central part. Systematic cross-cutting relationships indicate that the different types of veins are of different ages. In contrast, conflicting cross-cutting relationships among two types of veins indicate that they are broadly contemporaneous. It further indicates cyclic, sequential development of these veins (Robert, 1990). Because conflicting relationships are not necessarily exposed at the same place, it is important not to base interpretations of age relationships among veins on a single or small number of observations which may not be representative.

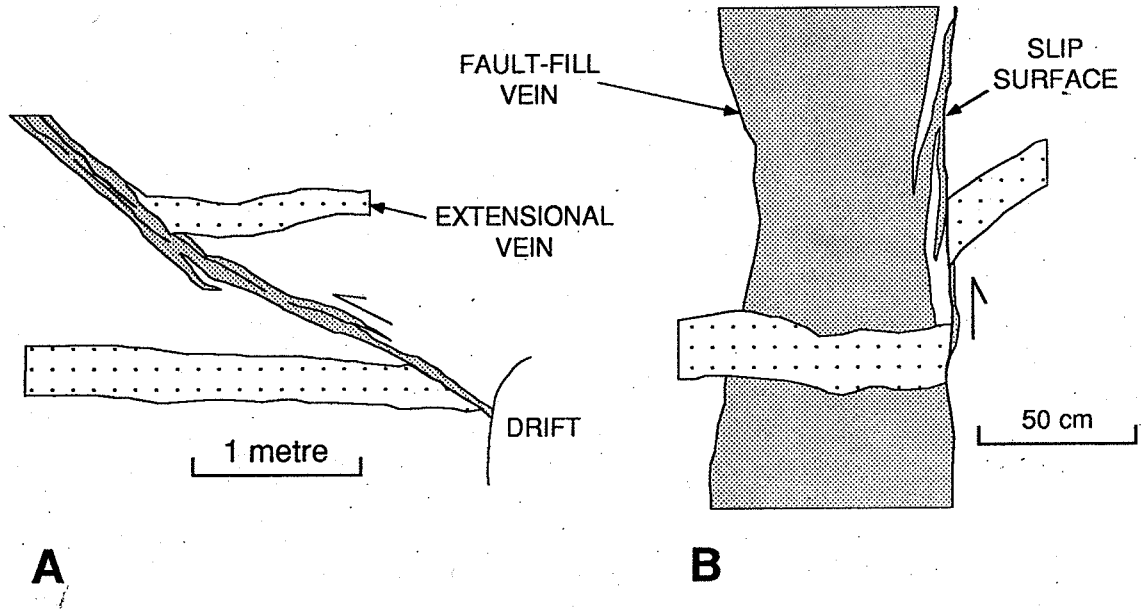

Figure 3.21. Cross-cutting relationships among veins. (**A**) Cross-section of a fault-fill vein along which there is reverse offset of a horizontal extensional vein; Perron deposit, Val d'Or. (**B**) Cross-section showing complex relationships between a subvertical fault-fill vein and a sub-horizontal extensional vein. The extensional vein truncates part of the fault-fill vein but is in turn offset by vertical movement along a slip surface on the edge of the fault-fill vein; Sigma deposit, Val d'Or.

In the section presenting the characteristics of fault-fill and extensional veins, the incremental and dynamic nature of the development of these veins was emphasized. It is important to realize that the cross-cutting relationships observed among veins represent the final product of their incremental development, and does not necessarity reflect cross-cutting relationships at different stages in their incremental development. As shown in Figure 3.22A and discussed by Scholz (1989) and Pollard and Segall (1987), extensional veins are expected to develop

at the frontal and lateral terminations of shear fractures and faults, as a result of the attenuation of movement at such terminations. The orientation and distribution of these extensional veins reflects the stress field in which the fault develops. Such spatial arrangements fault-fill veins and extensional veins are only observed in rare cases, such as that illustrated in Figure 3.22B. The array of large sigmoidal extensional veins shown in Figure 3.15A occurs at the lateral termination of a ~100 m long fault-fill vein. The reverse sense of movement indicated by the vein array is consistent with that deduced for the fault-fill vein based on stepped hydrothermal slickenfibres.

The distribution of extensional veins illustrated in Figure 3.22A represents that which occurred at a fixed time in the development of the fault. If this fault propagates frontally and laterally, existing extensional veins will be truncated by the fault and by any resulting fault-fill vein, and new extensional veins may form at the new frontal and lateral limits of the larger fault. The end result of this dynamic process is that at any location along a fault or a fault-fill vein other than its termination, extensional veins will always be cut by the fault or the fault-fill vein. These relations are illustrated in Figure 3.22B: the largest extensional vein is clearly truncated by the fault-fill vein, whereas other smaller extensional veins are not and occur beyond the down-dip termination of the fault-fill vein. The truncated extensional vein probably formed at an earlier stage at which the fault-fill vein had not yet propagated to its current position. Similarly, if the fault-fill vein had propagated further downward, it would have truncated and offset all extensional veins present at the point of observation. This would have resulted in incorrect interpretation of age relationships among the two vein sets.

Identical hydrothermal characteristics (mineral assemblages and associated hydrothermal alteration) of different types of veins, as is the case for those in Figure 3.22B, may be used as a first indication that the veins are broadly contemporaneous.

Vein development vs shear zone activity

In the case of auriferous veins hosted in shear zones and in faults, one critical and difficult question to address is the relative timing of vein development relative to shear zone development. Structural and textural evidence for the emplacement of fault-fill veins in active shear zones versus their overprinting by the shear zones have already been presented in the section on the structural significance of fault-fill veins.

Such relative timing can also be established using relationships between extensional veins and shear zone foliation. Overprinting and crenulation of extensional veins by the foliation, best observed at the vein-wallrock interface, clearly establishes the veins to predate the shear zone. If extensional veins cut the

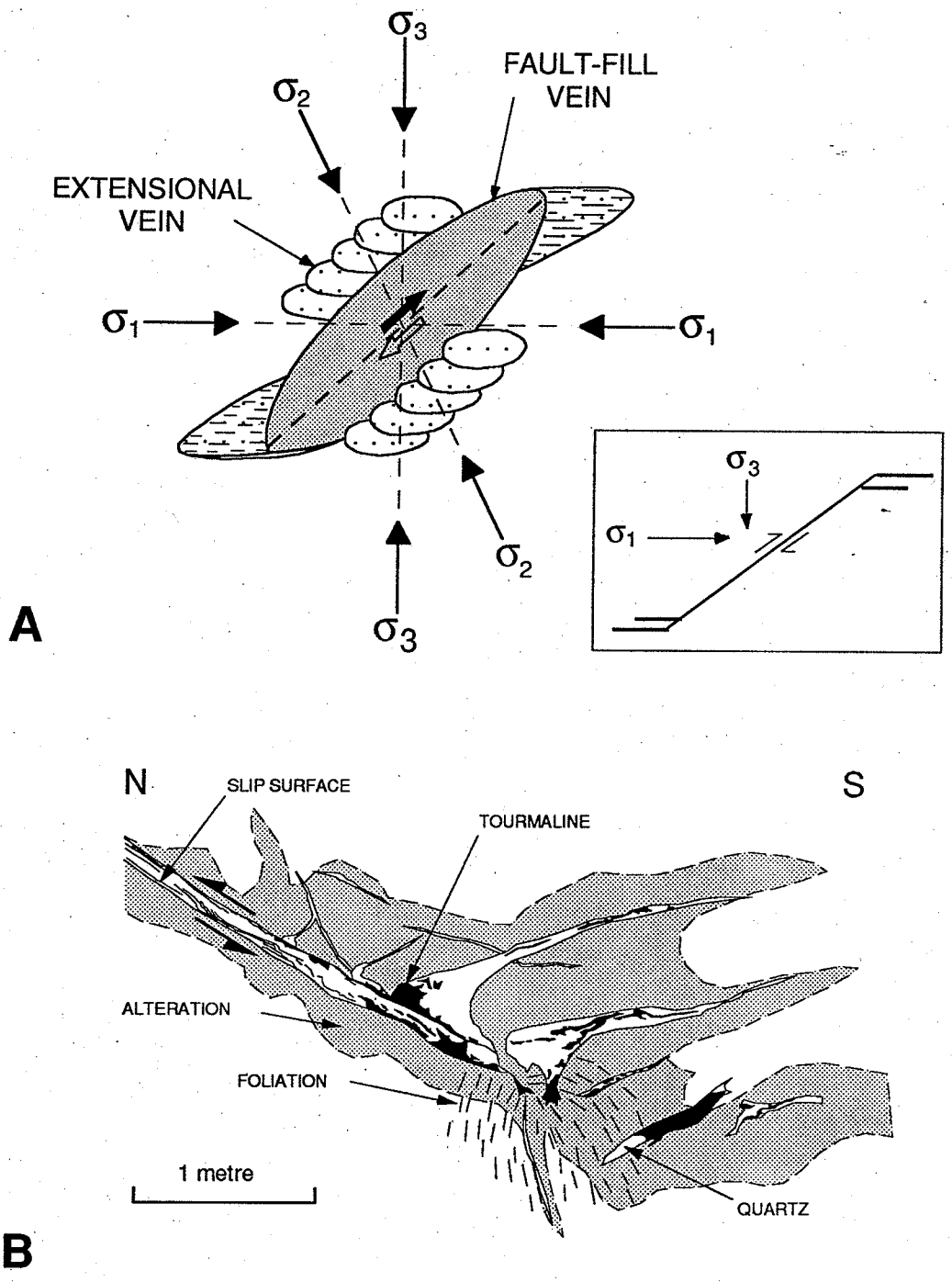

Figure 3.22. Spatial arrangements of fault-fill and extensional veins. (**A**) Diagram representing the expected distribution and geometry of extensional fractures around the edges of a shear fracture; adapted from Scholz (1989). (B) Cross-section showing the down-dip termination of a quartz-tourmaline reverse fault-fill vein with related extensional veins in the hangingwall. Note also the local development of foliation on the footwall side; Lucien Béliveau deposit, Val d'Or.

foliation planes and are not crenulated, they obviously postdate development of the foliation; if these extensional veins are perpendicular to the elongation lineation within the shear zone, their formation can be viewed as an integral part of shear zone development. Finally, it is not uncommon for extensional veins cutting across the foliation to be buckled to variable degree. Such gentle folding of extensional veins indicates continued shortening across the shear zone after vein development and should not be misinterpreted as evidence that the veins predated the shear zones.

Geometric relationships

The geomtric relationships between veins and structural elements of shear zones expected in cases of vein emplacement in active shear zones are summarized in Figure 3.23. As indicated above, the B-axis of the shear zone is given by the line perpendicular to the slip direction within the plane of the shear zone. This axis also coincides with the line of intersection of the oblique foliation to the shear zone boundaries and, in a number of cases, it may also coincide with the line of intersection between a shear zone and its splays. Elongation lineations on foliation planes, as well as striations and hydrothermal slickenfibres in fault-fill veins related to shear zone development will also be perpendicular to the B-axis of the shear zone.

Extensional veins within the shear zones, whether isolated or in vein arrays, are at high angle to the shear zone foliation and their line of intersection with the foliation is parallel to the shear zone's B-axis. This is also the case for the line of intersection between the shear zone and related planar extensional veins in adjacent low strain rocks.

The most important structural information about shear zones required for analysis of complex networks comprising many deposits (see Chapter 4) is their B axis of the shear zone. As indicated here, this axis can be determined from any of the following shear zone or vein component: intersection of foliation or extensional veins to shear zone boundaries, elongation lineations on foliation planes, and hydrothermal slickenfibres on slip surfaces within fault-fill veins.

Plunge of ore shoots

It is well known that fault-fill veins, stockwork zones and arrays of extensional veins within shear zones commonly occur at specific sites along shear zones and faults, such as bends and intersections with splays or with other structures (Newhouse, 1942; McKinstry, 1948). At such sites, orebodies will have elongate shapes with long axes corresponding to the plunge of the ore shoots they represent. Similarly,

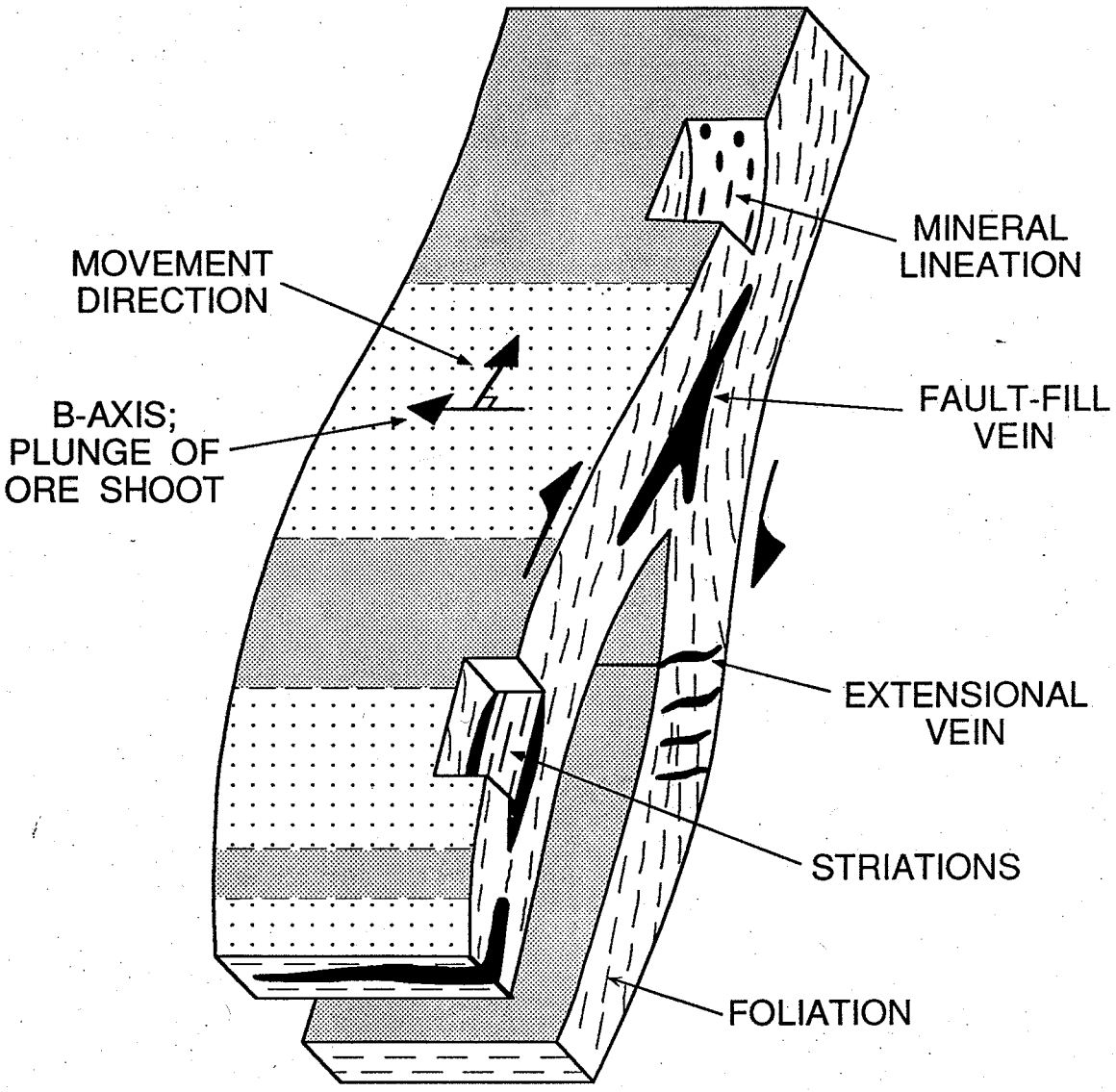

Figure 3.23. Block diagram showing the geometric relationships among structural elements of shear zones and associated veins and vein arrays; see text for discussion; adapted from Poulsen and Robert (1989).

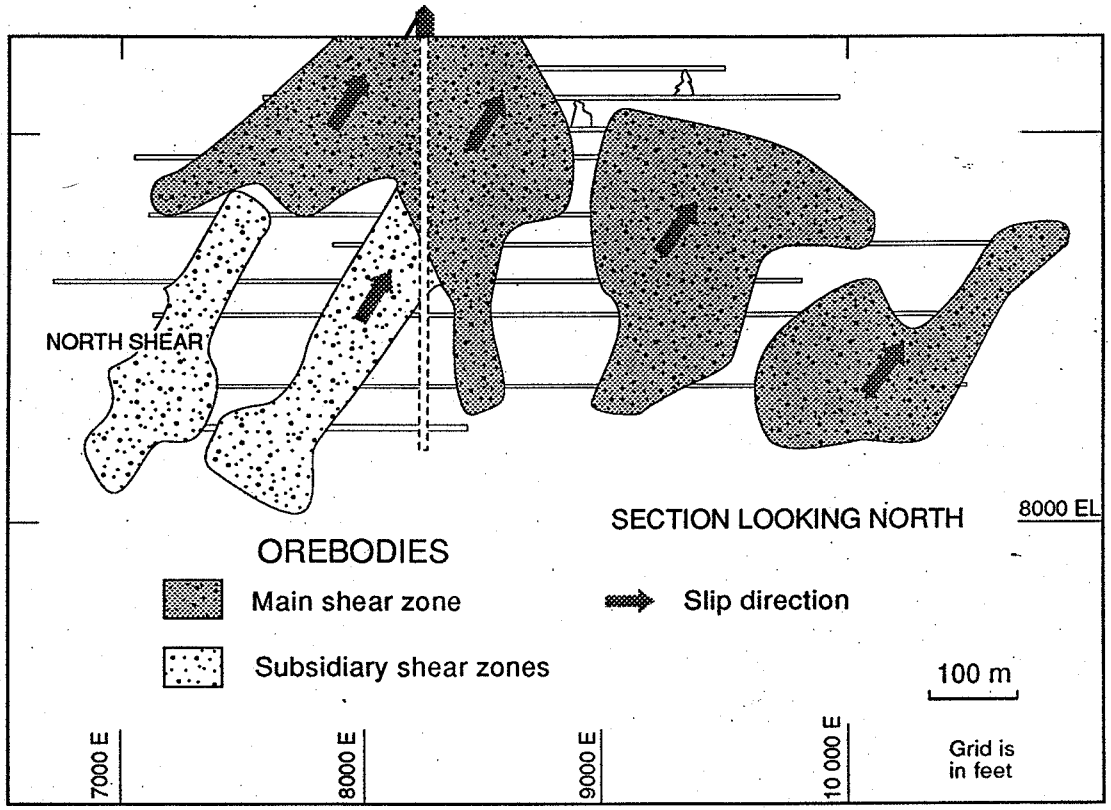

A

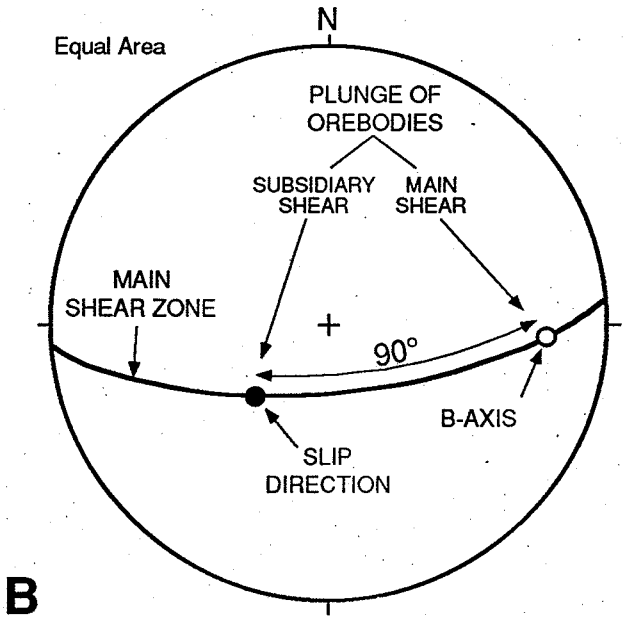

B

Figure 3.24. (**A**) Simplified longitudinal section along the main shear zone of the Dumont deposit, Val d'Or, showing the plunges of orebodies within the main and subsidiary shear zone relation to the slip direction; adapted from Belkabir (1990). (**B**) Stereographic representation of the main structural elements of the main shear zone.

intersection among different types of veins along a given shear zone are also the sites of high grade ore shoots. It is also well known that the plunges of these two types of ore shoots display specific relationships to the slip direction or to the B-axes of the shear zones .

As shown in Figure 3.23, ore shoots corresponding to vein intersections will be parallel to the B-axis of the associated shear zone. Ore shoots defined by the long axes of fault-fill veins, if they have emplaced in dilational jogs, are predicted to also lie parallel to this axis. In other cases, for reasons that are not fully understood at present, the long axes of such veins are rather perpendicular to the B-axis, or parallel to the slip direction. The possible plunges of fault-fill veins are particularly well illustrated by the Dumont deposit (Fig. 3.24), where both a main shear zone and a smaller splay contain fault-fill veins. The slip directions along the shear zone and its splays are well constrained (Belkabir et al., 1993), and rake at 60-65° to the west in both cases, which define a B-axis raking at approximately 25-30° to the east. In the main shear zone, fault-fill veins line up along an axis parallel to the B-axes, whereas fault-fill veins along the splay are parallel to the slip direction.

CHAPTER 4:
THE INFLUENCE OF FAR-FIELD STRESS / STRAIN REGIME

INTRODUCTION

The majority of lode gold deposits comprise several orebodies within single or multiple structures that may be part of single or multiple sets. A large number of deposits, especially those of syn-tectonic vein type, consist of multiple sets of shear zones and veins which define *three-dimensional networks* of a wide range of complexities. In fact, an empirical observation one commonly makes is that large lode gold deposits tend to be geometrically the most complex ones. This specifically focusses on such syn-tectonic vein gold deposits.

The networks comprising syn-tectonic vein gold deposits, especially those of the vein-type, typically involve shear zones of the third-order, as defined in Chapter 2, with which most of the orebodies are associated. Second-order shear zones are also mineralized in a number of deposits, especially at their intersections with other shear zones and veins. The different sets of shear zones and veins composing the networks may have formed during the same deformation increment, as established by conflicting cross-cutting relationships among the various sets or by identical hydrothermal characteristics (see Chap. 3), or they may be of different ages and systematically overprint each other. In this chapter, we are only concerned with the analysis of networks of broadly contemporaneous structures; examples of networks composed of multiple ages of structures are considered in Chapters 5 and 6.

The geometry of gold deposit networks, i.e. their orientation and complexity, are determined by factors operating at both the regional and the local scales. The dominant factor at the regional scale is the *far-field stress/strain regime* under which the auriferous structures are formed or deformed; at the local scale, *strength anisotropy* related to lithological heterogeneities is an important factor. The influence of these two main factors on the geometry of gold deposits is schematically illustrated in Figure 4.1. In a homogeneous rock mass, such as a pluton, shortening about a particular axis will produce a relatively simple and predictable pattern of shear zones along which slip directions can easily be related to the orientation of the three principal stress axes (Fig. 4.1A). However, if the same rock mass contains local "weakness planes", such as pre-existing faults or incompetent dykes, the resulting shear zone pattern will be more complicated and less predictable (Fig. 4.1B): pre-existing faults and incompetent dykes of a range of

orientations can be reactivated or become the locus of shear zones. Thus, the geometry of shear zone and vein networks will reflect the interplay between the regional stress/strain field and local anisotropies. Networks controled dominantly by the far-field regional stress/strain field are considered in this chapter; those in which anisotropies play an important role are considered in Chapter 5.

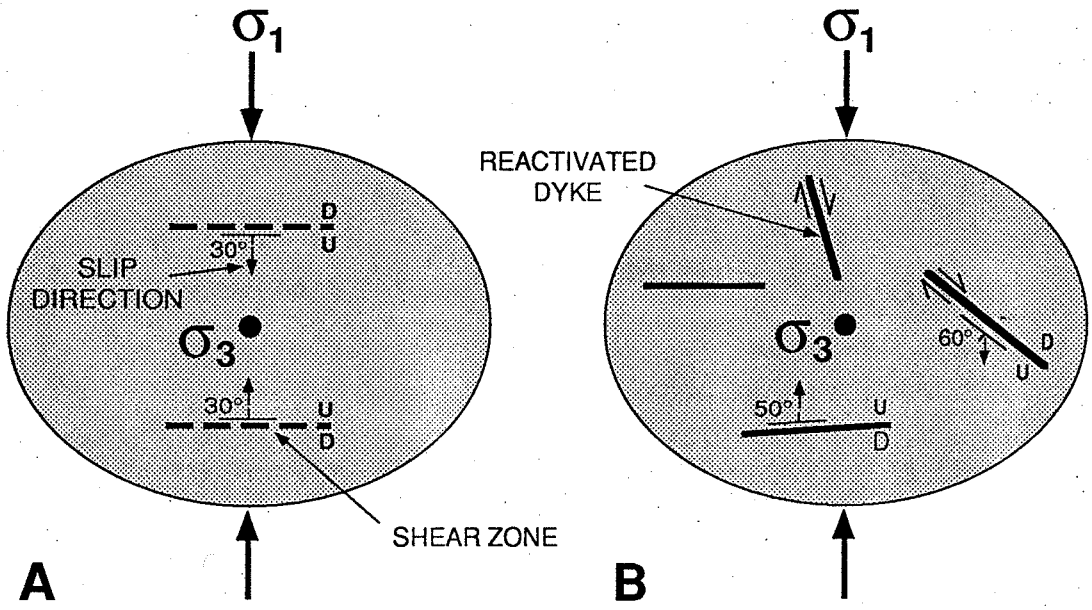

Figure 4.1. Expected shear zone patterns to develop under a given stress field (**A**) within a homogeneous rock mass and (**B**) within a rock mass containing weak layers.

ANDERSONIAN FAULTING AND STRESS REGIMES

Anderson (1905) pointed out that, because the surface of the Earth is a free horizontal surface (in areas of low relief) across which there is no shear stress, one of the principal stress axes must be vertical at the surface and for some depth. This led him to define three major classes of faults corresponding to the three possible stress configurations in which one of the principal stress axis is vertical: thrust faults where $\sigma v = \sigma 3$, strike-slip faults where $\sigma v = \sigma 2$, and normal faults where $\sigma v = \sigma 1$ (Fig. 4.2). These three stress configurations also correspond to compressional, wrench or strike-slip, and extensional regimes, respectively. As emphasized in Chapter 2, deformation in a large number of gold districts took place under compressional regimes, where $\sigma 1$ is horizontal.

Theory predicts that, in intact rocks, faults will develop at an angle of approximately 30° to $\sigma 1$ (Fig. 3.9). If conjugate sets of faults develop, their intersection will be parallel to $\sigma 2$, and $\sigma 1$ will lie in the acute angle between the two sets, which is predicted to be $2\theta = 60°$ (Fig. 4.2). However, it can be demonstrated

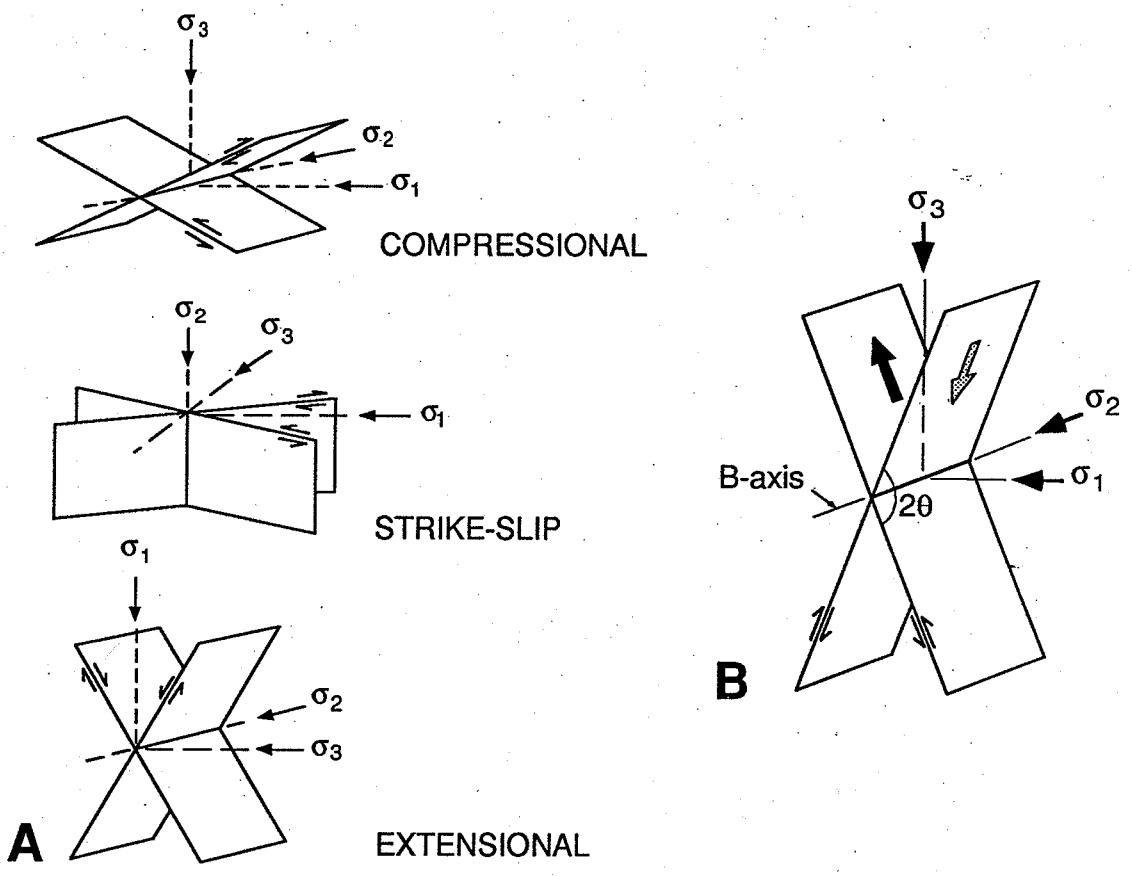

Figure 4.2. Relationships between conjugate sets of faults and principal stress axes. (**A**) Fault patterns corresponding to the three main stress regimes; from Anderson (1905). (**B**) Conjugate sets faults for which σ1 lies in the obtuse angle between the sets, as commonly observed in gold districts.

for shear zones of medium to high metamorphic grades, as well as those in a number of gold deposits that σ1 rather lies in the obtuse angle between two conjugate sets of shear zones, as depicted in Figure 4.2B (Ramsay, 1983; Robert and Brown, 1986a). It was further noted by Ramsay (1983) that the 2θ angle between conjugate shear zones changes with crustal depths, ranging from ~60° in the upper 5 km of the crust, in good agreement with theory, to 60-90° at depths on the order of 5-10 km, which corresponds to depths of erosion of a large number of gold districts, to 90-120° at depths greater than 10 km. This increase in the 2θ angle cannot entirely result from rotation of initially properly oriented shear zones towards σ3 as a result of shortening in the intervening rocks. Other interpretations relate such increase in the 2θ angle to either an increase in mean stress with depth or to volume loss within the shear zone (Ramsay, 1983).

Figure 4.2B illustrates the geometric relationships between the principal stress axes and conjugate sets of reverse shear zones with $2\theta > 90°$. It is important to note that the line of intersection of the two shear zones is perpendicular to their respective slip directions, and that the B-axes of the two shear zones are coincident; this is one of two necessary conditions for interpreting two sets of shear zones as conjugates. The other condition is that the sense of movement on the two sets must be opposite to one another. Splays along a master fault or a shear zone may present geometries similar to those illustrated in Figure 4.2B, and their intersection with the master fault may also be perpendicular to the slip direction. However, both the master fault and the splays will have the same sense of movement.

AXES OF NETWORKS

Shear zone and vein networks record part of the deformation of the enclosing volume of rocks in response to applied regional stresses. The volume of rocks undergoes shortening in some directions and elongation in others. For such a volume of rock, it is therefore possible to define three orthogonal principal directions of elongation and/or shortening, which will be referred to here as *bulk strain axes*, in contrast to far-field regional strain axes. Figure 4.3 illustrates how a volume of rocks can be deformed in two dimensions by combined movement along conjugate sets of faults and penetrative deformation of the intervening rocks, and also illustrates the corresponding bulk elongation (**X**) and bulk shortening (**Z**) axes. In such a general case, movement on the faults and dilation associated with them are reponsible for only part of the bulk strain. Therefore, shortening and/or elongation axes determined from the analysis of a deposit network represent only part of the deformation associated with the development of the network .

We believe it is preferable to analyze gold deposit networks in terms of their relationships to bulk strain axes rather than in terms of principal stress axes for two main reasons. First, auriferous shear zones are ductile to brittle-ductile in character and do not strictly lend themselves to brittle analysis. Second, although structural axes of the networks correspond to the far-field stress/strain axes in a number of cases (Fig. 4.3), such as those considered in this chapter, they are not coincident in other deposits such as some of those discussed in Chapter 5.

It is possible to use the data derived from mesoscopic observation of veins and contemporaneous shear zones in order to reconstruct the deposit-scale axes of incremental strain that the veins and shear zones represent. This is useful in that these *deposit-scale strain axes* of vein and shear zone networks can be compared with independantly determined bulk strains recorded by enclosing rocks, as well as with far-field stress/strain axes. If the different sets of shear zones and veins in a given network are shown to be broadly contemporaneous, then the resolved

deposit fabric axes are those corresponding to the increment of the deformation producing the auriferous structures. If these different sets systematically overprint each other, then deposit fabric axes represent to the sum of multiple increments of deformation.

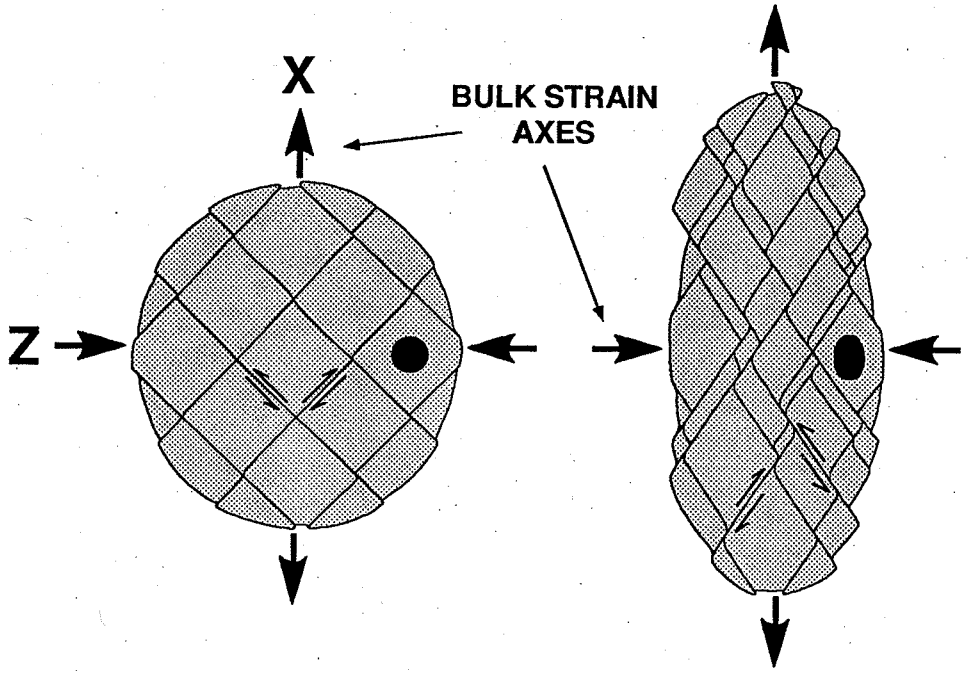

Figure 4.3. Diagram illustrating how volume of rocks can undergo significant bulk strain by combination of penetrative deformation and movement along conjugate sets of faults. The axes of elongation (X) and shortening (Z) of the volume of rocks correspond to bulk strain axes; from Ramsay and Huber (1987).

An important point about the strain recorded by deposit networks is that there may be more than one axis of elongation, or more than one axis of shortening. As illustrated in Figure 4.4, there are three possible types of bulk strain, which have in common one direction of shortening (horizontal) and one direction of elongation (vertical); they differ in the other horizontal direction. The first case is characterized by one axis of bulk shortening and one axis bulk elongation, and it corresponds to two-dimensional deformation, which we refer to as *plane bulk strain* by analogy with the corresponding shape of finite strain ellipsoids. The second case is characterized by two axes of elongation and represents *oblate bulk strain*, whereas the third case, characterized by two axes of shortening, corresponds to *prolate bulk strain*, or bulk uniaxial extension. Clearly, cases of oblate and prolate bulk strain represent deformation in three-dimensions and two-dimensional representations of

the corresponding networks deposits as level plans and cross-sections are inadequate.

Finally, as represented schematically in Figure 4.4, the three different types of bulk strain will lead to three different patterns of shear zones and veins, and to different complexities of networks. In the case of plane bulk strain, one set of extensional veins and two conjugate sets of shear zones can be predicted, all intersecting about the intermediate bulk strain axis (Y), corresponding to the shear zones' B-axes. Prolate bulk strain will lead to development of one set of extensional veins and multiple shear zones of a wide range of orientations but forming a similar angle to the bulk elongation axis (X). In the case of oblate strain, two orthogonal sets of extensional veins can be produced, as well as multiple shear zones of a wide range of orientations but forming a similar angle to the bulk shortening axis (Z). In the last two cases, the different sets of shear zones and veins produced will not intersect about a common axis. All examples considered in this chapter record plane strain.

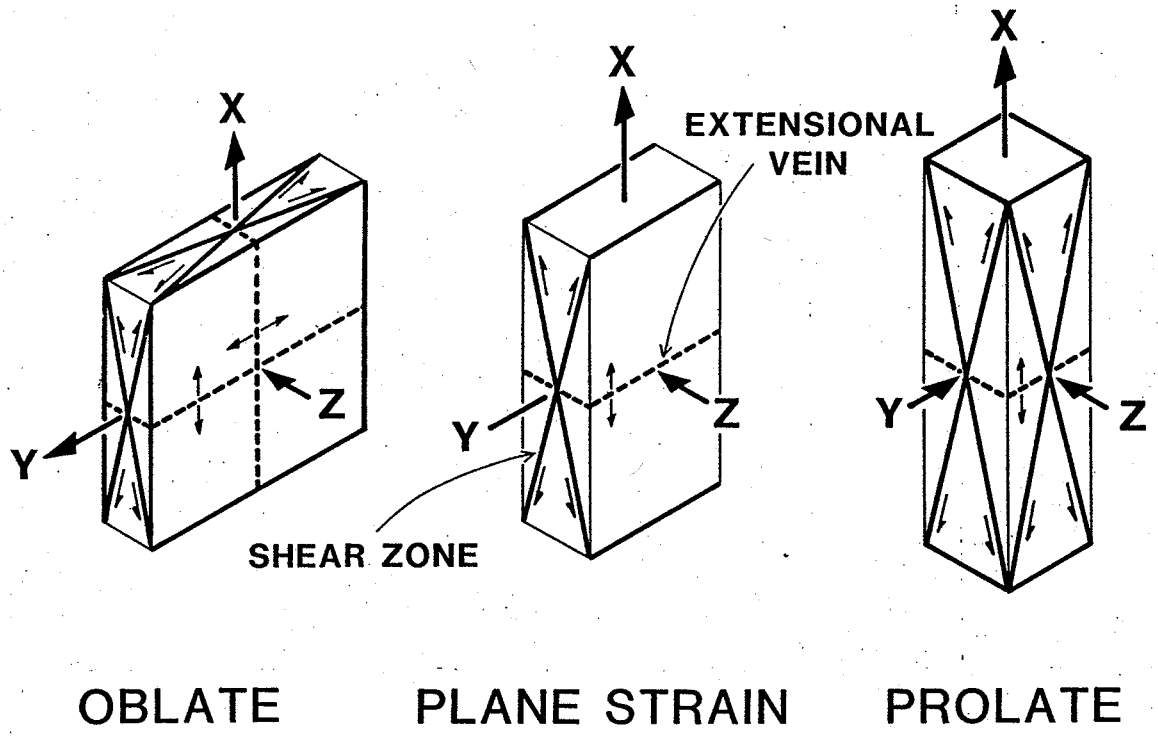

Figure 4.4. Diagrams showing predicted orientations of conjugate sets of shear zones and extensional veins as a function of the type of bulk strain. See text for explanations.

Determination deposit-scale strain axes from vein and shear zone data

Strain axes of gold deposit networks are determined in a way similar to reconstruction of the three principal stress axes from fault data. It is not always possible from the available data to constrain the position of all three axes, but in general, at least one of the axes can be determined.

The geometric relationships between elements of gold deposit networks and deposit-scale strain axes are illustrated in Figure 4.5. If the direction of slip along a fault-fill vein and and its host shear zone is known, the B-axis of the shear zone may correspond to the Y-axis of deposit-scale strain in two cases: if the network comprises a single set of shear zones, or if the different sets of shear zones are conjugate sets, i.e. if their B-axes are parallel. In cases where the B-axes of multiple sets of shear zone are not parallel, these axes do not represent the Y axis, and other techniques should be used to determine the orientation of deposit-scale strain axes, as discussed in Chapter 5. In cases where conjugate sets of shear zones are present and the direction and sense of movement are known, all three deposit-scale axes can be determined (Fig. 4.5B): the Y axis corresponds to the intersection of the shear zones. The X and Z axes fall on a great circle perpendicular to the Y axis; on that great circle, the orientation of these two axes is such that they bisect the angles defined by the two conjugate shear zones, and their position is determined from the sense of movement along the shear zones.

In cases where planar extensional veins are present in less deformed rocks outside shear zones, the opening vector of these veins, which is generally perpendicular to their walls, defines the direction of elongation or the X axis (Fig. 4.5). The position of the three deposit-scale strain axes can also be fully constrained for deposits combining extensional veins with a single set of shear zones. As indicated above, the Y axis can be determined from the shear zone's B axis which, combined with the position of the X axis determined from the extensional veins, fixes that of the Z axis. It should be noted that in most cases, extensional veins external to shear zones will have a line of intersection with the shear zones which is coincident with the B axis (Fig. 4.5B).

Determination of deposit-scale strain axes is illustrated using the Paramaque gold showing at Val d'Or as an example (Fig. 3.6). Structural data obtained on outcrop are summarized in Figure 4.6, together with their stereographic projection. As shown in Figure 3.6, small extensional veins extend outside the main shear zone; these veins are slightly buckled as a result of superimposed shortening, but their envelopes give a reasonable approximation of their initial orientation. The pole of these veins, which are oriented at 194-33° on average, corresponds to the elongation direction, or the X axis of the deposit-scale strain ellipsoid. Because we are analyzing a single shear zone, the B-axis of that shear zone corresponds to the Y axis of the strain ellipsoid. The B-axis of the shear zone corresponds to the line of

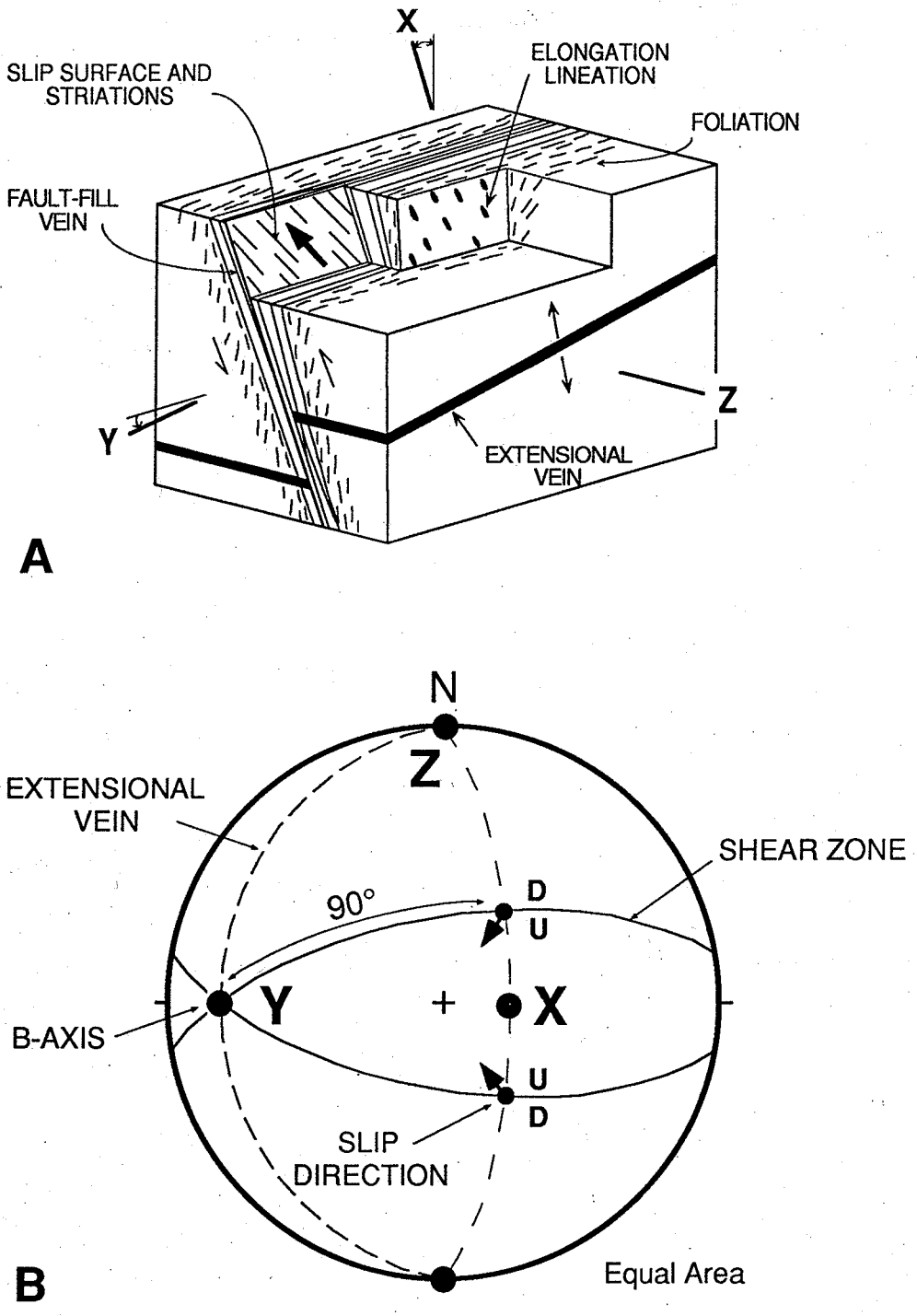

Figure 4.5. (**A**) Diagram illustrating geometric relationships between structural elements of veins and shear zones and deposit-scale strain axes. (**B**) Stereographic projection of structural elements and deposit-scale axes corresponding to the case depicted in A.

intersection of the shear zone with its internal oblique foliation or with the extensional veins outside the shear zones. It also corresponds to a line, within the plane of the shear zone, perpendicular to the slip direction along the shear zone, as determined from slickenlines within the fault-fill veins or from the projection of the elongation lineations onto the plane of the shear zone.

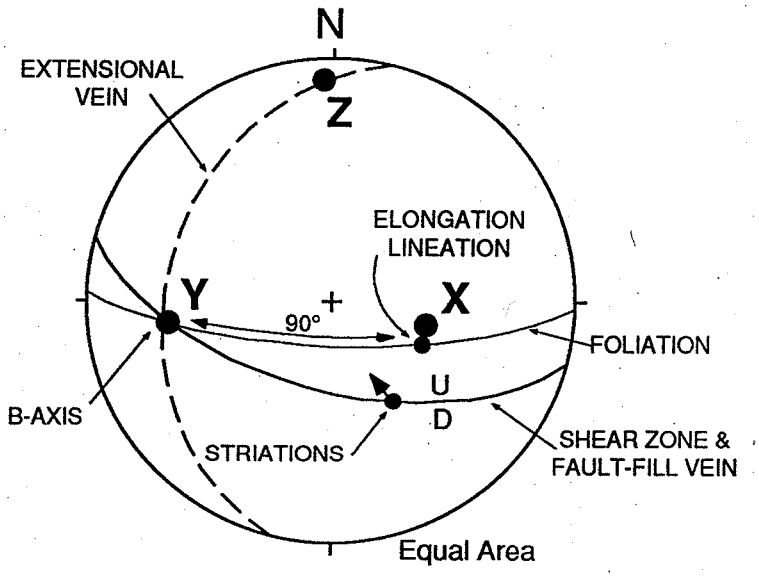

AVERAGE ORIENTATION OF STRUCTURAL ELEMENTS

SHEAR ZONE:	
Foliation	092-75
Elong. lineation	116-56
FAULT-FILL VEIN	
Orientation	105-60
Striations	148-50
EXTENSIONAL VEINS	
Orientation	194-33

Figure 4.6. Stereographic projection of structural elements of the Paramaque gold showing, Val d'Or, with the interpretation of the corresponding deposit-scale strain axes.

STRUCTURE OF DEPOSITS AND THEIR ANALYSIS

In this section, geological examples of networks of increasing complexities are described and analyzed. They range from networks composed of single shear zone sets, to those combining different sets of shear zone and veins, including conjugate sets, to geometrically more complex networks. Important geological and structural aspects of the deposits are presented and the network axes are determined and interpreted in terms of deposit-scale strain axes. This section also serves to illustrate a variety of difficulties commonly encountered in analyzing and interpreting the structure of gold deposits.

Ferderber deposit

The Ferderber deposit at Val d'Or (Fig. 2.2), hosted in the synvolcanic quartz diorite Bourlamaque pluton, consists of a single set of shear zones and fault-fill veins (Vu et al.,1987; Vu, 1990). Several mineralized fault-fill veins occur in a shear zone

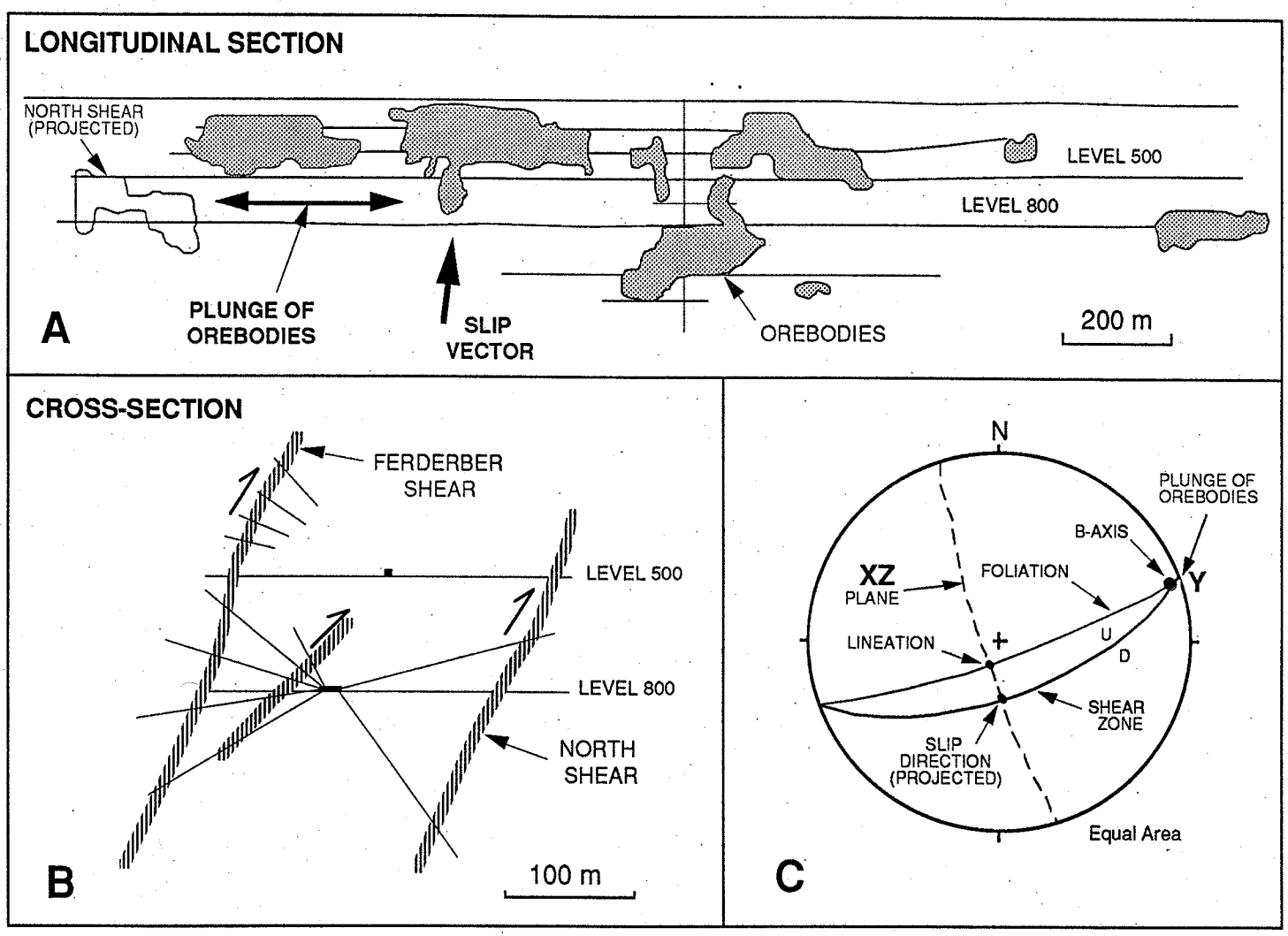

Figure 4.7. The Ferderber deposit, Val d'Or district. (**A**) Longitudinal section of the Ferderber shear zone showing the position and shape of the mined fault-fill veins; from Vu (1990). (**B**) Simplified cross-section looking west showing the position of the Ferderber and North shear zones; from Vu (1990). (**C**) Stereographic projection of the structural elements of the deposit.

striking at 070° and dipping 65° to the south, and additional orebodies occur in smaller subparallel shear zones in the western part of the deposit (Figs. 4.7A and B). The main shear zone, known as the Ferderber shear, has been traced for over 2.5 km along strike and to a depth of 450 m; it follows and overprints one of numerous mafic dykes present throughout the host intrusion. Shear zone lithologies include both foliated quartz-diorite and chlorite-carbonate schists derived from the mafic dyke. The obliquity of foliation to shear zone boundaries (Fig. 4.7C), together with the presence of down-dip elongation lineations and striations and of shear bands clearly indicate that the Ferderber shear is a reverse shear zone (Vu et al., 1987).

The orebodies consist of individual laminated fault-fill veins, typically ranging from 10 cm to 10 m in thickness, from 200 to 300 m in their longest and horizontal dimension, and from 75 to 150 m vertically (Fig. 4.7B). The fault-fill veins are central to the shear zone and are slightly oblique to the boundaries in cross-section, leading to an en echelon arrangement similar to that illustrated in Figure 3.10A. Both the veins and the shear zone foliation are folded; these folds have shallow plunges to the east or to the west and have an asymmetry which is consistent with the reverse movement recorded along the shear zone (Vu, 1990). The veins in the Ferderber shear can be interpreted as having emplaced during, and outlasted by, reverse movement along the shear zone, rather than having been deformed during subsequent reactivation of the shear zone in a different deformation regime.

As is the case in many deposits, the orebodies in the Ferderber deposit have well-defined long axes with subhorizontal plunges (Fig.4.7B). Their plunges are parallel to the B-axis of the shear zone, as determined from the elongation lineations and from the intersection of the foliation with the shear zone boundaries (Fig. 4.7C). It should be noted that the fold axes are also parallel to the shear zone's B-axis. The deposit-scale axes cannot be entirely constrained at the Ferderber deposit: the intermediate axis (Y) parallels the shear zone's B-axis, and the shortening (Z) and elongation (X) lie on a plane perpendicular to Y, but their plunges are not constrained.

Star Lake deposit

The Star Lake deposit in the La Ronge belt, Saskatchewan (Fig. 2.5), occurs in one of several shear zones which transects a zoned granitoid pluton. The mineralized shear zone is oriented at 240-85; it has been traced for a distance of 1 km and consists of several anastomosing splays and branches reaching thicknesses of 30 m (Fig. 4.8a). The shear zone rocks consist of protomylonites and mylonites derived from the host granite (Poulsen et al., 1986). The mylonitic foliation is oblique to the shear zone boundaries, with a more northerly strike and a shallower dip than the shear zone and it contains a prominent mineral lineation plunging at

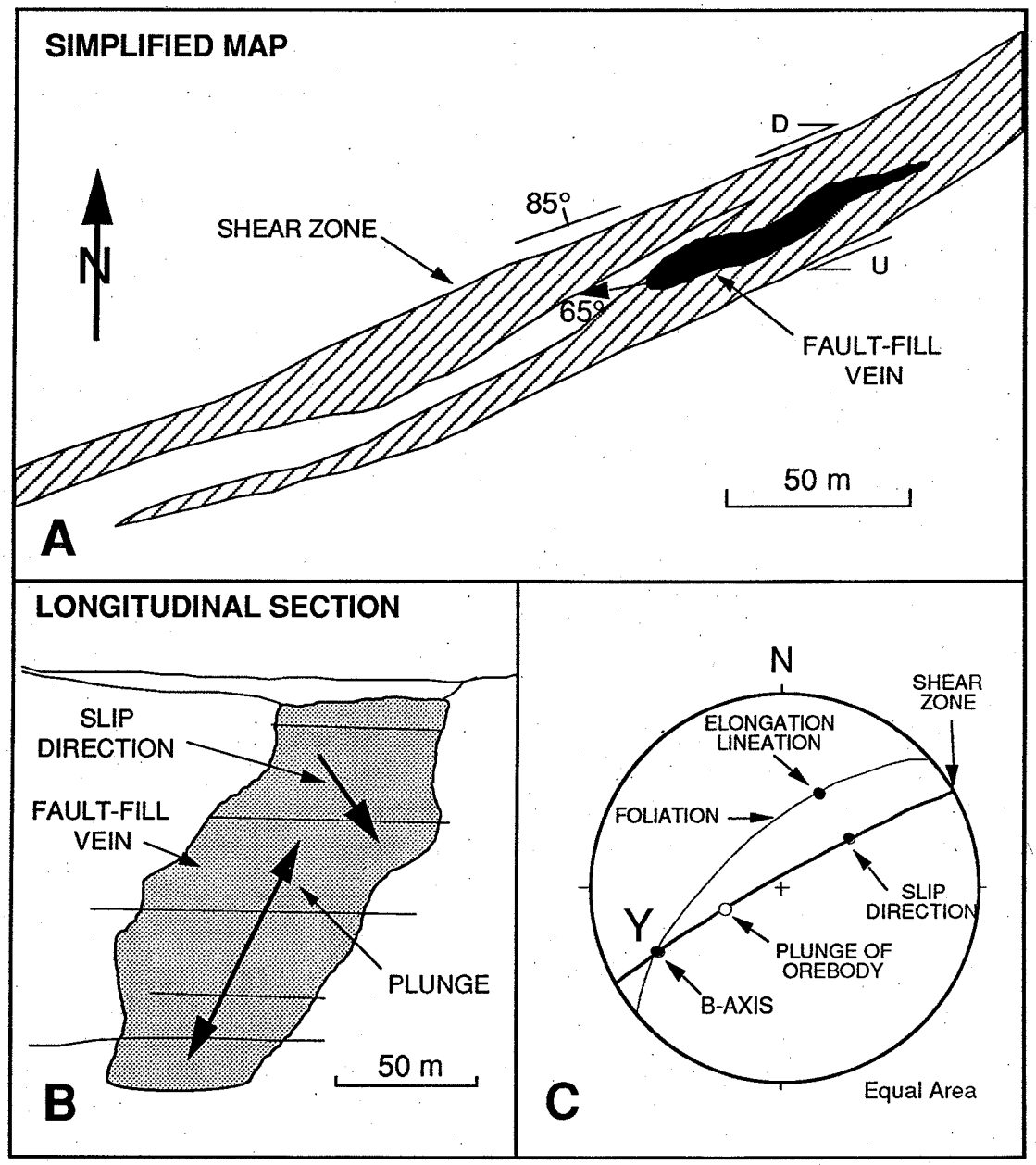

Figure 4.8. The Star Lake deposit, La Ronge district. (**A**) Simplified geologic map of the mineralized shear zone, showing the surface projection and plunge of the # 21 mineralized vein. (**B**) Longitudinal section looking northwest showing the plunge of the # 21 vein. (**C**) Stereographic projection of the structural elements of the deposit.

55° to the northeast (Fig. 4.8C). The obliquity of the mylonitic foliation to the boundaries and dragging of the regional metamorphic foliation indicate oblique-normal displacement with a dextral horizontal component. A superimposed extensional crenulation cleavage, at low angle to the mylonitic foliation, is compatible with this kinematic interpretation (Poulsen et al., 1986).

The #21 zone Star Lake consists of a fault-fill vein in the central portion of the shear zone, slightly discordant to the mylonitic foliation. This quartz vein plunges at 65° to the southwest and has dimensions of ~300 m down its plunge and 60 m across the plunge (Fig. 4.8B). As for the Ferderber deposit, only the Y axis of the deposit-scale strain can be determined. In this case, the plunge of the orebody lies at an angle of ~30° to the shear zone's B-axis and bear no geometric relationships to the shear zone (Fig. 4.8C). At Star Lake, there is evidence of overprinting of mineralization by static metamorphism, as indicated by recrystallization of the mylonites and quartz veins, and of further reactivation of the shear zone producing mylonitic quartz. The observed angle between the shear zone's B-axis and the plunge of the orebody could be explained in part by an overall reorientation of the orebody during reactivation of the shear zone.

Sigma-Lamaque deposit

The Sigma-Lamaque deposit at Val d'Or (Fig. 2.2), taken here to include the Lamaque Main and #2 mines, occupies an area of approximately 2.5 km by 1.5 km and extends to a depth of about 2 km (Figs. 4.9 and 4.10A.). It is centered on an area of abundant intermediate to felsic intrusions including, from the oldest to the youngest): an irregular body of synvolcanic porphyritic diorite, a swarm of easterly striking feldspar porphyry dykes of dioritic composition, and cylindrical plugs of diorite-tonalite. Mineralized structures include fault-fill veins in third-order shear zones, striking mostly east-west with steep to moderate dips to the south and locally to the north, and areas of laterally extensive sub-horizontal extensional veins which dip 10-15° to the west. The network also comprizes subvertical second-order shear zones, which are only locally mineralized, and one of which bound the deposit on its northern side (Fig. 4.9).

All documented third order shear zones are reverse to reverse-oblique and can be traced for distances up to several hundred metres horizontally and vertically (Figs. 4.9 and 4.10). Fault-fill veins within these shear zones reach a few metres in thicknesses and extend laterally for distances up to 100 m. They also record reverse to reverse-oblique movements (Robert and Brown, 1986a). Sub-horizontal extensional veins range in thickness from a few centimetres to 1 m, and are laterally continuous (in an E-W direction) for distances in excess of 100 m (Fig. 4.10B). In N-S section, these veins are typically bounded by mineralized shear zones or by feldspar porphyry dykes. The opening vector of extensional veins is

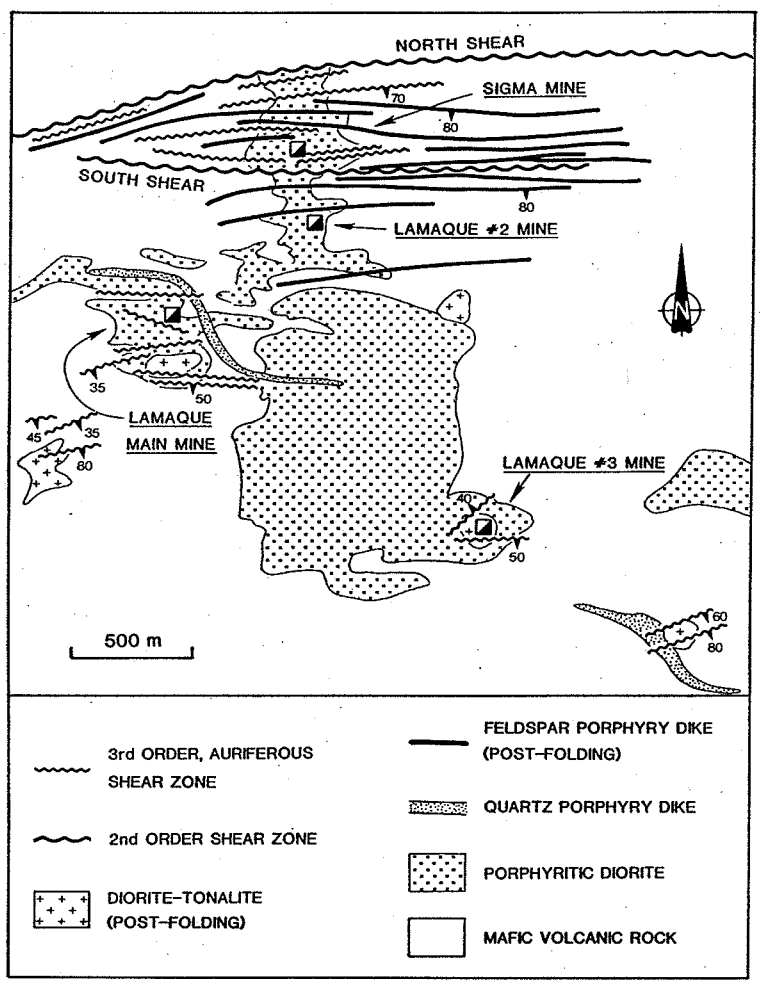

Figure 4.9. Simplified geologic map in the vicinity of the Sigma-Lamaque deposit showing the location of the most significant mineralized shear zones; modified from Sauvé et al. (1993).

typically subvertical, orthogonal to the vein walls. Conflicting cross-cutting relationships have been documented among these different sets of mineralized structures (Robert and Brown, 1986a), which indicate their overall contemporaneity. It is interesting to note that at the Lamaque main mine, as shown in the cross-section of Figure 4.10B, sub-horizontal extensional veins occur near the terminations of mineralized third-order reverse shear zones, as was discussed in Chapter 3, and illustrated in Figure 3.22.

There are significant variations in relative abundance of fault-fill veins and extensional veins from one part of the system to the other. For example, the Sigma mine combines cobines two sets of fault-fill veins and sub-horizontal extensional

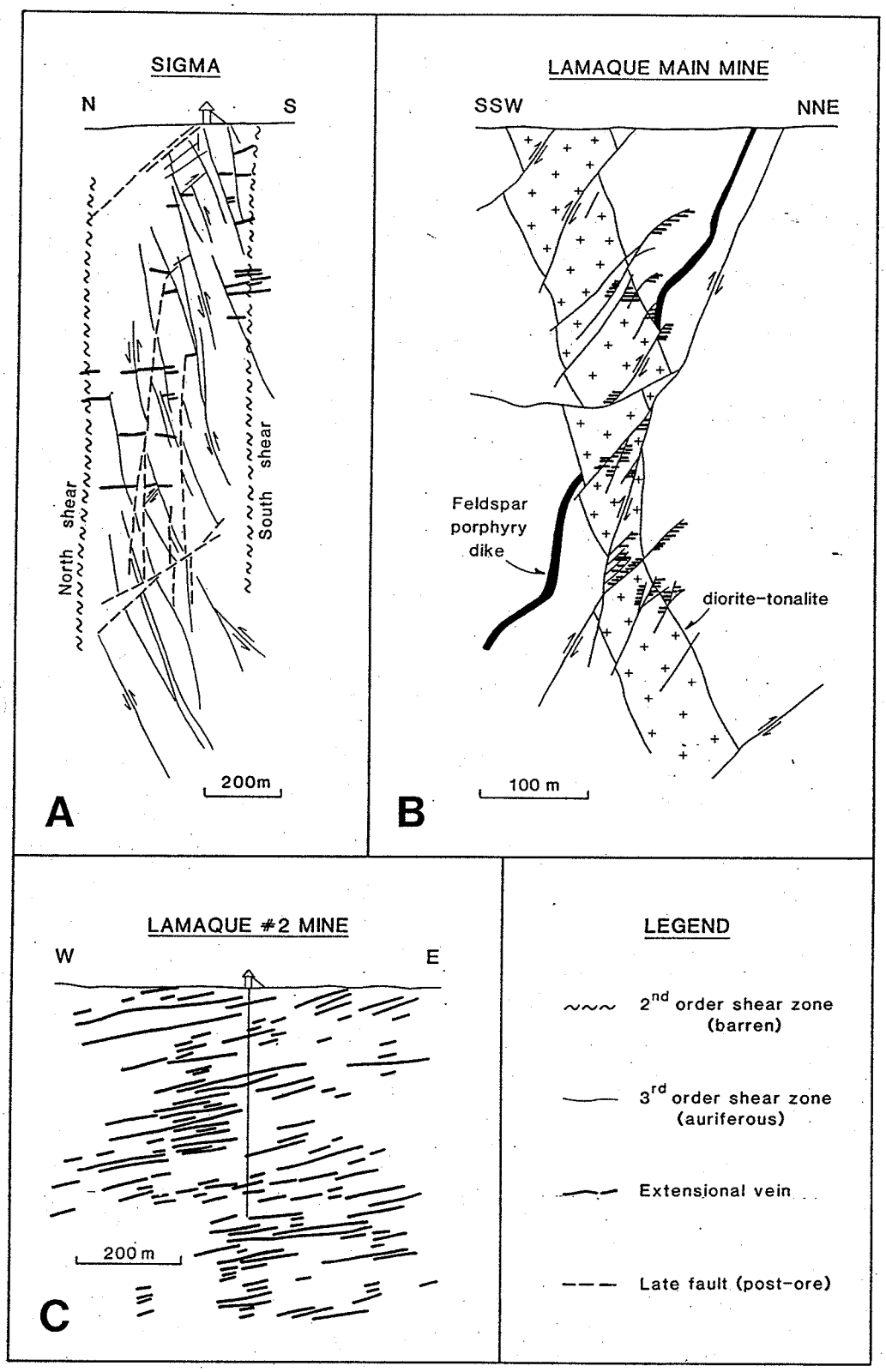

Figure 4.10. Representative cross-sections through portions of the Sigma-Lamaque deposit; see Figure 4.9 for the location of the sections. (**A**) Cross section looking east through the Sigma mine; modified from Robert and Brown, 1986a). (**B**) cross-section looking west through the Lamaque main mine; modified from Wilson (1948). (**C**) Cross-section looking north through the Lamaque #2 mine; from Bédard (1979).

veins (Fig. 4.10A), whereas the Lamaque #2 mine consists mainly of such extensional veins (Fig. 4.10C). The Lamaque Main mine is centered on a zoned diorite-granodiorite cylindrical intrusion plunging at 70° to the north-northeast, down to a depth of at least 1.5 km (Fig. 4.10B). Such variations in relative proportions of the two types of veins in part reflects the distribution of lithologies: extensional veins are more abundant in the within competent intrusions and in areas where such intrusions are volumetrically important. This large deposit illustrates the important point that some clusters of veins that appear to be isolated and to form a deposit by themselves should rather be viewed as part of a larger interconnected network.

The deposit-scale strain axes of this large network have been determined from the Sigma mine, where the best set of data is available. Two sets of reverse-oblique fault-fill veins and shear zones are oriented at 090-72° and 270-60° and both have slip directions raking ~60-65° to the east. Extensional veins are oriented on average at 180-14°. As shown in Figure 4.11, all vein sets at Sigma intersect approximately about a single axis perpendicular to the slip direction along the two shear zone sets, which can therefore interpreted as conjugates. This line of intersection corresponds to the B-axis of the two shear zone sets and represents the Y axis of the deposit-scale strain. The elongation axis corresponds to the pole of the extensional veins and plunges steeply to the east.

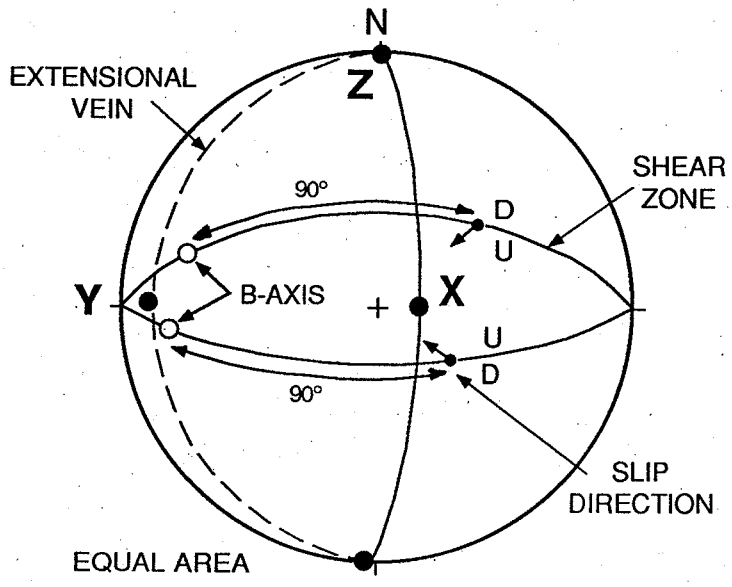

Figure 4.11. Stereographic projection of the structural elements of the Sigma deposit and the interpreted deposit-scale strain axes.

High grade gold oreshoots at Sigma occur at the intersection of horizontal extensional veins with fault-fill veins and second-order shear zones, in particular with the north shear (Fig. 4.10A). Such oreshoots plunge shallowly to the west, parallel to the line of intersection of extensional veins with other mineralized structures, parallel to the B-axis of the shear zones and to the Y axis of the network (Fig. 4.11).

CHAPTER 5:
THE INFLUENCE OF STRENGTH ANISOTROPY

INTRODUCTION

The structural characteristics and geometry of shear zone and vein networks presented in the previous chapter are those related to relatively simple cases where bulk strain is two dimensional and can be readily explained by theoretical concepts such as conjugate-type of shear zones and faults (Anderson, 1951). In such cases, the lode gold deposits are characterized by a relatively simple geometry that can be predicted by regional and local strain analyses. However, it is common in nature to find deposits made of complex shear zone and vein geometries which cannot be explained by simple two dimensional analysis and which depart from patterns and orientations predicted from regional stress axes. Strength anisotropy is one of the main factors responsible for such departures and structural complexities. Two types of deviations are induced by strength anisotropy: local two- or three-dimensional refraction of stress axes and variations in the type of bulk strain.

Strength anisotropy is clearly an important factor in the study of gold deposit. In this chapter, theoretical aspects of strength anisotropy and its influence are first considered. Then, two common geological situations were strength anisotropy is important are examined through the use of several examples. Techniques for approaching and analysing such complex structural situations are also discussed. It should be noted that the discussion of strength anisotropy as treated here only applies to the case of syntectonic development of veins and related structures as opposed to cases where overprinting deformation of deposits has taken place.

COMPETENCE AND ANISOTROPY

Definition

Rocks with identical mechanical properties in all direction are mechanically isotropic and the fracture criterion is the same regardless of the orientation of the principal stresses in the rock (Twiss and Moores, 1992). For example, massive limestones and plutonic rocks are often homogeneous and isotropic. However, in nature most rocks are anisotropic, either due to presence of bedding planes in sediments, foliations, magmatic or metamorphic layering, or, at larger scale, due to intercalation of contrasting rock types (felsic volcanic vs mafic volcanic, volcanic vs plutonic rocks, homogeneous granitoid cut by dikes or sills of different bulk

composition).

Table 1 presents a classification of relative competence for low grade metamorphic rocks (greenschist to lower amphibolite) such as those commonly encountered in lode gold deposits. At higher metamorphic conditions, the mineralogical transformation will influence the ductility and modify this classification (Ramsay, 1983). Competence contrasts induce anisotropy, which is defined as a variation in strength or physical properties of rocks in different directions (Ramsay and Huber, 1987).

Table 5.1. Classification of relative competence of low grade metamorphic rocks (greenschist to lower amphibolite), from most competent to least competent rocks; from Ramsay (1983).

Sedimentary rocks	
1- Dolomite	2- Arkose
3- Quartzsandstone	4- Greywacke
5- Coarse-grained limestone	6- Fine-grained limestone
7- Siltsone	8- Marl
9- Shale	10- Halite, anhydrite
Crystalline and metamorphic rocks	
1- Metabasic rocks	
2- Coarse-grained granite and granitic gneiss	
3- Fine-grained granite and granitic gneiss	
4- Banded quartz, two feldspar mica gneiss	
5- Quartzite	
6- Marble	
7- Mica schist	

Theoretical considerations

A simplified representation of the influence of strength anisotropy is illustrated in Figure 5.1 for the two dimensional case of a single oblique layer in an otherwise isotropic host rock. Where the layer is much more competent than its host, most of the strain will be taken up by the host rock, and it is expected that the layer will be submitted to an extension (or shortening) parallel to its length and will be decoupled from its hosts (Fig. 5.1A). In this case, shear zones of the sense indicated will develop in the host rocks along its contact with the layer. In the intermediate cases where there is less contrast between the layer and its host, the interface becomes the locus of deformation and the strain will be better develop in the weaker unit (Fig. 5.1B). However, where the layer is much weaker than its host,

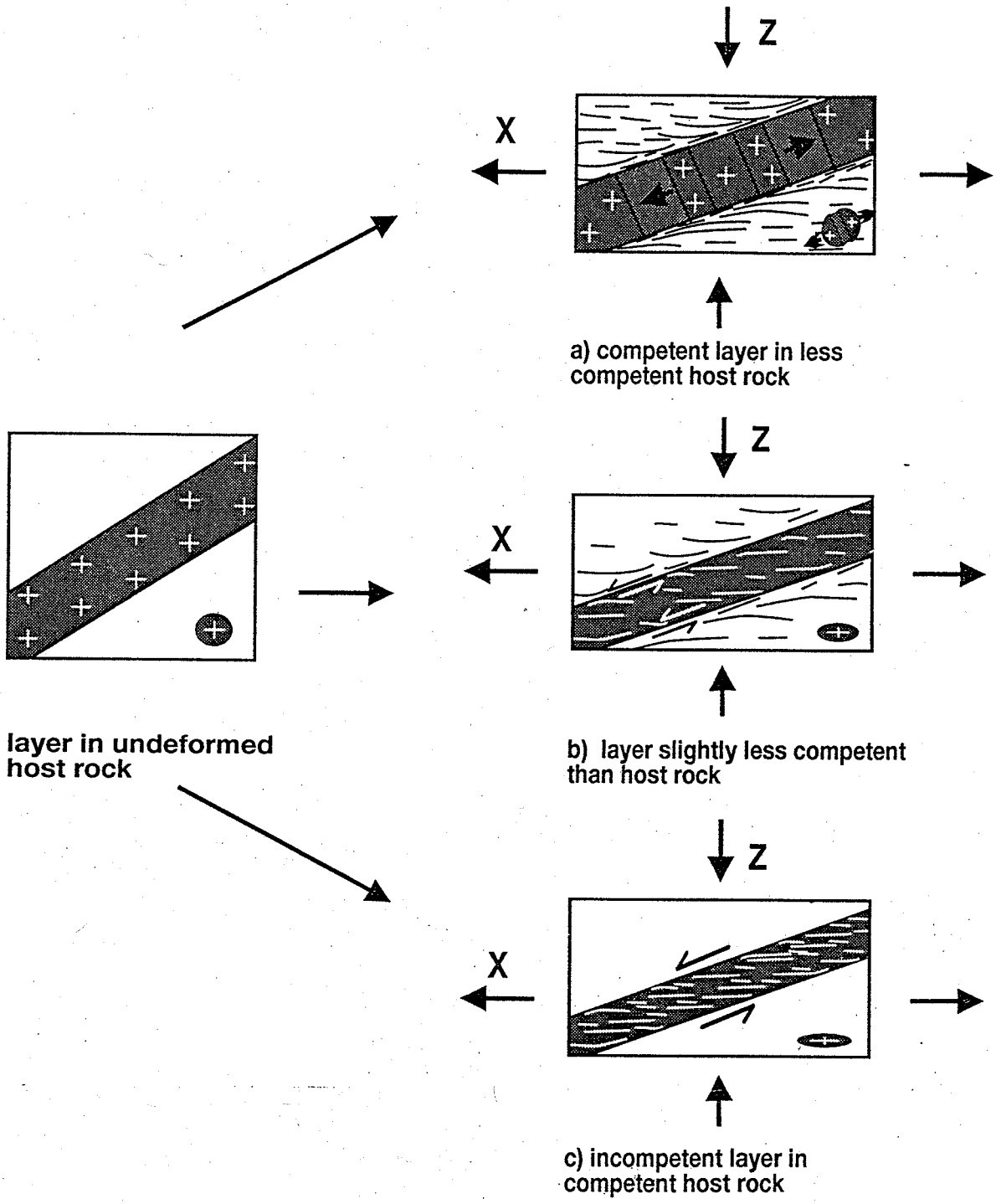

Figure 5.1. Schematic diagram illustrating the effects of layer anisotropy in a medium undergoing bulk strain; the far-field or external strain axes are parallel to the edges of the rectangles. Single layers and initially spherical inclusions are: (**A**) more competent than host rock, (**B**) slightly less competent than host rocks, and (**C**) significantly less competent than host rock. Modified from Poulsen and Robert (1989).

strain will be localized within the layer; as a result, the layer will effectively become a shear zone (Fig. 5.1C). Field examples corresponding to these different anisotropic effects are shown in Figures 3.15B and 5.2.

Two geological situations where competence contrasts or strength anisotropy is particularly relevant to gold deposits are also illustrated in Figure 5.1. The first corresponds to the case where mineralized veins and shear zones occupy a specific competent lithological unit (Fig. 5.1A) such as gabbroic sills. The other corresponds to the case where mineralized veins and shear zones are spatially controlled by the presence of incompetent layers within competent host rocks, such as mafic dikes within isotropic competent granitoid bodies (Fig. 5.1C). These two particular settings of gold mineralization represent two end-member types of influence of strength anisotropy:

1- that of stiff layers within incompetent material

2- that of planes of weakness or of incompetent layers within competent units.

These two end-members also correspond to different scales of strength anisotropy-induced deviation. In the first case, the entire layer (sill) is the deforming body and the type of bulk strain within it may differ from that in adjacent rocks. In the second case, the deviation occur locally along 'small-scale' incompetent layers which localize the deformation and become activated as shear zones, whereas the entire host body remains little deformed and passive.

It has long been recognized that rock anisotropy strongly influences the deformation and fracture patterns and leads to complexities not observed in isotropic rocks (Wallace, 1951; Ramberg, 1959, 1960; Donath, 1961, 1962; Cobbold, 1976; Treagus, 1981, 1983, 1988; Dubé et al., 1989; Lisle, 1989; Treagus and Sokoutis, 1992). In anisotropic sequences, the deformation is inhomogeneous and strong variations in orientation, size and shape of the finite strain ellipsoids may result (Treagus, 1981). One important consequence is that stresses and incremental strains need not be coaxial (Cobbold, 1976).

In this chapter, we will mainly consider strength anisotropy induced by competence contrasts. In the context of gold deposits, such strength anisotropy has at least two significant effects: it localizes the deformation and it induces deviation of the strain axes and variation of their relative length due to strain refraction. At least three parameters directly influence strain refraction: the competence contrast between the units, the orientation of the layers with respect to the stress axes, and the type of bulk strain and its intensity.

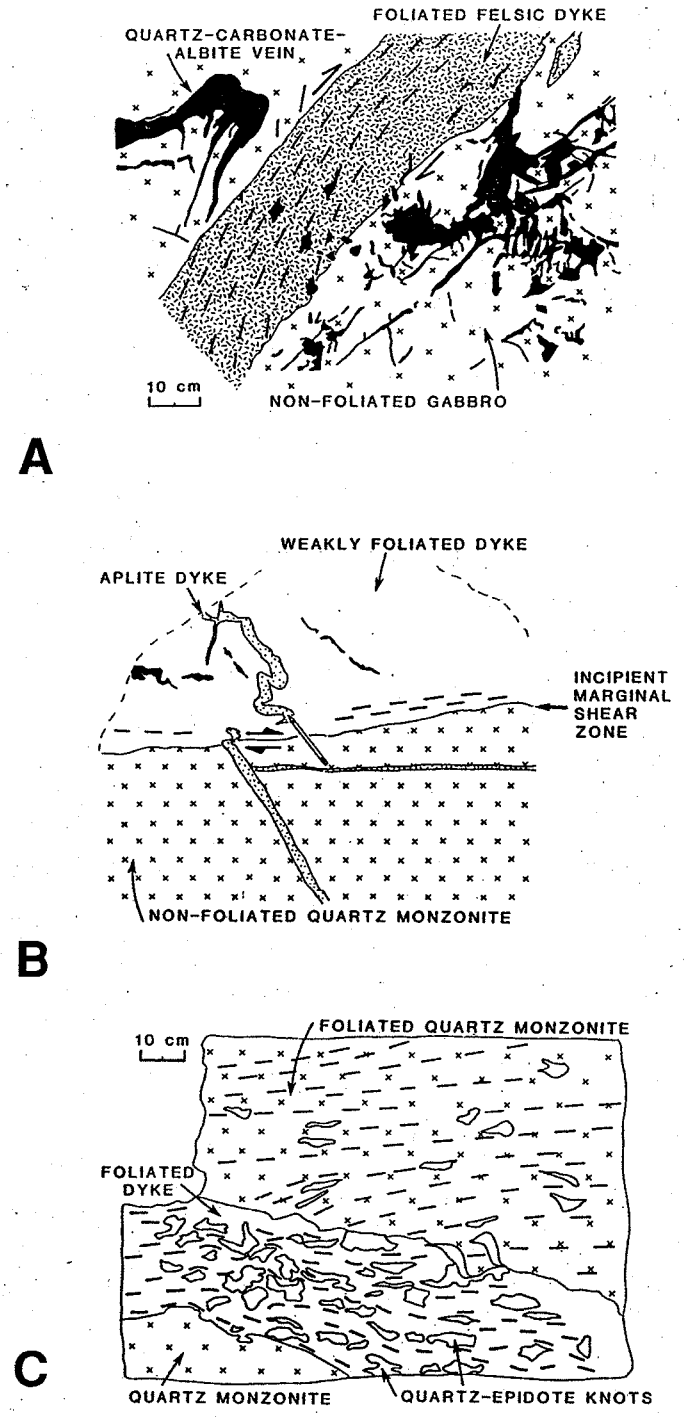

Figure 5.2. Field examples illustrating the effects of layer anisotropy. (**A**) Intensely foliated and altered felsic dyke in competent gabbroic matrix; San Antonio deposit, Rice Lake. Note the angular relationship between the foliation within the dyke and the wall of the dyke indicating the sense of motion. (**B**) Incipient shear zone developed at the margin of a dyke slightly less competent than the adjacent quartz monzonite; Star Lake deposit, La Ronge. (**C**) Shear zone developed on both dike and quartz monzonite of similar competence; Star Lake deposit, La Ronge. From Poulsen and Robert (1989).

Strain refraction

If two rocks are submitted to an identical stress field, the most competent one will develop less total amount of finite strain than the incompetent rock, and planar structures such as cleavage, schistosity and extensional veins will refract from one layer to the next relative to their competence (Ramsay, 1983). This phenomenon is illustrated in Figure 5.3, where extensional veins are refracted across the contact between a felsic dyke and slates.

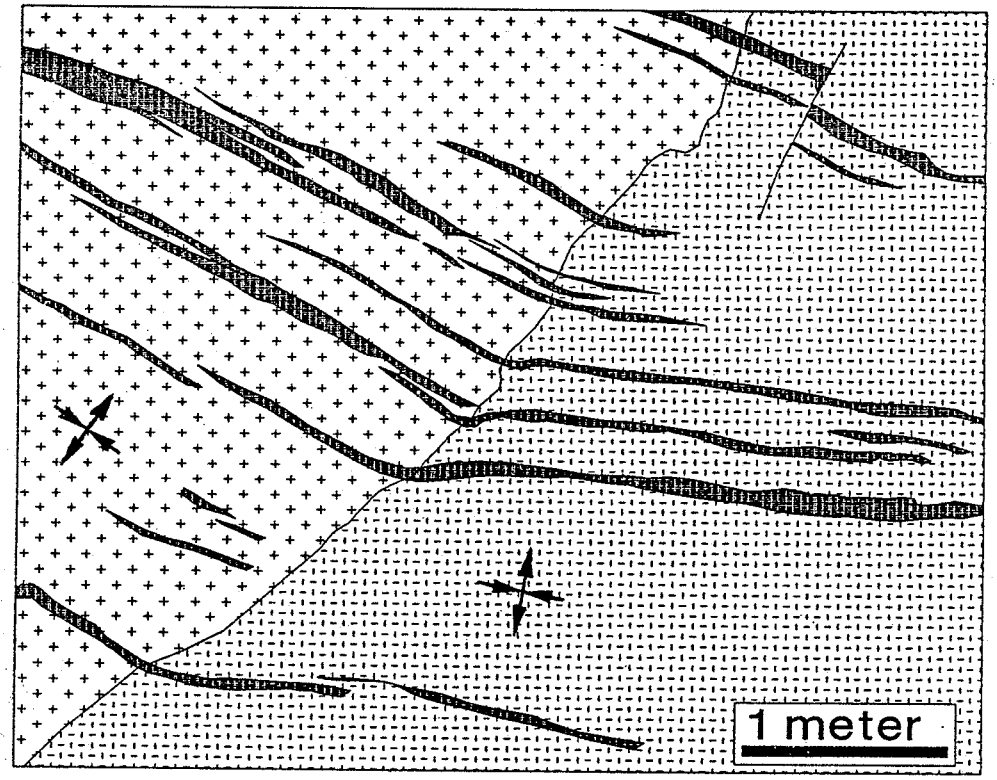

Figure 5.3. Cross-section of extensional veins (black) refracted across the contact between a felsic dyke (left) and laminated chert with magnetite layers (right); Victory mine, Western Australia. As indicated by the arrows, the elongation direction, which would corresponds to the trace of the foliation, is refracted within the dyke towards parallelism with its walls, indicating that the dyke is less competent than the host sedimentary rocks.

According to Treagus (1988), strain refraction implies changes of homogeneous strain across layer competence contrasts inducing variation in strain ellipsoids from layer to layer in sequences of varied lithology. Variations will be in strain intensity and shape (variations from prolate to oblate strain for example). Treagus (1983, 1988) presented an elegant and simple model of strain refraction in which the finite-strain refraction can be decomposed in two components acting

contemporaneously: (1) a homogeneous layer-orthogonal pure shear strain that affects the whole multilayered sequence equally, and (2) a heterogeneous layer-parallel simple shear component. All layers show the same sense of shear, but the amount of layer-parallel shear strain is inversely proportional to competence. These two components are illustrated for a two-dimensional model on Figure 5.4, which clearly shows that the strain refraction is induced by the simple-shear component. As shown by Treagus (1983), homogeneous strain in anisotropic material should only exist if the principal strain axes are layer-parallel and layer-orthogonal. In such a cases, there will be no strain refraction because no component of layer-parallel shear developed (Treagus, 1988). In all other cases of layering oblique to regional strain axes, principal strain axes will refract from layer to layer, and their magnitudes vary sympathetically (Fig. 5.4).

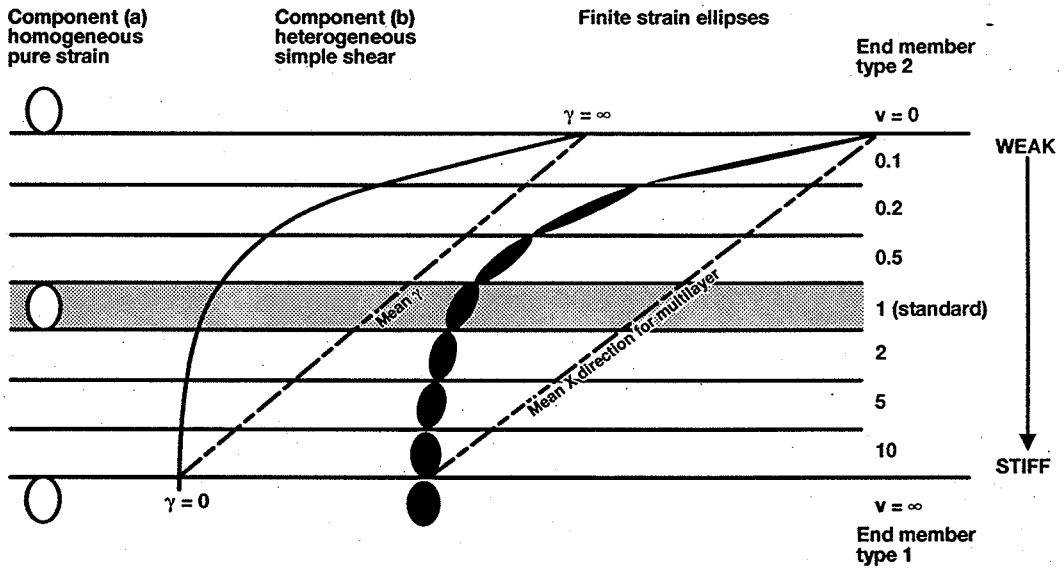

Figure 5.4. 2D model of strain refraction showing the layer-orthogonal pure shear (white ellipses) and layer-parallel simple shear components of finite strain. Variations in intensity and orientation of finite strain (black ellipses) results from variations in the amount of layer-parallel simple shear, which is inversely proportional to the competence contrasts (expressed here as viscosity ratios) across a set of layers; the reference layer with viscosity ratio of 1 is shaded. Note that the standard layer (V = 1) does not represent the average strain for this system. From Treagus (1988).

Thus, strain refraction represents local deviations of the orientation and length of finite strain axes from their more regional or mean orientations (Fig. 5.4). These regional, or external, finite strain axes provide a framework for discussion of strain refraction.

The San Antonio deposit in the Rice Lake district (Fig. 2.4) is a good example where various orientations of planar and linear structures developed during a progressive deformational event. At San Antonio, a moderately-dipping layered gabbroic sill hosts a complex network of veins, shear zones and faults that are restricted to this competent unit (Fig. 5.5; Lau, 1988; Poulsen and Robert, 1989). The competence contrasts between the competent sill and the incompetent host volcanic sandstone resulted in the development of zones of sericite schist, tens of metres thick, in both the footwall and hangingwall of the sill and sub-parallel to the its walls. These zones of sericite schist represent shear zones localized at the sill margins (Poulsen et al., 1986), a case analogous to that shown in Figure 5.1A. The fracture and vein pattern at within the sill at the San Antonio deposit is complex and consists of five major fracture sets filled with dikes or veins showing consistent cross-cutting relationships (Lau, 1988) As shown in Figure 5.5, the five sets of structures are, from oldest to youngest: (1) E-W dikes dipping ~65°N, (2) NW-SE stockwork zones dipping ~80°NE , (3) ENE-WSW shear zone-hosted fault-fill veins of the "16-type" dipping ~70°NW, (4) NE-SW shear zone-hosted fault-fill veins dipping 70° SE, and (5) NW-SE vein-filled fractures dipping 75°SW.

Lau (1988) demonstrated that although, the mineralized structures are of different ages and the slip histories of individual shear zones are complex, the differences in the rheological behaviour between the stiff sill and incompetent hosts best accounts for the complexity developed. The changes of principal stress orientation relative to the sill during the progressive fracturing history can be related to (1) a progressive rotation of the maximun principal stress axis relative to a fixed orientation of the sill and\or to (2) rigid body rotation of the sill within a ductile matrix under a fixed stress field (Brisbin and Lau, 1990).

In the case illustrated in Figure 5.1C, all the strain is accommodated within the incompetent layer, which undergoes non-coaxial deformation. As predicted by the theory, the finite extension direction and the foliation plane rotate towards parallelism with the layer with increasing strain and decreasing layer competency (Fig. 5.4). Thus in this case, anisotropy has induced development of a shear zone within the incompetent layer. Depending on its thickness, all the incompetent layer could become a shear zone, if it is narrow or, if it is wider, only the interface with the neighbors will become a shear zone. A similar situation occurs where the anisotropy corresponds to planes of weakness such as faults.

The general case of strain refraction in three dimensions (i.e. cases in which none of the principal external strain axes are contained in the plane of layering) involves refraction of all three finite strain axes and associated changes. The deviations from the external strain axes are difficult to predict because theoretical models and corresponding laboratory experiments are still being developed. Figure 5.6 illustrates the refraction of all three principal finite strain axes (X,Y,Z) in where the external axes are all oblique to layering. Note in particular the variation

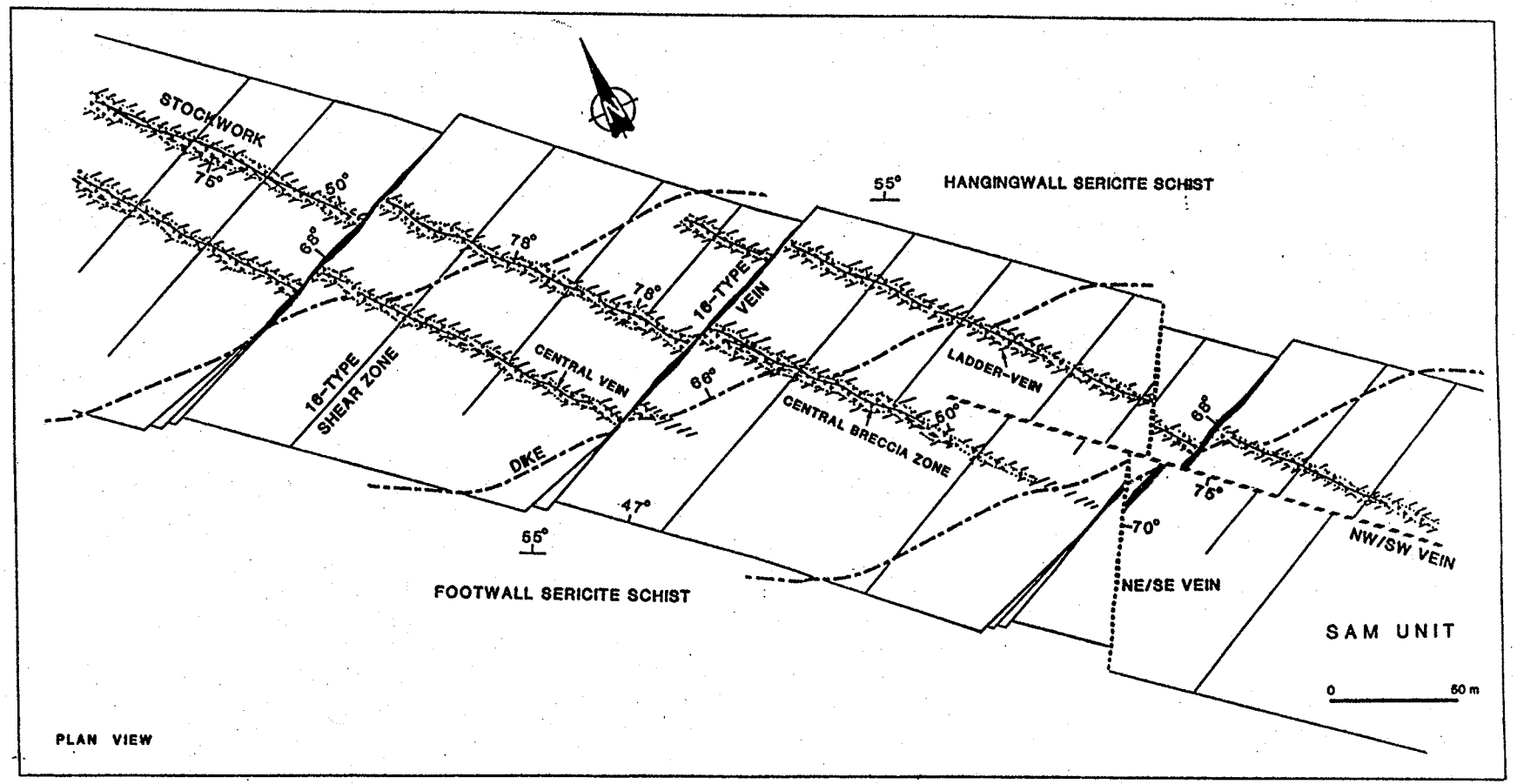

Figure 5.5. Simplified schematic plan view of the San Antonio deposit showing the gabbro sill (SAM unit), the enveloping sericite schist zones and the different sets of structures within the sill; from Lau (1988).

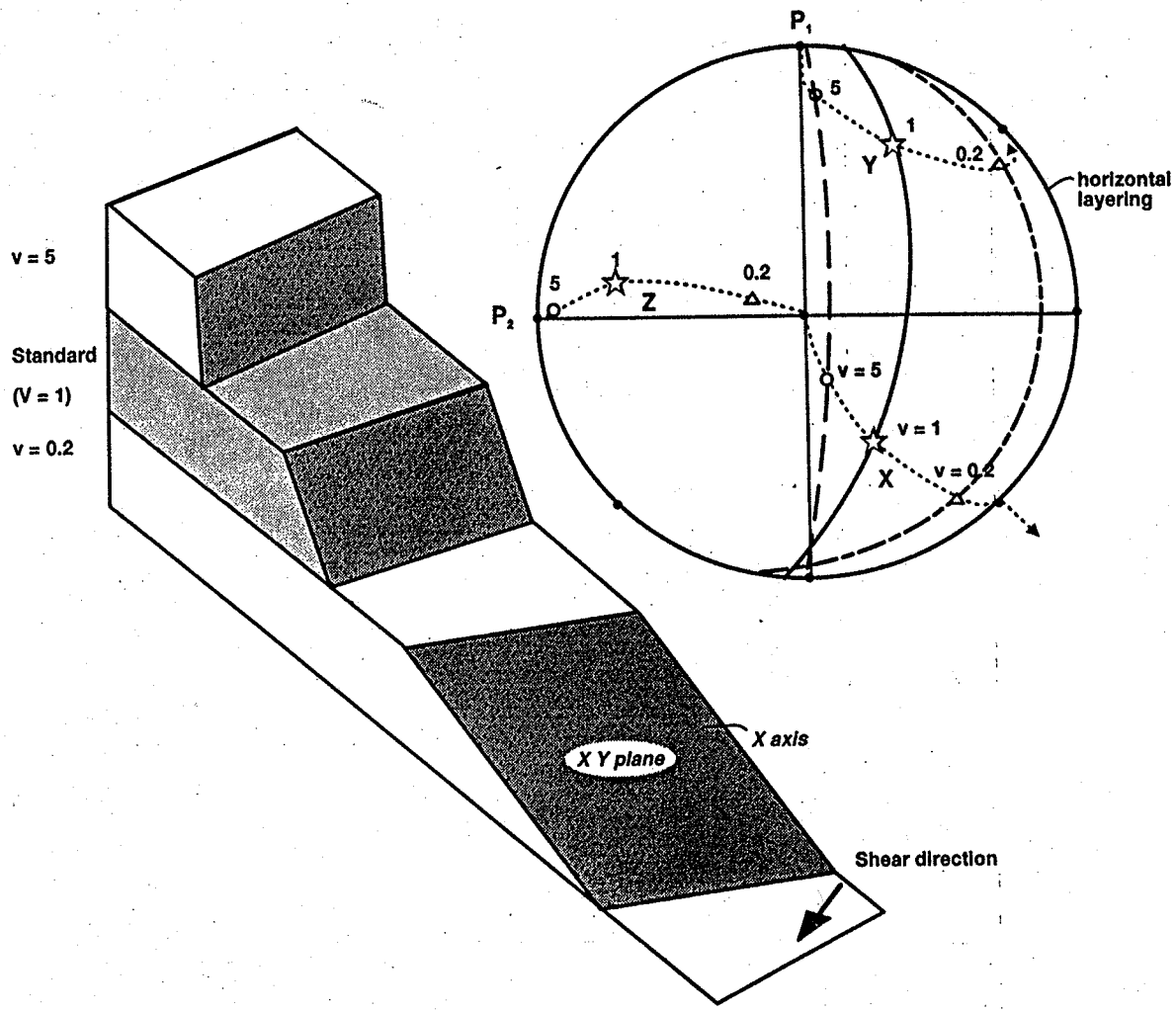

Figure 5.6. 3D strain refraction. (**A**) Variation of the orientation of all three principal finite strain axes (X,Y,Z) with competence contrasts for viscosity (V)=1 (stars), V=5 (circles) and V=0,2 (triangles) layers. End-member refractions trends illustrated by broken curves with small arrows indicating positions of X, Y and Z axes. Variation of XY plane in strike and dip shown by solid curve for V=1, broken for V=5 and dot-dash for V=0,2. Lower-hemisphere equal-area projections with layering horizontal. (**B**) Schematic 3D illustration of the strain refraction in (A). XY plane shaded with lines parallel to X for each layer. Note the increase in dip of the XY plane and plunge of the lineation (X) with the augmentation of the competence. From Treagus, 1988.

of the plunge of the X axis from shallow to steep with the increase in competence. In the context of gold mineralization, such refraction would strongly influence the orientation of extensional veins within the layers which could range from high to low angle to the layer. The consequence of 3D refraction will be illustrated below using the Norbeau deposit as an example.

Summary

Homogeneous strain is predictable only in homogeneous rocks or in layers submitted to an exact layer-parallel and layer-perpendicular principal strain axes; deformation involving principal external strain axes oblique to layered sequences of rocks is relatively common in nature (Treagus, 1988) in which case strain refraction will take place. With increasing amount of strain, the X-axis (elongation lineation) and X-Y plane (foliation) of the finite strain ellipsoid will become subparallel to least competent layers and sub-perpendicular to most competent layers. As a result, least competent layers or their contacts with more competent ones, effectively become shear zones, whereas most competent layers will undergo internal coaxial deformation with principal strain axes parallel and perpendicular to the layers.

Strain ellipsoids of different shape, intensity and orientation, with sometimes exchange of principal strain axes, are expected in a layered sequence of different rocks types submitted to given external stress/strain field (Fig. 5.4; Treagus, 1988). For example, oblate ellipsoids may refract to prolate ellipsoids at competence interfaces (Treagus, 1983). As many ore zones are hosted by lithologies of contrasting competence, various vein geometries and ore shoots are expected to be found in a given deposit. One can readily realize that the orientation of a cleavage and\or extension lineation in a single lithology may not indicate the bulk or regional strain axes (Treagus, 1983) and how cautious we should be when trying to define the external strain axes and use it to predict vein geometry and potential ore shoots. Competent layers will most probably exhibit bedding-symmetrical fabrics and structures characteristic of an approximate coaxial strain history, whereas incompetent layers should exhibit non-coaxial asymmetric fabrics and structures (Williams, 1979; Lister and Williams, 1983, Treagus, 1988).

STIFF LAYERS WITHIN INCOMPETENT MATRIX: THE EXAMPLE OF SILL-HOSTED GOLD DEPOSITS

Introduction

Gold deposits hosted by differentiated gabbroic sills are common world wide; some of the best known examples include the Archean lode gold deposits of the Golden

Mile in Kalgoorlie Australia (Boulter et al., 1987) and the Victory deposit in Kambalda, Australia (Clark et al., 1986, 1989), the San Antonio deposit in Manitoba, Canada (Poulsen et al., 1986; Lau, 1988), and the Norbeau deposit in Chibougamau, Canada (Dubé et al., 1989). Most of these deposits have complex vein geometries and represent good examples where anisotropy has played a key role in the development of the deposit.

In this group of gold deposits, the fracture and vein networks are typically better developed and more complex than for other deposits outside the sills but in the same districts. The complex geometry of the vein and fracture networks is also typically difficult to reconcile with the regional strain patterns. Mineralized quartz veins occur in three or more differently oriented sets, as described by Dubé et al., (1989) for the Norbeau deposit and Boulter et al., (1987) for the Golden Mile. Veins are sub-parallel to the layering within the differentiated sills but they are more frequently oblique and at high angle to the layering. In several cases, the gold-bearing veins are better developed in the quartz- or granophyric-rich upper facies of sills which could be ascribed to their greater competence relative to other facies within the sills.

Following the approach of Anderson (1951), it is common in the analysis of multiple sets of shear zones and faults to regard them as conjugate or second order shears and to consider the common line of intersection of two or more shear directions as the intermediate axis of stress as discussed in Chapter 4. This type of analysis is only valid if the line of intersection among the various sets of shear zone is perpendicular to the slip direction along each set, in other words if their B-axes are parallel (Fig. 4.2B). This condition is met in a number of cases illustrated in Chapter 4. However, in many complex networks, this condition is not met and the line (s) of intersection among the various shear zones sets is not perpendicular to their respective slip directions, as discussed by Lau (1988) for the San Antonio deposit, and as will be further illustrated below for other deposits. The Andersonian analysis is inadequate in such cases because it reduces the bulk strain analysis in two-dimensions, whereas the multiple orientations of shear zones and veins develop to accomodate three-dimensional strain (Dubé et al., 1989; Poulsen and Robert, 1989).

Such sill-hosted gold deposits offer an opportunity to study the effects of the strength anisotropy on these complex structural patterns and will also serve to illustrate methods that can be used to determine the orientations of internal strain axes from complex shear zone and vein networks. The Norbeau and Cooke gold deposits in the Chibougamau district (Fig. 2.3) are both hosted by the Bourbeau Sill, a thick gabbroic sill and will be used to illustrate these effects. The interest in comparing these two deposits lies in their contrasting geometries: complex at Norbeau and relatively simple at Cooke (Dubé et al., 1989; Dubé and Guha, 1992). Such differences will serve to illustrate the effects of the orientation of stiff layers

(the gabbro sill) relative to external strain axes. The analysis of the two deposits will be summarized followed by their comparison and by a discussion of the parametres believed to influence strain refraction in stiff layers. One important conclusion is that the development of shear zones of multiple orientations and slip directions within the sill reflect internal bulk strain different from that outside the sill.

Norbeau deposit

The Norbeau deposit consists of shear zone-hosted auriferous quartz veins within a differentiated gabbroic sill (Dubé et al., 1989). The local stratigraphic section, in which the Bourbeau sill was intruded, comprises ultramafic to mafic rocks of the Roberge and Ventures sills, followed by volcaniclastic and pyroclastic rocks of the Blondeau Formation (Fig. 5.7). This sill is a hundred metres thick and extends laterally for up to a hundred kilometres. It is differentiated and comprises, from base to top, peridotite-pyroxenite, leucogabbro, quartz ferrogabbro, and quartz granophyre ferrodiorite layers.

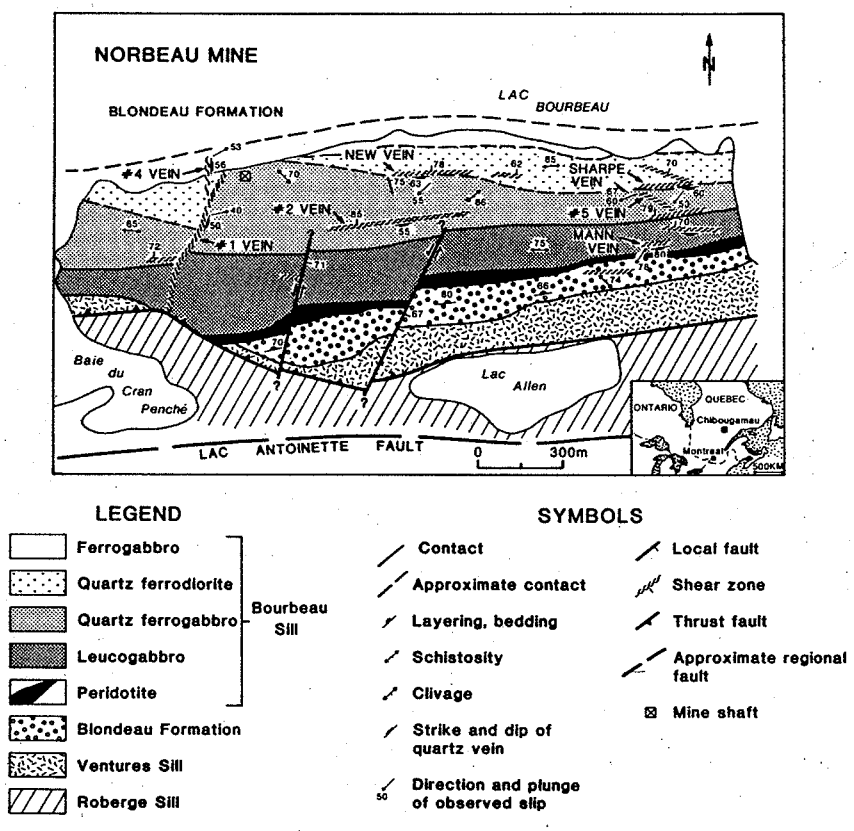

Figure 5.7. Geological setting of the Norbeau mine showing the stratigraphic units, main structures and vein distribution; from Dubé et al. (1989).

Four sets of auriferous shear zones are present: a northeast set (035°/50°), represented by vein #1, and a north-south set (000°/56°), represented by vein #4, and east-west and northwest sets (Fig. 5.7). All sets of shear zones are mineralized but the northeast and north-south sets are economically the most important.

The shear zones are defined as zones of chlorite schist, within which the foliation is oblique in dip to the shear zone boundaries, indicative of a reverse sense of motion which is compatible with downdip elongation lineations developed on foliation planes. All mineralized shear zones contain a central laminated fault-fill vein, parallel to their boundaries, as well as many extensional subhorizontal veins. The walls of the fault-fill veins are commonly marked by slickenlines subparallel to the mineral lineation in adjacent schists, leading to the interpretation that they are compatible with, and related to the same progressive deformational event.

The structural similarities between the four sets of auriferous shear zones, their common patterns of alteration and the absence of exposed clear crosscutting relationships among themselves strongly suggest that they are contemporaneous and related to the same deformation event (Dubé et al., 1989). The next step is to combine the shear zone orientation, slip direction and sense of motion and test their mechanical compatibility.

Structural analysis

Figure 5.8 shows the orientation and slip data for all shear zones at Norbeau. A large number of shear zones, including those of the east-west and northeast sets, intersect in the southeast quadrant about a common axis. However, this intersection axis does not correspond to the B-axes of the shear zones (Fig. 5.8), as should be the case if all shear zones were conjugate sets and if bulk deformation took place in two dimensions, illustrating the inadequacy of the Andersonian approach.

Several graphical and theoretical methods have been formulated for the analysis of multiple sets of faults exhibiting various orientations and kinematics. All these methods have been established for the analysis of brittle faults produced or reactivated under a single stress field. They are based on the stress-shear relationship established by Wallace (1951) and Bott (1959). They have shown that, the direction and sense of displacement on faults, whether newly created or pre-existing, are determined by their orientation and the shape of the three-dimensional stress ellipsoid. At Norbeau, the structures are not perfectly brittle faults. However, because these ductile-brittle shear zones are discrete, narrow and widely spaced structures in an otherwise weakly deformed medium, we assume that this criterion is met (Dubé et al., 1989). As well, because of the ductile components of deformation within the auriferous shear zones, it is more appropriate to treat the results in term of bulk strain (i.e. axis of extension, X, and

shortening, Z) than in terms of stress ($\sigma 1$, $\sigma 3$, etc) (Dubé et al., 1989).

These graphical methods have been described previously (Dubé et al., 1989) and their principles are only be summarized here. It should be noted that other graphical methods also exist (Lisle, 1987, 1989; Aleksandrovski, 1985) and that computer-assisted methods are now available for treatment of large data sets (Angelier, 1984; Lisle, 1988).

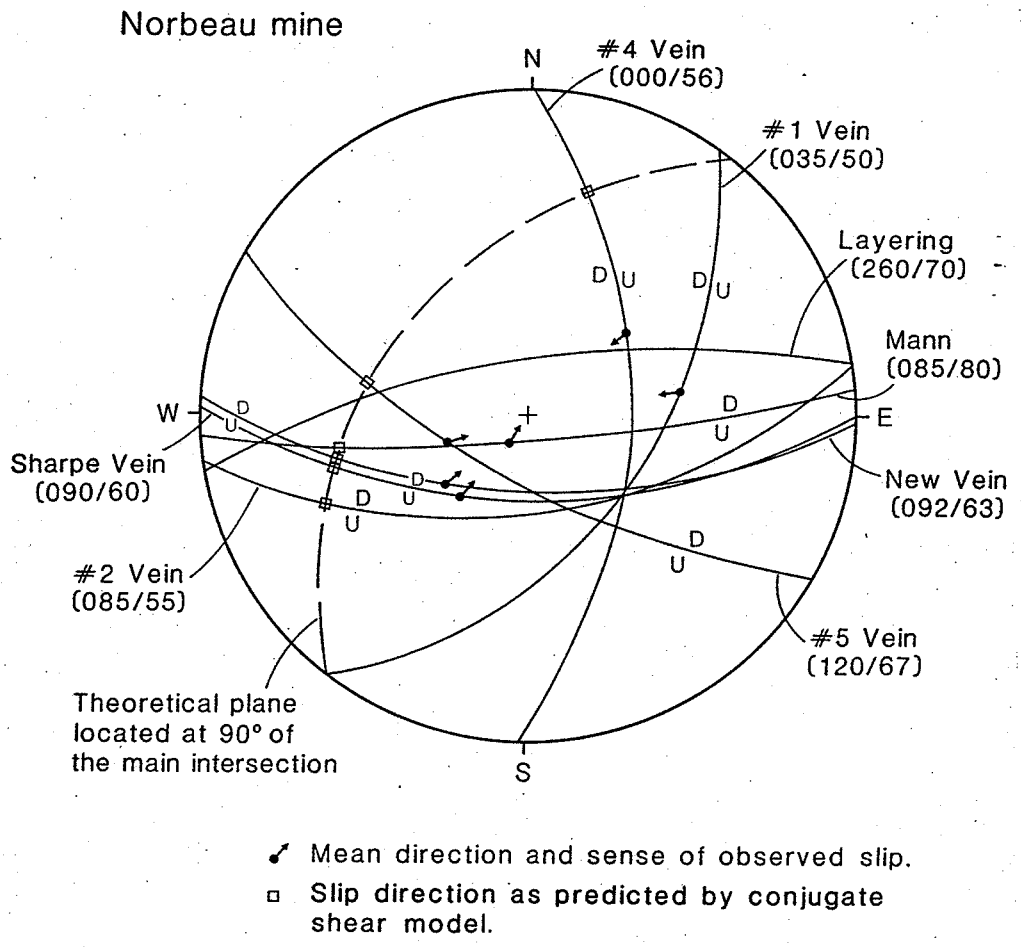

Figure 5.8. Stereographic projections of the mean orientation of the major mineralized shear zones at Norbeau. The mean observed direction and sense of slip and the theoretical slip direction for a conjugate model are also indicated. Equal angle, lower hemisphere projections. From Dubé et al. (1989).

The *method of Angelier and Mechler* (1977) is an elegant graphical method for determination of stress axes from fault-slip data. This method was subsequently modified using computer-assisted analysis for a more complete determination of paleostress axes and stress ratio (Angelier, 1984). However, Angelier and Mechler's method is presented here because it is a simple method, easy to visualize and it can be graphically done by hand. Lisle (1987, 1989) indicates how

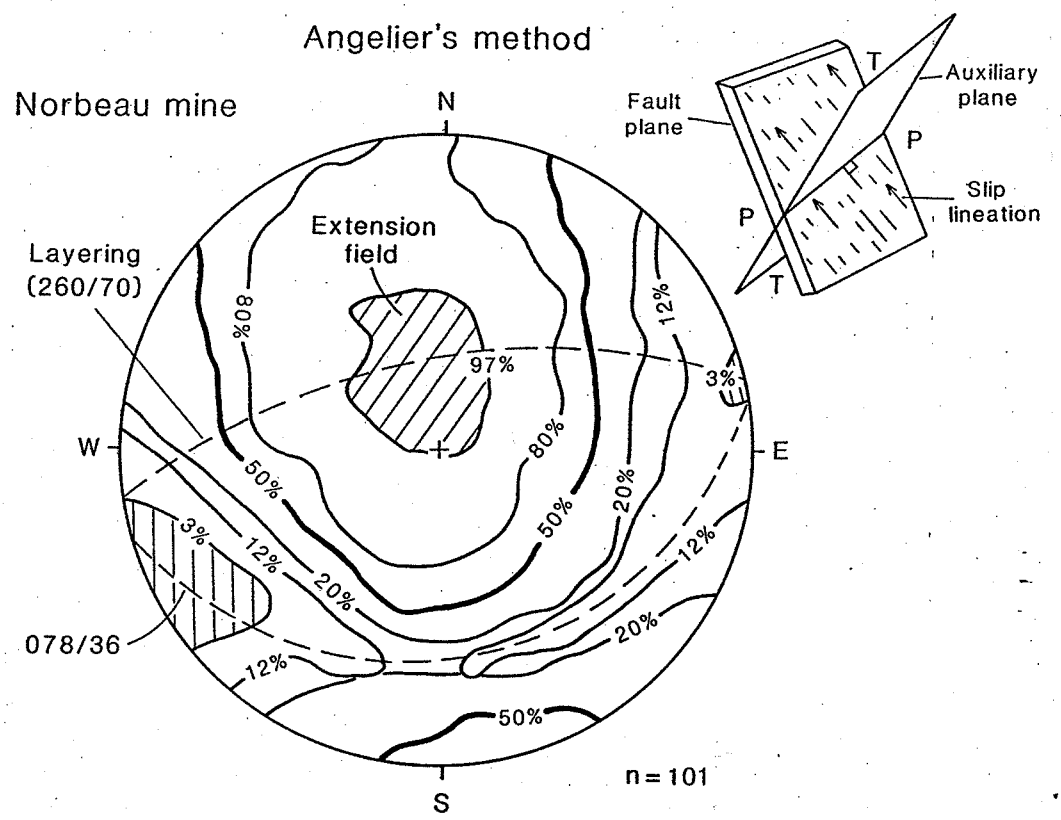

Figure 5.9. Application of Angelier's method to the Norbeau data set. Equal area, lower hemisphere projections, n = number of measurements. From Dubé et al. (1989).

this method can be refined for more efficient graphical determination of principal stress.

Angelier and Mechler's method was defined for a fault population of any kind, which were formed or reactivated under a homogeneous stress field within inhomogeneous material, and it requires knowledge of direction and sense of slip along the faults. The method is based on the principle established by Bott (1959) that slip along a given fault plane occurs along the direction of maximun shear stress. By analogy with the approach used by seismologists to analyze focal mechanisms for earthquakes, the space around the fault can be divided into four dihedras by defining a second plane, purely geometric and referred to as auxiliary plane, perpendicular to the slip direction along the fault (inset, Fig. 5.9). Thus, for a given fault, $\sigma 1$ will lie within two opposed, compressive, dihedras (P) and $\sigma 3$ will lie within the two other extensional (T) dihedras. The determination of the compressive and extensional dihedras is based on both the sense of slip along the fault plane as well as its orientation. For each field measurement of the fault plane orientation, slip direction, and shear sense, it is possible to define compressive and extensional dihedra as shown in Figure 5.9 (inset). By combining the observations

for all measured faults, areas of compression and extension common to all faults can be displayed on a stereonet (Fig. 5.9). The orientation of $\sigma 1$ and $\sigma 3$ are constrained to two corresponding fields on the stereonet which represent the intersection of all compressional and extensional dihedras respectively. In this case, high percentage contours correspond to extension and low percentages to compression. For example, for any direction located on contour 80%, 80% of the fault are in extension whereas 20% are in compression. One should keep in mind that the geometrical centres of the compressional and extensional fields thus defined do not necessarily correspond exactly to the attitude of the stress axes (Angelier and Mechler, 1977). However, if the number and the variety of orientation faults and slips directions are large enough, the correspondence will often be close (Angelier, 1984).

As shown on Figure 5.9, the Norbeau data set presents a well defined field of extension resulting from the overlap of 97% of the extensional dihedra, whereas an axis of shortening defined by the 3% contour is located on a great circle perpendicular to the extension direction. Both these axes are almost confined within the plane of the Bourbeau sill. The clear definition of the axis of extension, coupled with the poorer definition of the axis of compression, suggests a deformation which is approximately uniaxial. In such a case, the method of Arthaud (1969) is another graphical method more appropriate for cases of uniaxial deformation.

The geometric *method of Arthaud* (1969), which was later modified by Aleksandrowski (1985), was defined for a brittle deformation in anisotropic material and is based on the concept of the 'plane of movement'. This plane is defined as orthogonal to the fault plane and containing the direction of slip. The pole (B-axis) of this 'plane of movement' is the perpendicular to the slip direction in the fault plane (Fig. 5.10Ai). Contrary to Angelier's method, this method does not take into account the sense of slip. In the conjugate, or quasi-conjugate case, B-axis on each of the fault planes will tend to be parallel to their common line of intersection, whereas in the oblique slip case, the B-axis will have a different orientation on each fault plane and consequently will not parallel the intersection axis (Fig. 5.10Aii). As indicated by Carey (1979), this method is valid only for uniaxial deformation. Thus, it is well appropriate to test the results obtain at Norbeau with Angelier and Mechler's method.

The B-axes of the four sets of auriferous shear zones at Norbeau define a single great circle oriented at 078\36 (Fig. 5.10B). By definition, the pole of this great circle corresponds to a principal axis of deformation. Because all shear zones have an oblique-reverse sense of displacement, this axis must correspond to an axis of elongation. As all the B-axes fit on a single great circle, the deformation is approximately uniaxial.

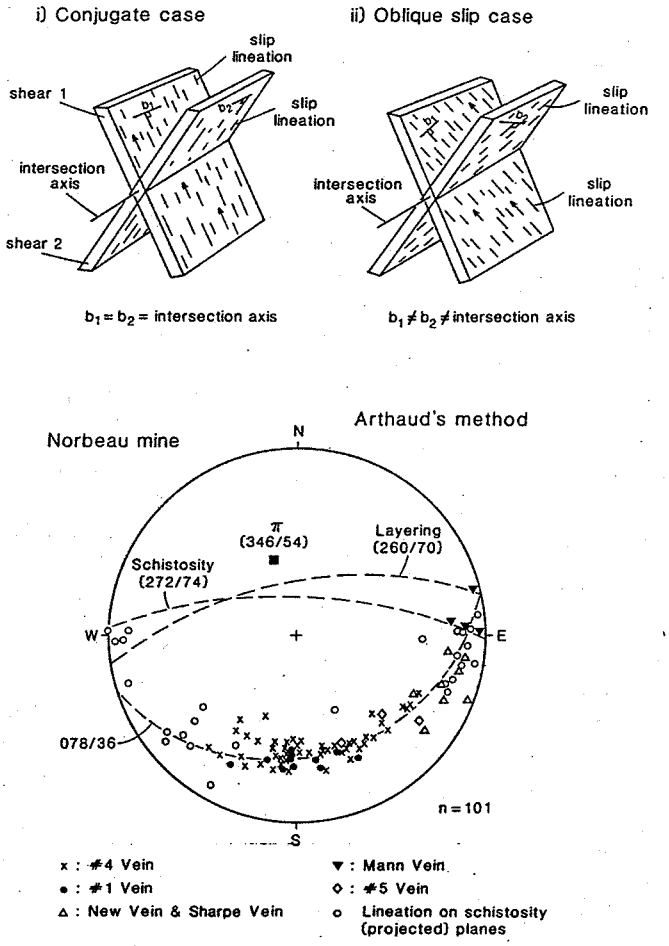

Fig. 5.10. (**A**) Schematic illustration of the B-axis concept for (i) the conjugate and (ii) the oblique slip cases. (**B**). B-axes of the different auriferous shear zones based on to Arthaud's method. The pole of the great circle defines the principal axis of extension. Equal area, lower hemisphere projections; n = number of measurements. From Dubé et al. (1989).

Results and discussion

Both methods of analysis yielded similar results: the shear zones are not compatible with a conjugate system but are rather related to a uniaxial deformation with a relatively steep deposit-scale elongation axis oriented approximatively at 346°\54 and almost contained within the plane of the Bourbeau sill (Fig. 5.9). This result is compatible with the presence of several extensional sub-horizontal veins developed adjacent to the four sets of auriferous shear zones, which also indicates a steep component of extension. The uniaxial deformation implies that the deposit-scale strain ellipsoid is approximately prolate rather than plane and explains the non-conjugate shear zone pattern within the sill. The other two deposit-scale strain axes are located on a great circle oriented at 078/36°. In the case of uniaxial bulk

strain, the maximum and intermediate bulk strain axes should not theoretically be distinguishable from one another. However, the results obtained using the method of Angelier and Mechler (1977) show a poorly-defined field of compression oriented west-southwest and sub-horizontal, and also contained within the plane of the sill (Fig. 5.9). Thus deposit-scale axes of elongation and shortening are approximately confined within the plane of the Bourbeau sill.

In the area surrounding the Norbeau deposit, rocks display penetrative foliations and elongation lineations which may be used to estimate the orientation of bulk strain axes external to the Bourbeau sill. Foliations are oriented east-west and are subvertical, and elongation lineations are essentially down-dip, i.e. sub-vertical. Thus, such fabrics suggest that the regional bulk shortening axis (Z) is N-S and sub-horizontal, whereas the regional bulk elongation axis (X) is subvertical (Fig. 5.11). This contrasts the deposit-scale elongation and shortening strain axes within the sill, which are both parallel to the sill and which have therefore been refracted.

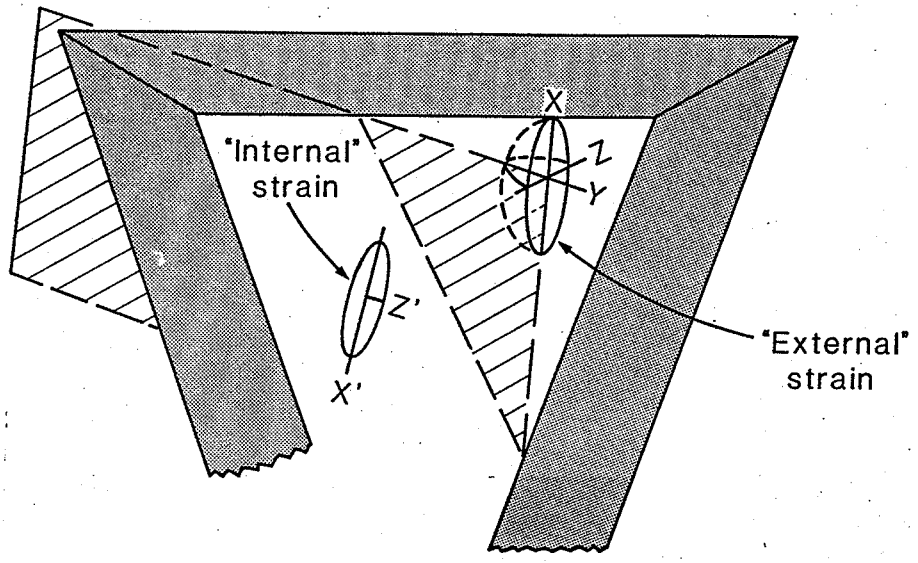

Figure 5.11. Schematic illustration of refraction of strain axes within a stiff layer (shaded) by contrast with external strain. From Dubé et al. (1989).

Thus, both the refraction of the bulk strain axes within the sill and the uniaxial down-dip stretching experienced by the sill can be ascribed to the effects of the strength anisotropy induced by the sill itself, which behaved as a stiff layer. The deposit-scale strain axes within the sill were controlled by the plane of the sill due to strain refraction along its boundaries (Fig. 5.11).

Cooke deposit

The Cooke deposit, located at 50 km SW of the Norbeau deposit, comprises Au-Cu-Ag bearing quartz-sulfide veins hosted by the Bourbeau sill, mostly within the leucogabbro and the upper quartz ferrogabbro (Fig. 5.12; Dubé et Guha, 1992). Figure 5.13 shows the distribution of the mineralized shears zones and cross-cutting faults. Overall, the mineralized shear zones are sub-parallel to the local stratigraphic units and to layering within the sill.

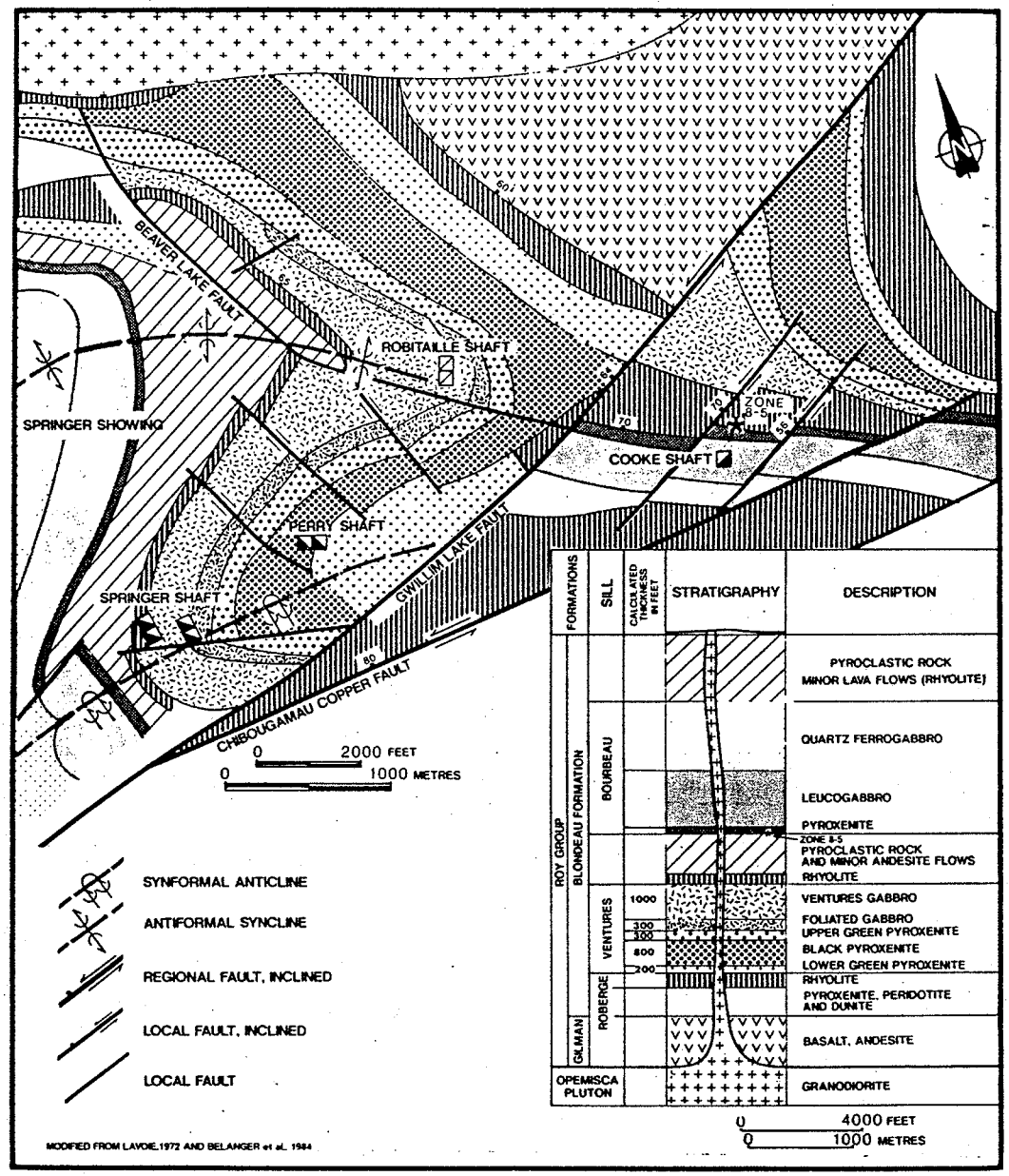

Figure 5.12. Geological setting of the Cooke mine showing the stratigraphic units and the main structures. From Dubé and Guha (1992).

There are two principal mineralized shear zones known as "veins" 7 and 9 (Fig. 5.13). They are made up of several cm- to m-wide shear zones delineated by relatively schistose rocks containing quartz-calcite veins. Ductile-brittle to brittle deformation characterizes these shear zones. Locally, the mineralized veins also occupy brittle fractures/shears sub-parallel to the overall orientation of shear zones (Dubé and Guha, 1992). The shear zones vary in strike from E-W to NW-SE and their dip is generally steep (70° to 80°) to the north (Fig. 5.13). Contacts between shears and host rocks are commonly sharp.

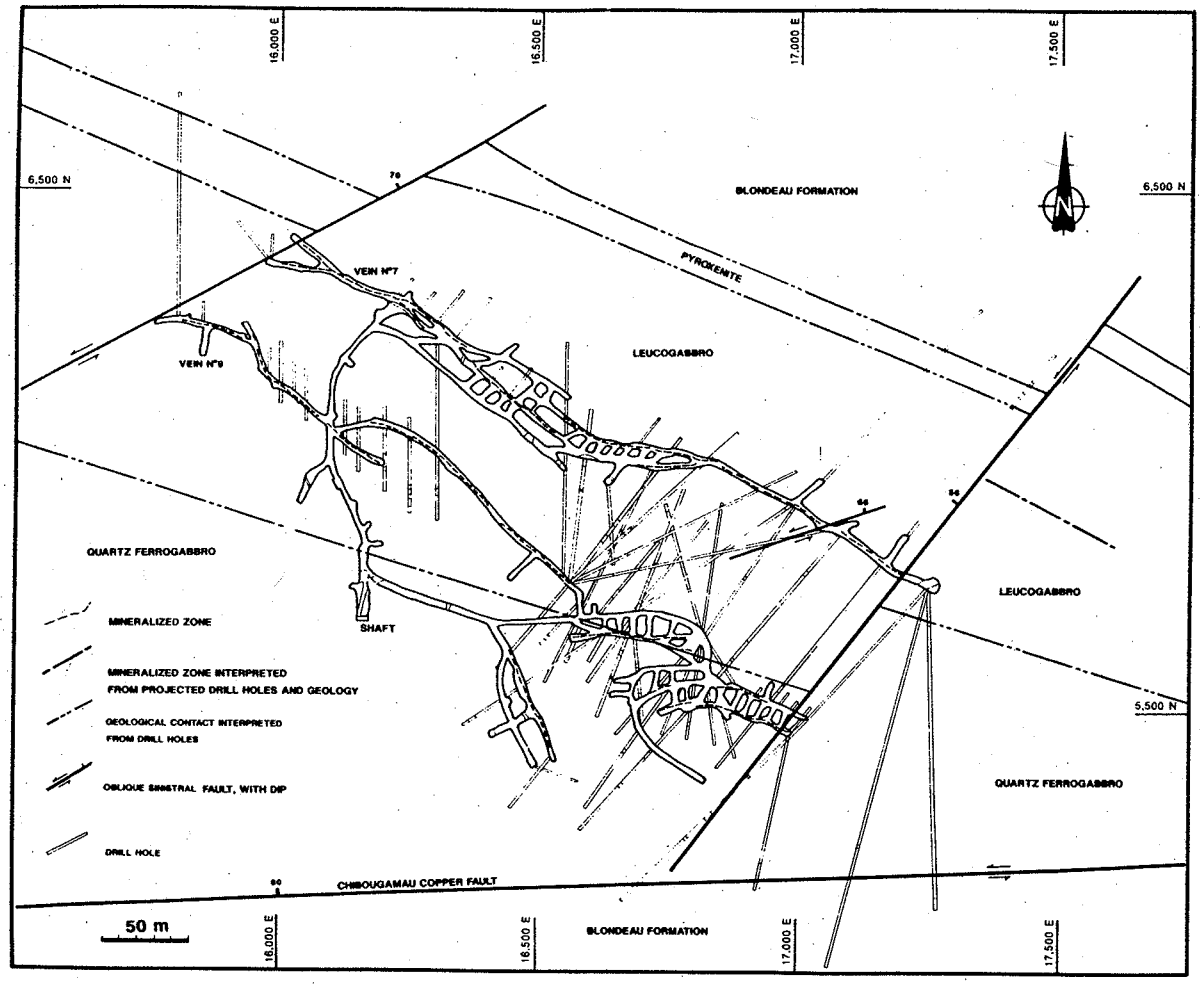

Figure 5.13. Geologic map of level 6 at the Cooke mine showing the distribution of the mineralized shear zones and the late cross-cutting north-east faults. From Dubé and Guha (1992).

Non-coaxial deformation within the shear zones is indicated by the obliquity in dip between the shear zones and the foliation developed within them. This angular

relationship, combined with the relative steep plunges of the lineations and striations present on foliation planes, demonstrate that the E-W to NW-SE shear zones are characterized by reverse-oblique movement in which the reverse vertical component is dominant over the dextral horizontal component (Dubé and Guha, 1992). This interpretation is consistent with the local presence of sub-horizontal extension veins formed outside the shear zones.

Structural analysis

Using the method of Angelier and Mechler (1977), the data set for the mineralized shear zones shows a well defined extension field resulting from the overlap of almost all the extensional dihedra (90% in extension field) and suggests that the X axis of the bulk strain is oriented at 251°/75° (Fig. 5.14). This result is compatible with the local presence of extensional sub-horizontal veins outside the shear zones, which also indicates a steep elongation. The 3% contour defines a sub-horizontal north-south (0°/04°) axis of bulk shortening (Z) located in a small field, whereas the intermediate bulk strain axis (Y) is oriented at 090\24. Note that the distribution of the fields are similar to conjugate systems presented by Angelier and Mechler (1977).

The results suggest that the mineralized shear zones at the Cooke deposit are compatible with internal strain characterized by a sub-horizontal north-south shortening, an intermediate axis plunging shallowly to the east and a sub-vertical elongation axis. The orientations of bulk strain axes within the sill at Cooke are coincident with those outside the sill determined from foliations and elongation lineations in the area (e.g. Daigneault et al., 1990; Dubé and Guha, 1992), in contrast to what is observed at Norbeau.

Influence of strength anisotropy

The Cooke and Norbeau deposits are comprised of oblique-reverse auriferous structures and occur in the same lithological setting. However, they show major differences in their geometries. Such differences are probably related to various parameters influencing the effects of layer anisotropy including: the orientation of the layers relative to the external bulk strain axes, type of external bulk strain, and the competence contrasts and the type of internal bulk strain induced by such contrasts due to strain refraction. Each parameter and its influence at the two deposits is examined below.

First, the Bourbeau sill at both Cooke and Norbeau mines is at high angle (60-75) to the regional N-S shortening direction. It is thus unlikely that layer orientation is a major cause of geometric differences between the two deposits. Second,

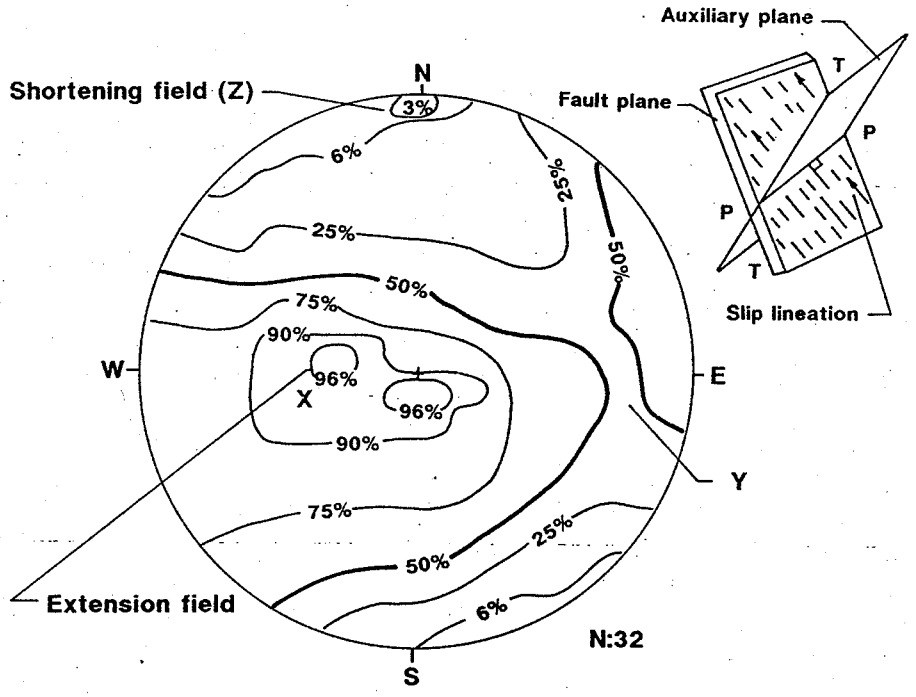

Figure 5.14. Application of Angelier and Mechler's method to the data set of the Cooke deposit. Equal area, lower hemisphere projections. N = number of measurements. From Dubé and Guha (1992).

neither was the type of external bulk strain critical as regional tectonic study done by Daigneault et al., (1990) indicated that all Chibougamau greenstone belt has been submitted to a deformation regime dominated by coaxial strain with N-S oriented subhorizontal shortening. Thus, the external bulk strain was not significantly different in both deposits. However, field study suggests that the deformation is better developed and more ductile at Norbeau compared to Cooke.

From these parameters, the competence contrast was probably the most significant factor. The internal stratigraphy of the Bourbeau sill at Cooke is slightly different from that observed regionally and at Norbeau. Only three petrological facies have been observed at Cooke as opposed to five at Norbeau (Dubé and Guha, 1989). These three facies show lesser amount of magmatic differentiation and the quartz ferrodiorite facies, interpreted to be more competent than the other facies, is absent or poorly developed at Cooke but is very well developed and is more than 100 metres thick at Norbeau. This facies is interpreted to be very competent because of its quartz and granophyric content. Thus, it is probable that the competence contrast between the sill and its host at Cooke was not as important as at Norbeau and for the same reason, the vein complexity was limited because of the reduced refraction of strain.

Our study suggests that the orientation of the internal bulk strain axes of the finite ellipsoid within the Bourbeau sill, resulting from the strength anisotropy of the

sill, were relatively different in the two deposits. At Cooke, the maximun shortening axis (Z) is N-S and sub-horizontal, the intermediate axis (Y) is E-W and shallowly plunging, and the elongation axis (X) is sub-vertical, whereas at Norbeau, Z is W-SW and sub-horizontal, Y is south-directed and shallowly plunging and X is approximately oriented at 346\54 (Fig. 5.9 and 5.14). Furthermore, these orientations do not correspond to the same axis of strain. The Y- and Z-axes were interchanged. Contrary to Cooke, the intermediate internal bulk strain axis (Y-axis) at Norbeau is not parallel to the layer, instead both the X and Z axes are contained within the layer. The internal maximun shortening was sub-parallel to the strike of the sill whereas regionaly and at Cooke, it is at high angle.

The N-S and subhorizontal internal maximun shortening and subvertical elongation deduced at Cooke is compatible with the external bulk strain proposed by Daigneault et al., (1990) for the Chibougamau area. Whereas, the uniaxial internal bulk strain at Norbeau clearly deviated from it and resulted from strain refraction. One explanation for such deviation and interchanged of internal strain axes, is that because of the higher competence contrast at Norbeau between the sill and its host, there was a change through time of the maximun principal shortening axis from high angle to sub-parallel to the layering.

The refraction of strain within the Bourbeau sill at Norbeau probably reflects the stronger competence contrast between the sill and its enclosing rocks. This refraction induced variation of the internal type of bulk strain and its intensity compared to the strain outside the sill. The uniaxial elongation of the sill resulting from such deviation was critical in the development of the complex vein pattern. In such a case, the intermediate principal stress axis played an important role, theoretically as important as the main stress axis and multiple shear zone directions were necessary to accommodate the three-dimensional strain. So, the variation in the strain complexity between the Norbeau and the Cooke mines could be related to the type of internal bulk deformation: plane strain and two-dimensional deformation at Cooke and uniaxial deformation and three-dimensional at Norbeau. And these type of deformation were controled by competence contrast and related refraction of strain.

INCOMPETENT LAYERS WITHIN COMPETENT UNITS: THE CASE OF ENFORCED SHEARING

Introduction

As indicated above, the second end-member type of anisotropy relevant to gold deposits is that of a soft layer in a competent matrix (Fig. 5.1C). This situation is important in deposits where ore zones occur in strongly foliated dykes which are enclosed in less foliated, more competent host rocks. The weak dykes localize the strain and, if they are oblique to the external shortening direction, shear zone will

develop along their margins (Fig. 5.3A). This simply reflects the preferred accomodation of strain in the less competent layers by layer-parallel simple shear (Treagus, 1988). If the dykes are sufficiently narrow, or if the amount of strain is high enough, the entire dykes effectively become shear zones. This is in a way analogous to reactivation of faults.

The role of dykes as weak layers is particularly evident in granitoid intrusions within which mineralized veins and shear zones occur along or within the mafic dykes. Examples include gold deposits within the Star Lake pluton, La Ronge district, the Eldrich and Silidor deposits within the Flavrian pluton, Noranda and those of the Bourlamaque pluton at Val d'Or. In other cases, auriferous shear zones occur along the margins of felsic dykes within gabbroic sills or mafic metavolcanics, such as the Joe Mann deposit, Chibougamau and Hammer Down deposit, Newfoundland repectively, illustrating the diversity of geological situations where dykes are important in localizing orebodies.

In all cases, there is typically a strong spatial coincidence among shear zones, dykes and veins leading inevitably to the question as to which formed first (Poulsen and Robert, 1989). However, in most cases, the foliation developed within the dykes, especially along its walls, is a clear indication that they are pre-tectonic and thus pre-mineralization.

In a homogeneous intrusion, parallel shear zones will develop with a Andersonian relation to regional strains axes (Fig. 4.1A). If soft dykes are present, some shear zones will develop along or within the dykes (Fig. 4.1B). Some shear zones will be initiated in the host and if it intersects a dyke as it propagates, it will be deflected along the dyke and will follow and\or overprint it for some distance. This is well documented at Star Lake (Fig. 5.15) where shear zones are generally located independently of dykes but with similar orientations, and it is common for dykes and shears to be perfectly coincident along part of their course (Poulsen and Robert, 1989). These coincident segments are therefore 'enforced' shear zones that deviate from the overall shear zone trend. The ore zones in the Eldrich and Silidor deposits within the diorite sills of the Flavrian pluton, Noranda, present a similar situation (Richard et al., 1990; Picard, 1990). As dykes have commonly varied orientations within intrusions, so will the overprinting shear zones. This may result in complex shear zone patterns, which deviate from that predicted based on regional strain patterns.

In order to further illustrate the influence of soft layers within competent bodies and the complex shear zone and vein patterns they may induce, we will examine in detail shear zone-hosted gold deposits within the Bourlamaque pluton at Val d'Or (Fig. 2.2), based largely on the work of Belkabir et al., (in press).

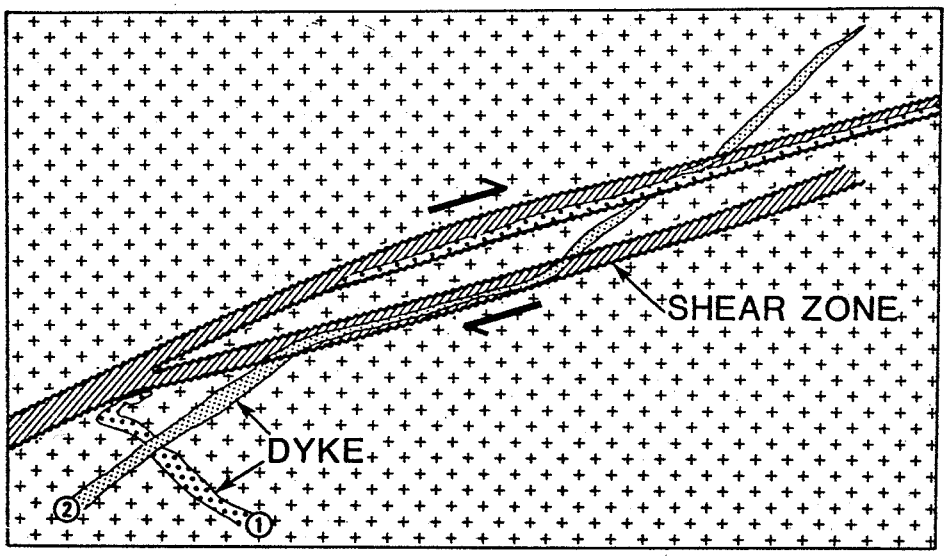

Figure 5.15. Schematic representation of dyke-shear relationships at Star Lake. Where shear zones entrap, or follow the margins of, suitably oriented dykes, the dykes are variably foliated; elsewhere they lack shear fabric and the correct sequence of cross-cutting relationships (1, 2) as well as their pre-shear origin can be readily deduced. From Poulsen and Robert (1989).

Gold deposits within the Bourlamaque pluton

Introduction

The Bourlamaque pluton is a synvolcanic quartz diorite intrusion injected by several generations of dykes of different composition. These different types of dykes are overprinted or cut by gold-bearing shear zones and related quartz-tourmaline-pyrite veins (Belkabir et al., in press). Seven gold deposits are distributed throughout the pluton and along its margins a show a significant diversity of orientations (Fig. 5.16); they consist of fault-fill veins within moderately to steeply dipping shear zones and associated sub-horizontal extensional veins as is typical of the Val d'Or district (Robert, 1990a). The majority of mineralized shear zones within the pluton are spatially coincident with diorite dykes.

Dykes and ore relationships

Several types and generations of dykes occur throughout the Bourlamaque pluton and diorite dykes, which are the most abundant, systematically cut across aplitic and pegmatitic felsic dykes (Fig. 3.17A; Belkabir et al., in press). Thickness of these dykes varies from tens of centimetres for the felsic dykes to up to a few metres for the diorite ones over along strike distance up to 100 m and 1 km respectively. These dykes were submitted to the regional greenschist grade metamorphism and based on their mineralogy and pre-kinematic hydration, the chloritic diorite dykes

constitute incompetent layers whereas the felsic ones are expected to be equally or more competent than the host pluton (Belkabir et al, in press). This interpretation is further supported by the fact that the diorite dykes are typically foliated and felsic ones are not. Both felsic and diorite dykes show the same spectrum of orientation and define four major sets (Figs. 3.18 and 3.19): three subvertical sets strike N-S, E-W and NE-SW; and a fourth set is shallowly dipping (30>) and has a variable strike.

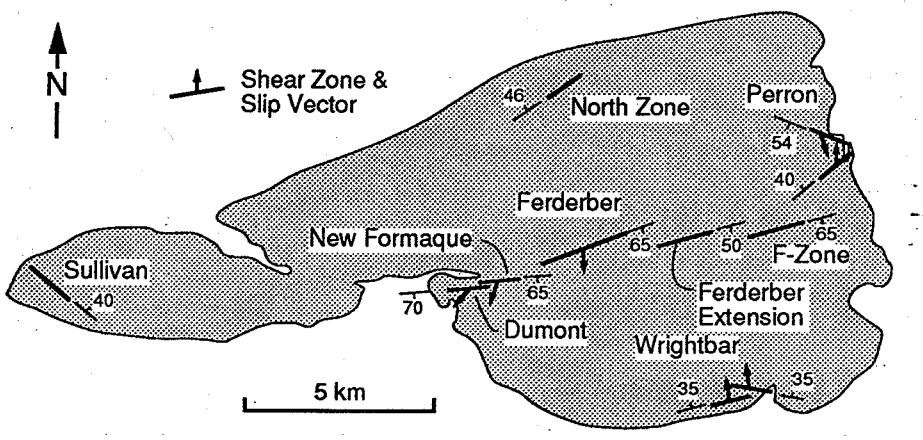

Figure 5.16. Schematic representation of the distribution and orientations of auriferous shear zones within the Bourlamaque pluton; slip vectors are indicated where known. Only the main shear zone orientations are illustrated for each deposit for the sake of clarity. From Belkabir et al. (in press).

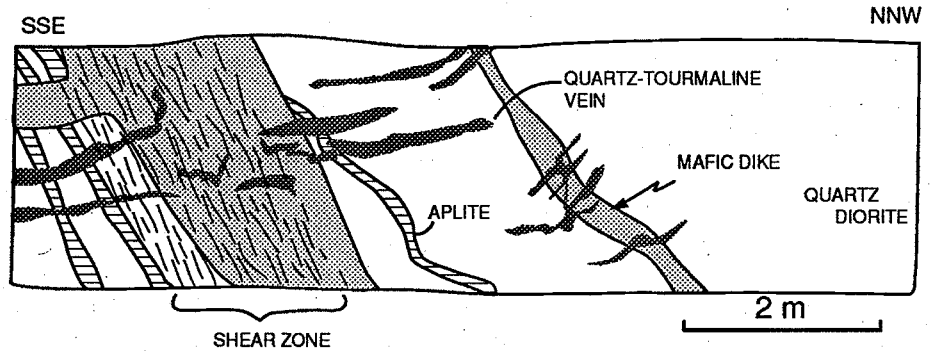

Figure 5.17. Typical cross-cutting and overprinting relationships among dykes, shear zones and veins: diorite dykes cut aplite dykes but are overprinted by a shear zone, which is in turn cut by mineralized quartz-tourmaline veins; Perron mine, Val d'Or. From Belkabir et al. (in press).

Within the Bourlamaque pluton, the gold-bearing shear zones are abundant and widely distributed (Fig. 5.16). They range from a few cm to several metres thick, from 100 to 2000 m laterally and extend for more than 500 m at depth. In all deposits, most mineralized shear zones are spatially associated with diorite dykes. They are coincident with the diorite dykes along at least part of their lengths, and dykes or dyke segments overprinted by the shear zones now consist of chlorite-carbonate schists (Fig. 5.19). However, many shear zone segments are devoid of such dioritic protoliths, as the shear zones are more continuous than the dykes themselves.

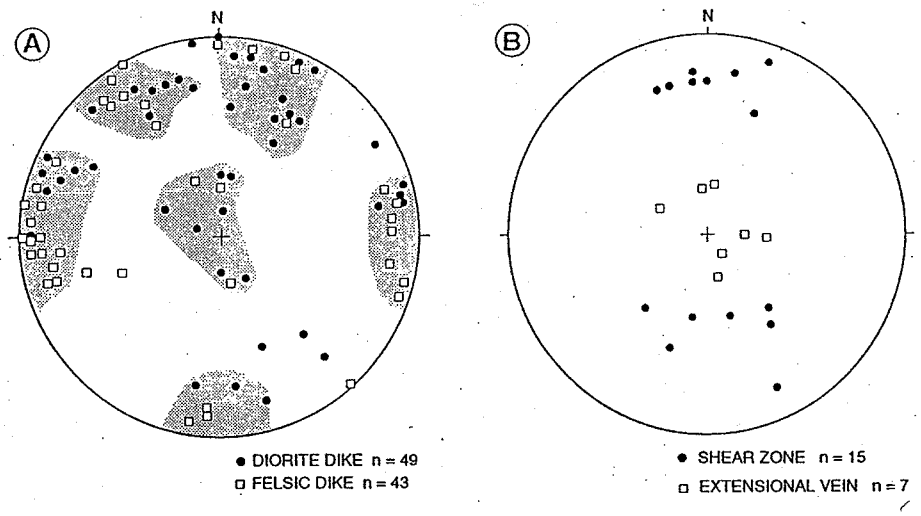

Figure 5.18. Stereographic projections (lower hemisphere). (**A**) Poles of diorite and felsic dykes in the Dumont-New Formaque-Ferderber area. (**B**) Poles of auriferous shear zones and associated extensional veins within the Bourlamaque pluton. From Belkabir et al., (in press).

In contrast to the diorite dykes which they typically overprint, the mineralized shear zones show a more restricted range of orientations: they strike from NE-SW to NW-SE and dip steeply to moderately to the north or to the south (Figs 19 and 21b). This indicates that only specific dyke orientations were activated as shear zones. At the Dumont-New Formaque deposit for example (Fig. 5.19), the main mineralized shear zones only follow the diorite dykes oriented at 090-65, despite the presence of similar diorite dykes oriented at 020-90 or of felsic dykes oriented at 075-80 and subparallel to the shear zones. These relationships indicate that the development of shear zones was controlled by both the orientation and the composition of the dykes (Belkabir et al., in press).

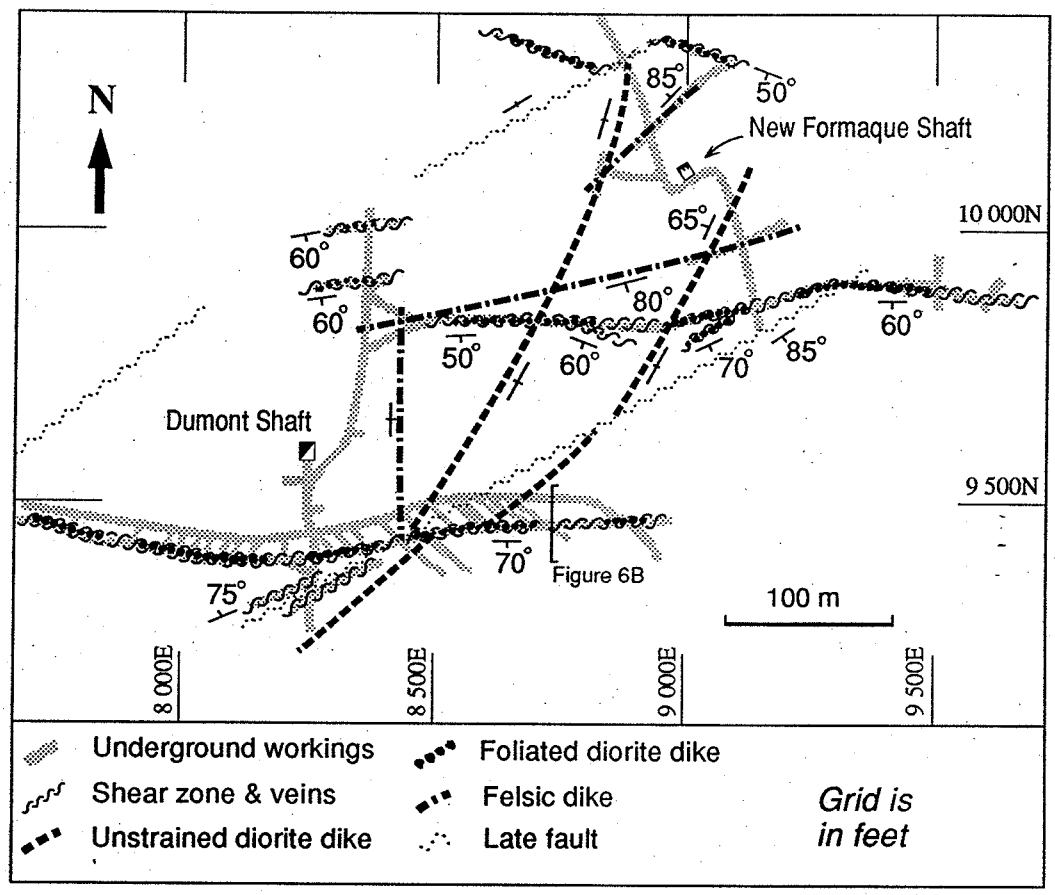

Figure 5.19. Simplified geologic map of level 250 of the Dumont-New Formaque deposit, showing the relation between diorite and felsic dykes and auriferous shear zones and veins. From Belkabir et al. (in press).

Kinematic analysis

All well constrained shear zones within the pluton have a reverse-oblique sense of movement based on: the obliquity of the foliation to the shear zone boundaries (Fig. 3.12A), elongation lineations on the foliation planes, striations and steps on laminated surfaces of the fault-fill veins and shallow dips of extensional veins Belkabir et al., (in press). The auriferous shear zones display a significant range of orientations and rakes of slip motion within the Bourlamaque pluton (Fig. 3.18B) which contrasts with the typical east-west strikes and rakes of slip direction >70° for the majority of the auriferous shear zones, outside the pluton (Robert, 1990a).

Despite these deviations in orientation and slip directions, similarities in structural features and hydrothermal alteration indicate a common origin for the veins and shear zones within and outside the pluton (Robert, 1994; Belkabir et al., in press). The strength anisotropy induced by the incompetent dykes has played a

key role in causing such deviations, as most of the strain within the pluton was accommodated by the development of shear zones along or within these weak layers.

Determination of deposit-related strain axes within the pluton

As the diorite dykes have acted as incompetent layers accommodating most of the strain, they represent structures which are dynamically analogous to reactivated faults (Lisle, 1989). Thus, these structures can be analyzed in a similar way to fault-striation data using the Angelier and Mechler's technique described above. It should be noted that a modified version of Angelier and Mechler's method has been proposed by Lisle (1989) when dealing with a very similar situation than the one described here. This graphical method, named the 'right trihedra method', was developed for paleostress analysis from sheared dyke sets and allows determination of principal axes of stress and their ratio.

Figure 5.20 presents the results obtained with the Angelier and Mechler's method using the data in Belkabir et al. (in press). The results show that the dyke-controlled auriferous shear zones within the Bourlamque pluton are recording horizontal north-south shortening and near-vertical elongation. Such deposit-related strain axes within the pluton are parallel to those determined from auriferous shear zones outside the pluton, as well as those determined from regional planar and linear fabrics in the Val d'Or district (Robert, 1990a). Thus, despite their difference in orientation and slip direction, the dyke-controlled auriferous shear zones are recording the same bulk strain as those outside the pluton (Robert, 1990a).

Summary

Three important points should be emphasis when dealing with such an environment. Fisrt, it is common for dykes within a single intrusion to commonly present various compositions and orientations. However, to be activated as shear zones, the dykes must be much weaker, or less competent than the host rock (Berger, 1971; Treagus, 1988; Dubé et al., 1989; Lisle, 1989; Poulsen and Robert, 1989; Talbot and Sokoutis, 1992; Belkabir et al., in press). In doing so, these incompetent layers enforce shearing and become a shear zone in the classical sense and the relationship between their internal oblique foliation with the dyke wall can be used to deduce sense of motion (Berger, 1972, Lisle, 1989) (Figures 4B and 26). Felsic dykes emplaced within less competent rocks could also enforced shearing along their margins and controlled the location of auriferous veins as indicated at the Joe Mann (Dion et al., 1990) and Hammer Down deposits (Dubé et al., 1992).

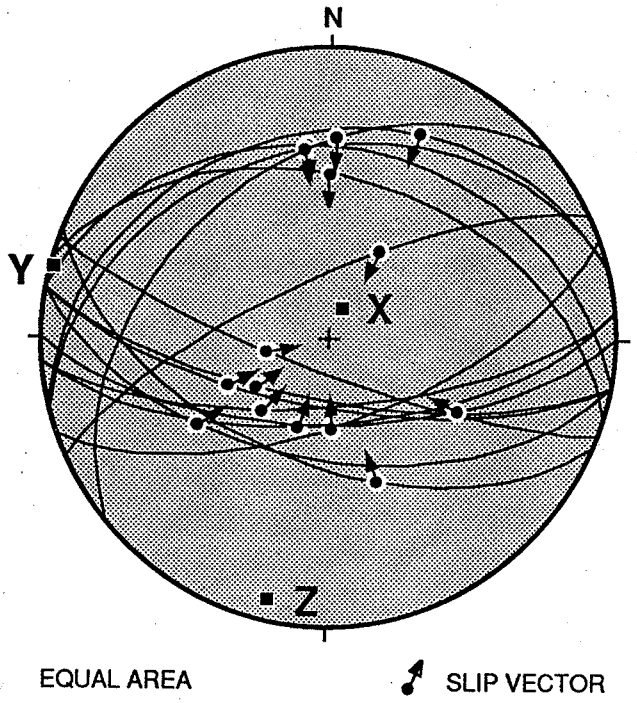

Figure 5.20. Stereographic projections of shear zone and shear vein orientations (where they differ) and slip data in Belkabir et al., (in press). The axes of the stress tensor were determined by the method of Angelier and Melcher (1977).

Second, in a given intrusion it is also common to see only certain dykes being activated and this is strongly controlled by their orientation in respect to the external bulk strain axes (Talbot and Sokoutis, 1992). However, this relationship need further considerations before complete understanding.

Third, as for the strength anisotropy within gabbroic sill described above, because of the strain refraction induced by the dykes (Treagus, 1988), shear zones will deviate from the Andersonian type geometry and kinematics predicted for isotropic material. In such a context, the variations in dyke orientation will consequently induce different direction of slip motion. As the orientations and plunges of orebodies are commonly related to slip directions along the host shear zones (McKinstry, 1948; Poulsen and Robert, 1989), it is important, for exploration purposes, to understand the role and influence of these dykes in order to be able to predict the slip directions along these variously oriented dyke-controlled shear zones (Belkabir et al., in press).

CHAPTER 6:
STRUCTURAL HISTORY OF DEPOSITS

INTRODUCTION

The structural analyses of gold deposits outlined in chapters 4 and 5 are based on the underlying assumption that the structures in question formed syntectonically with respect to a particular increment of deformation and that they have not been significantly deformed any further. This assumption need not always be valid and one must continually consider alternate ways of interpreting observed mesostructures. For example, workers in the 1930's (e.g. McKinstry 1948, Newhouse, 1942) recognized the same links between quartz veins and shear zones as are made today but interpreted them quite differently. The early workers viewed faults and shear zones (to them, multiple closely spaced fault strands) to repesent zones of "ground preparation" which subsequently served as passive conduits for hydrothermal fluids. Slickenlines in veins, for example, were viewed to be pre-mineral fault striations that were "replaced" by hydrothermal minerals (e.g. McKinstry and Ohle, 1949). A similar post-kinematic emplacement of gold into vein systems is implicit in the observations of modern day workers who infer isotopic ages of hydrothermal minerals to be as much as 100 million years younger than the major orogenic events in the gold districts. In sharp contrast, other workers have advanced the hypothesis that many vein-gold deposits are actually of pre-tectonic origin, either of porphyry or exhalative affinity. In this case, zones of pre-deformational hydrothermal alteration can be viewed as loci of subsequent high strain but without the need for significant displacement along structures.

The question of whether a particular gold deposit is pre-, syn- or post-tectonic with respect to a phase of deformation is therefore crucial to a correct structural analysis. In the case of vein deposits we can distinguish three possible situations:

(1) veins that are genetically related to faults and shear zones and formed syntectonically, but early, in a single deformation increment so that they are subject to continued deformation confined to the shear zone environment; these correspond to fault-fill veins within shear zones but that are overprinted by continuation of shear zone displacement.

(2) veins that formed syntectonically in relation to movements on faults and shear zones but during successive deformational events so that vein sets consistently overprint one another; these correspond to fault-fill veins, extensional veins or stockworks formed successively rather than simultaneously.

(3) veins that formed pretectonically, or syntectonically during one or more increments of deformation, and subsequently were pervasively overprinted by a later increment of deformation; this corresponds to the case of deformation affecting an entire vein deposit as well as its host rocks.

Although it is often difficult to decide which situation is relevant to a particular vein deposit, the problem is even more severe in deformed sulphidic gold deposits where the absence of veins also usually means the absence of markers that can track the deformation history of a deposit. Among deformed sulphidic gold deposits, two situations are distinguishable: (1) disseminated sulfide deposits (e.g. Hemlo-type) where the abundance of sulphide minerals is low enough to have little effect on the rheology of the ore relative to adjacent rocks so that ore deformation is effectively passive, and (2) massive sulphide deposits (e.g. Bousquet-type) where the sulphides induce strong competency contrasts and take an active part in deformation.

DEFORMED VEIN GOLD DEPOSITS

Nearly all vein gold deposits have been overprinted by subsequent deformation in one way or another. Folded and/or boudinaged quartz veins are commonplace mesoscopic features of deposits and this can potentially result from situations ranging from the simple reactivation of existing host shear zones to the pervasive folding and shearing of orebodies or entire deposits. Recognition of overprinting deformation and deciphering structural elements related to mineralization and to subsequent deformation is therefore a difficult but important part of structural analysis of vein deposits. Given the multiple deformation increments observed in greenstone terranes, it is not surprising that deposits that are entirely pre-tectonic, or those that formed during one early increment of a progressive deformation, become overprinted by subsequent deformation. At Val d'Or, for example, the Sigma-Lamaque deposit appears to have formed between the D2 and D3 increments of deformation (Robert, 1990a). It is located in a part of the district where the effects of D3 are minimal and overprinting is generally confined to reactivation of some shear zones and local overprinting of veins adjacent to those zones. Had deposits of the same type and age formed within the Cadillac Tectonic Zone or the western part of the district, where the effects of D3 are important, they would surely be overprinted more strongly by D3 deformation. Thus, with some knowledge of the structural history of a particular district, it is possible to make some predictions as to the probability and nature of overprinting deformation. The following sections illustrate some of the effects of overprinting deformation on vein deposits.

Overprinting by continuation of shear zone displacement

Deformation within shear zones (by definition!) and of shear zone-hosted veins is a relatively common feature of lode gold deposits. This is commonly reflected by the development of striations on vein and foliation surfaces, by folding of veins and of shear zone foliation, and by development of crenulation cleavages. Such deformation can be related to either continued shearing after mineralization or to shear zone reactivation under a different stress field. In the first case, where shear zone deformation outlasts vein development, the orientation of all structural elements, including those overprinting shear veins and wallrock foliation should be consistent with a single slip direction (and sense) along the shear zone (Fig. 6.1A). If the superimposed strains are not large, the axes of folds developed on extensional and shear veins as well as foliation will be at high angle to the slip direction. These axes are expected to be perpendicular to lineations on foliation planes and striations within the veins, and parallel to the shear zone's B-axis (Fig. 6.1A). Similarly, extensional crenulation cleavages and shear bands resulting from continued deformation will have a line of intersection with the foliation that is parallel to the shear zone's B-axis. This is the case at the Ferderber deposit, where asymmetric folds of veins and foliation have shallowly plunging axes, perpendicular to measured elongation lineation and compatible with reverse movement along the mineralized shear zone, (Fig. 4.7; Vu, 1990). New striations produced on existing veins will parallel those formed during vein development.

In the case of shear zone reactivation with a second displacement different from first one, the orientations of overprinting structural elements will be incompatible with the initial slip direction as indicated and best preserved by penetrative structural fabrics such as elongation lineations in the foliation planes (Fig. 6.1B). New sets of striations produced during reactivation on foliation and shear vein surfaces will likely be oblique to penetrative mineral lineations in the shear zones or to striations marked by hydrothermal minerals within shear veins (Fig. 6.1B). As described above, this is the case at Val d'Or where several shear veins containing down-dip striations are overprinted by weak subhorizontal striations related to strike-slip reactivation of the shear zones and veins.

In some other cases, asymmetric folds of the foliation, or of existing veins, may also be produced and their axes will have plunges that are oblique to the shear zone's B-axis (Fig. 6.1B). Structural elements with orientations not compatible with a single slip direction are a good indication of shear zone reactivation. In such cases, penetrative elongation lineations are probably the most reliable indicator of the early slip vector along the shear zone.

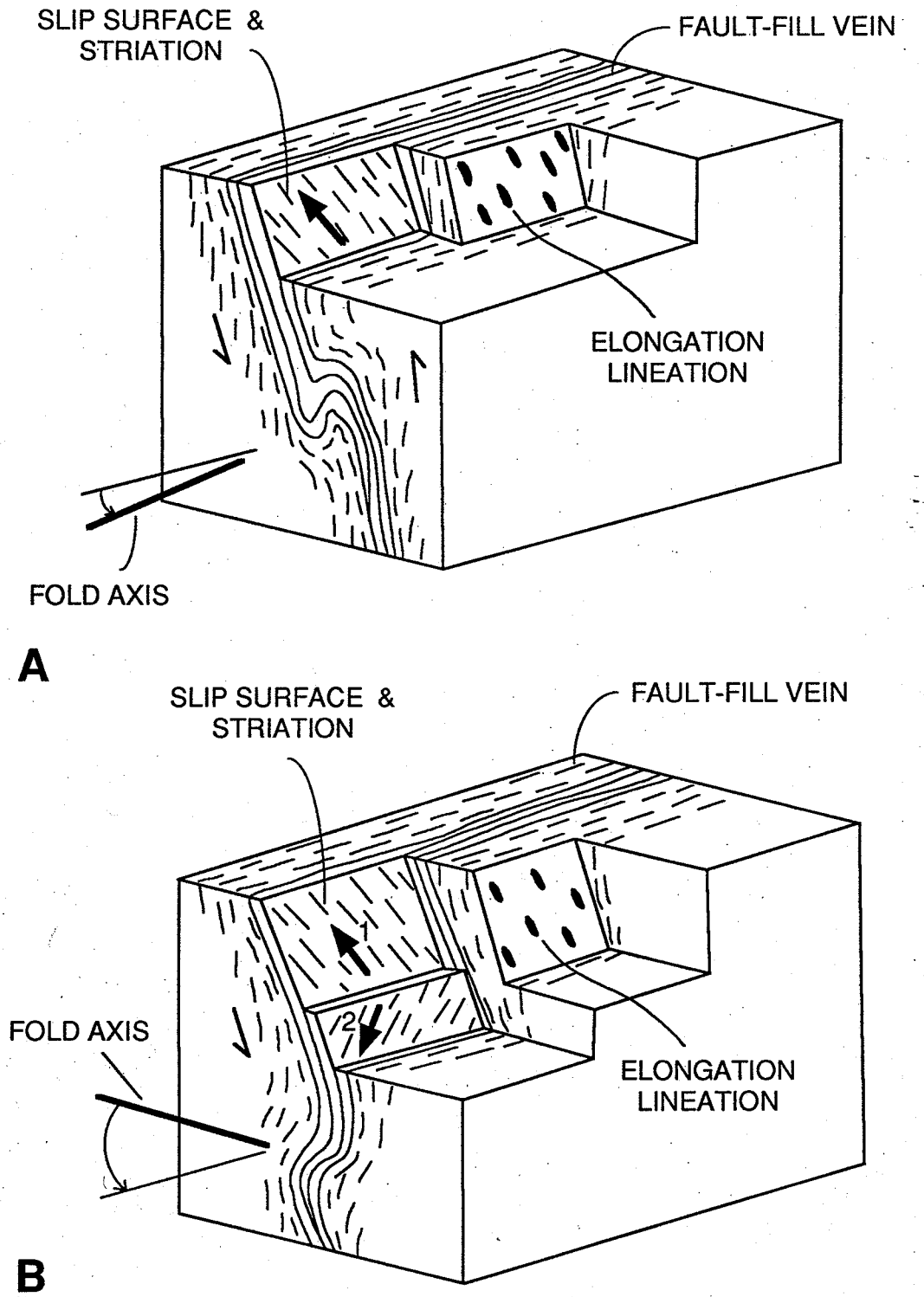

Figure 6.1. Schematic block diagrams illustrating (**A**) generation of a folded quartz vein and foliation resulting from continuation of displacement in a single direction in a shear zone; and (**B**) generation of a folded quartz vein and foliation resulting from displacement due to reactivation of a shear zone in a different direction (2) than that related to the syntectonic emplacement of the vein (1).

Overprinting vein sets of different generation

In some gold deposits the multiple orientations are the result of stuctures formed at different times in different stress/strain regimes. In such cases the structural analysis of the resulting network may not yield any simple coherent result but will put some constraints on the deformational history of the deposit. The San Antonio deposit in the Rice Lake (Fig. 2.4) belt offers an excellent example of such a complex vein network composed of vein sets of different generation (Lau, 1988).

San Antonio deposit

Most mineralized veins at San Antonio are hosted by a differentiated mafic sill intruding dacitic volcanic rocks. The sill strikes southeasterly and dips 50° to the northeast, and extends along strike for 6 km and reaches a thickness of 150 m in the mine area. It is cut by a series of dacitic feldspar porphyry dykes striking east-west and dipping 60-70° to the north, and enveloped by zones of sericite schists, reaching thicknesses of 140 m in the footwall and 20 m in the hangingwall (Fig. 5.5; Poulsen et al., 1986). Mineralized veins are preferentially developed in the most differentiated, granophyric layer of the sill as is the case at Norbeau (see chapter 5). Gold occurs mainly in two distinct sets of veins, which are cut two younger sets of barren veins and shear zones. Systematic cross-cutting relationships among the four sets of veins indicate that they likely formed at different times (Lau, 1988).

The first set of structures consists of stockwork zones that strike northwesterly and range in dip from subvertical to steeply northeast-dipping (Fig. 6.2). These zones, up to 10 m thick, are oblique to and steeper than the host sill, and they terminate at their intersection with the hangingwall or footwall of the sill. As a result the stockwork zones have a long axis that plunges at 20° to the northwest, parallel to their line of intersection with the host sill. The stockwork zones are internally complex (Poulsen et al., 1986; Lau, 1988): they are composed of stacked, moderately dipping extensional veins, referred to as ladder veins, linked by subvertical veins on the fringes of the zones. Due to an increase in vein abundance, stockwork zones grade into central breccias composed of angular wallrock fragments in up to 50% hydrothermal matrix. The central breccias are in turn cut by central shear veins which offset earlier dykes and along which all of the displacement along the stockwork zones has taken place (Fig. 3.19); no offset accompanies development of the ladder veins and central breccias, and the formation of central shear veins probably result from reactivation of the zone occupied by the central breccias. Movements along the central shear veins may also account for the sigmoidal shape of the ladder veins. The dyke offsets, combined with the sigmoidal shape of ladder veins indicate a reverse component of movement along the stockwork zone's central veins, with a slip direction raking moderately to the northeast (Fig. 3.19; Lau, 1988).

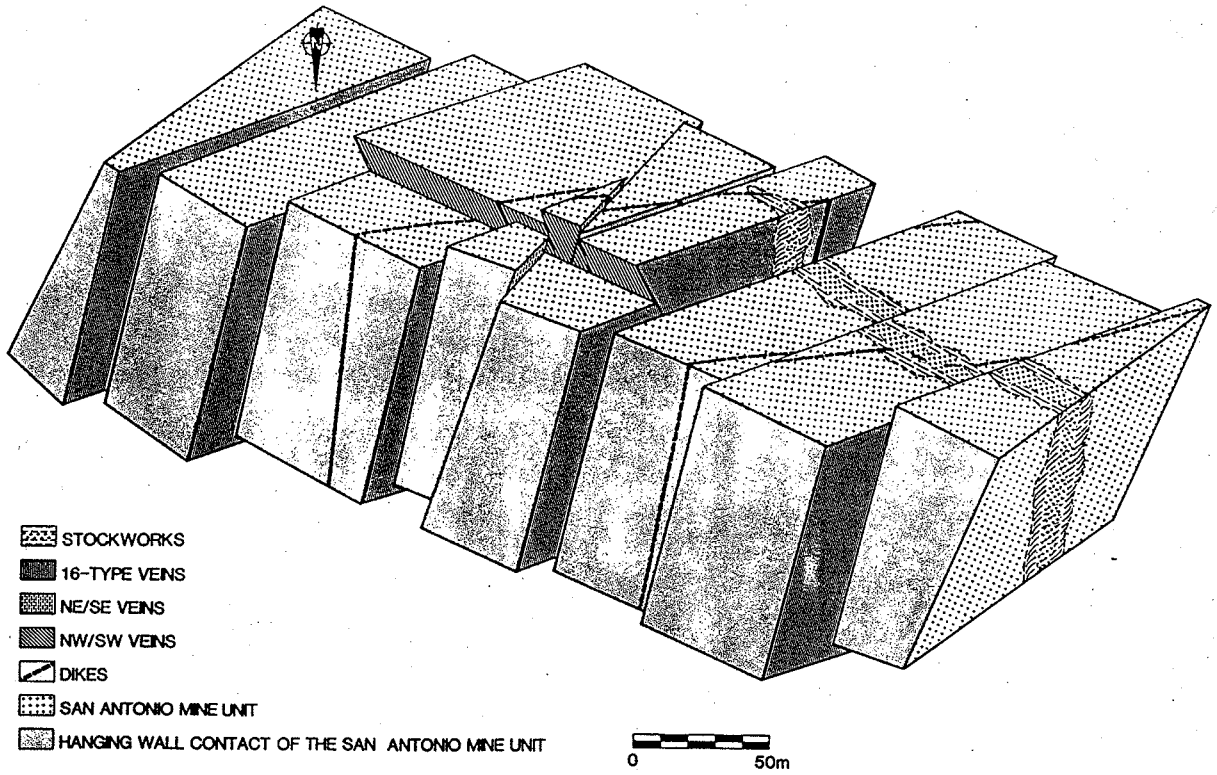

Figure 6.2. Three-dimensional representation of the early stockwork and later shear-zone styles of mineralization at the San Antonio Mine (after Lau, 1988).

The second set of mineralized structures, known as the 16-type veins, strikes approximately east-west and dips steeply to the north (Figs. 5.5 and 6.2). They consist of laminated shear veins in more continuous shear zones, some of which have been traced for more than 1 km in their longest dimension (down-dip). These shear zones offset both the stockwork zones and the walls of the host sill, but do not extend into the footwall and hangingwall sericite schists (Fig. 5.5). Laminated shear veins within these shear zones form lenses that are elongated down their dip and reach dimensions of 200 m along strike and 1200 m down dip. As for the stockwork zones, the long axes of 16-type veins are parallel to their line of intersection with the host sill. Offset of earlier markers and mineral lineations and striations in the host shear zones indicate reverse-sinistral movement along a slip direction raking at 40° to the NE (Fig. 6.3; Lau, 1988).

The third set of structures consists of barren laminated shear veins in more continuous shear zones striking northeast and dipping 70° to the southeast (Fig. 5.5). These structures offset all earlier ones; offset of markers, mineral lineations and striations on these shear zones indicate reverse-dextral movements along a slip direction raking 40° to the northeast, parallel to that along the 16-type veins (Fig. 6.3).

The last set of structures, which is barren and the least developed, consists of brittle faults, locally containing quartz veins; it strikes northwest-southeast and dips 75° to the soutwest. They offset all previous structures and the reconstructed movement is reverse-dextral along a direction raking at 45° to the southeast (Figs. 5.5 and 6.2; Lau, 1988).

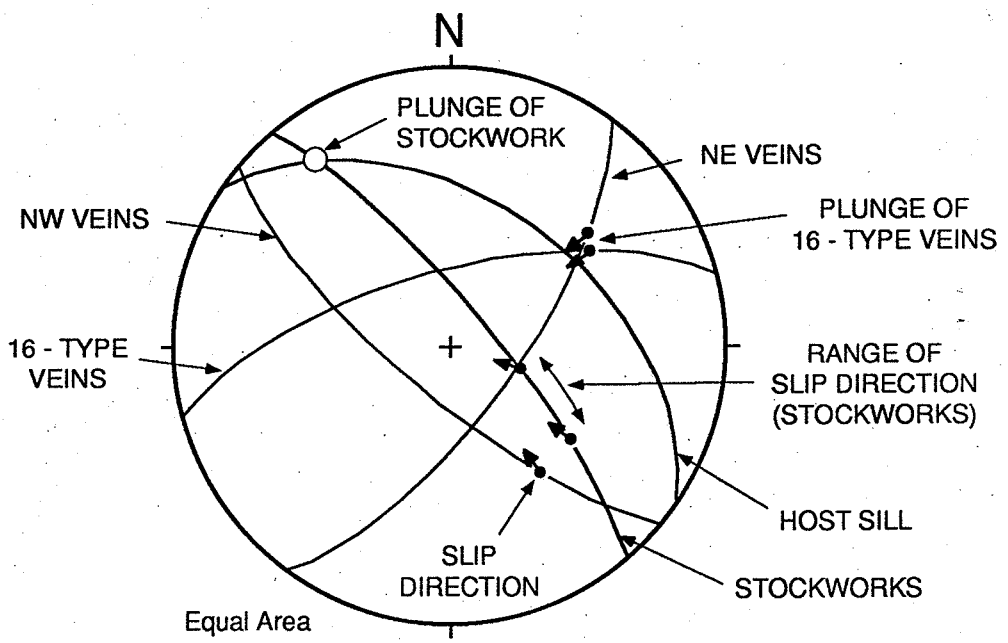

Figure 6.3. Stereographic representation of the orientation of the various sets of structures and related elements in the San Antonio Mine (After Lau, 1988).

The San Antonio deposit is a geometrically complex network of structures of multiple ages, some of which could have been considered as conjugates to one another without knowledge of age relationships. There are three important points to note about this network: first, movement along all the structres has an important component of reverse sense, which certainly must reflect persistent compressional deformation through time. The second is that the slip direction along the 16-type and NE/SE structures is parallel to their line of intersection with the host mineralized sill. Such coincidence is taken here to reflect the role of layer anisotropy (in this case the host intrusion) in localizing the development of mineralized structures and influencing their direction of slip, as was addressed in the previous chapter. Finally, it is interesting to note that the long axes of both the stockwork zones and the 16-type of veins coincide with the line of intersection with the host sill, rather than showing specific geometric relationships with the slip direction along the host shear zone.

Pervasively deformed vein deposits

In addition to cases discussed above, shear zones and entire vein deposits can be deformed and overprinted by subsequent deformation increments. The effects range from development of new fabrics within shear zone to folding and penetrative strain of orebodies and entire deposits. In some cases the veins may be pre-tectonic but become the locus of subsequent deformation as is the case of early porphyry-related veins in the Chibougamau district (Robert, 1994b) and in others the pre-existing veins formed during one increment of regeional deformation but deformed in a subsequent one as in the case of gold-quartz veins at Bell Creek in the Timmins disrict.

Because shear zones contain foliated rocks, they will be sites for preferential developement of crenulation cleavages and kink bands, which are known to readily develop in layered rocks. This point is important, because shear zones may be the only sites in a given area where the effects of small deformation increments will be recorded. Based on their occurrence solely within shear zones, some fabrics such as extensional crenulation cleavages could be misinterpreted as being part of the shear zone evolution, and misused as kinematic indicators, as discussed in Chapter 3. Such fabrics will also overprint and crenulate any mineralized vein present in the shear zone.

Orenada deposit

The Orenada Zone 4 deposit at Val d'Or (Fig. 2.2), is an example of a folded vein-type deposit occurring within the Cadillac Tectonic Zone (Robert et al., 1990). It consists of auriferous veins and altered wallrocks spatially associated with a large asymmetric fold. The mineralized veins are hosted by volcanic-derived intermediate to felsic schists (Fig. 6.4A and B), which display the intense subvertical S2 foliation of the CTZ. They occur principally within a large Z-shaped F3 fold which plunges at 30-45 to the east and which has been traced down plunge for a distance of approximately 400 m (Fig. 6.5A). The internal structure of this large F3 fold is complex and consists of a series of mesoscopic Z-shaped folds of S2 and of the lithological contacts, plunging subparallel to the larger structure (Fig. 6.5B).

Two types of mineralized veins occur within the Orenada Zone 4 deposit: abundant concordant V2 veins and rare discordant V3 veins (Fig. 6.4B). Concordant veins are typically parallel to S2 and are folded by the F3 folds. They are most abundant within the large F3 fold but also occur outside this fold. They are on the order of 10 cm thick and are surrounded by mineralized alteration envelopes of similar thicknesses. They commonly occur in groups of closely spaced, branching and merging veins (Fig. 6.4B) which make up mineralized zones reaching thicknesses of a few metres. Internal structures of the veins include laminations and and jigsaw puzzle breccias, suggesting that these are probably

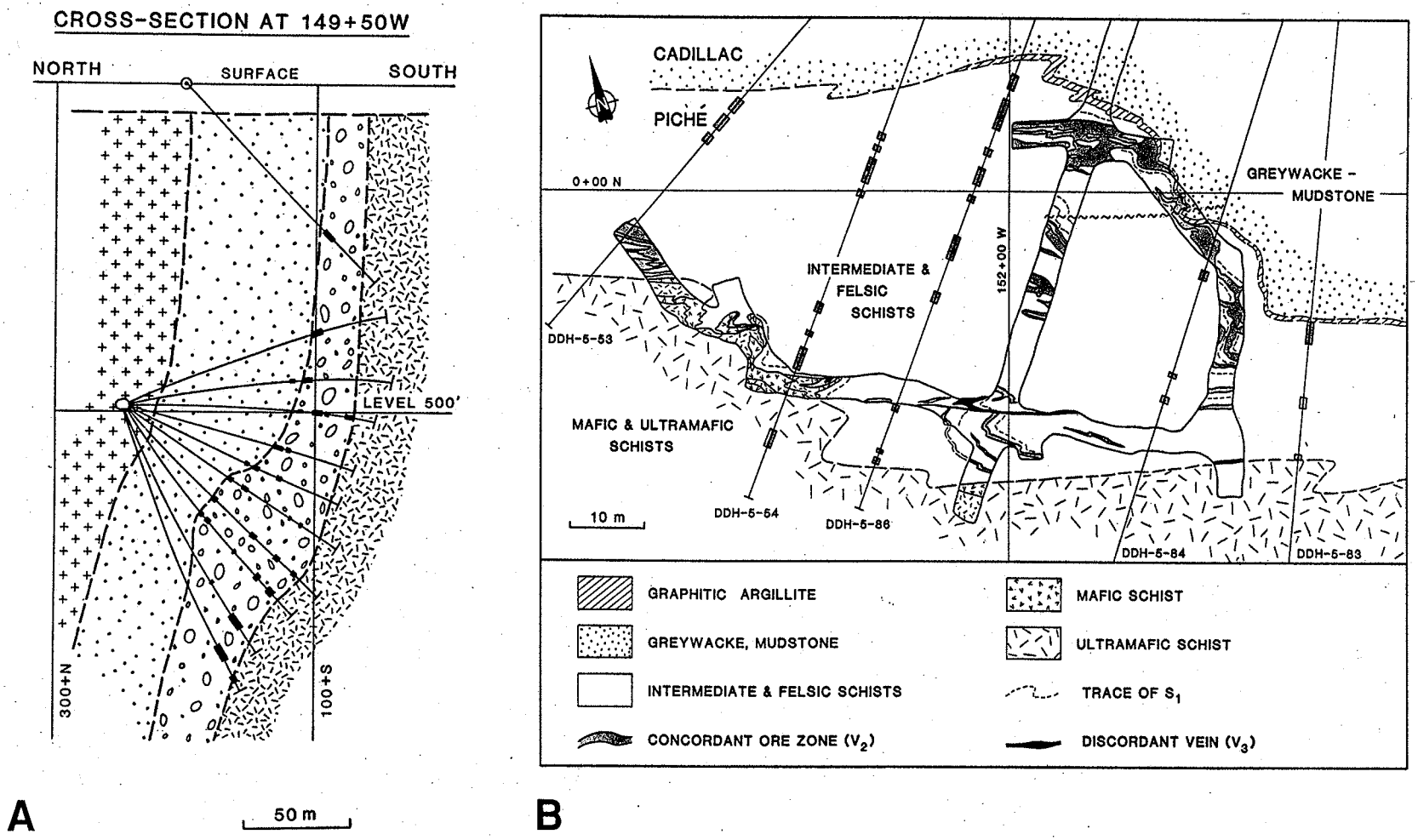

Figure 6.4. The Orenada Zone 4 deposit. (**A**) Simplified cross-section showing the envelope of lithological contacts and the distribution of mineralized drill-hole intersections. (**B**) Simplified geological map of level 500 showing details of the folding of both lithological untis and concordant mineralized veins. From Robert et al. (1990).

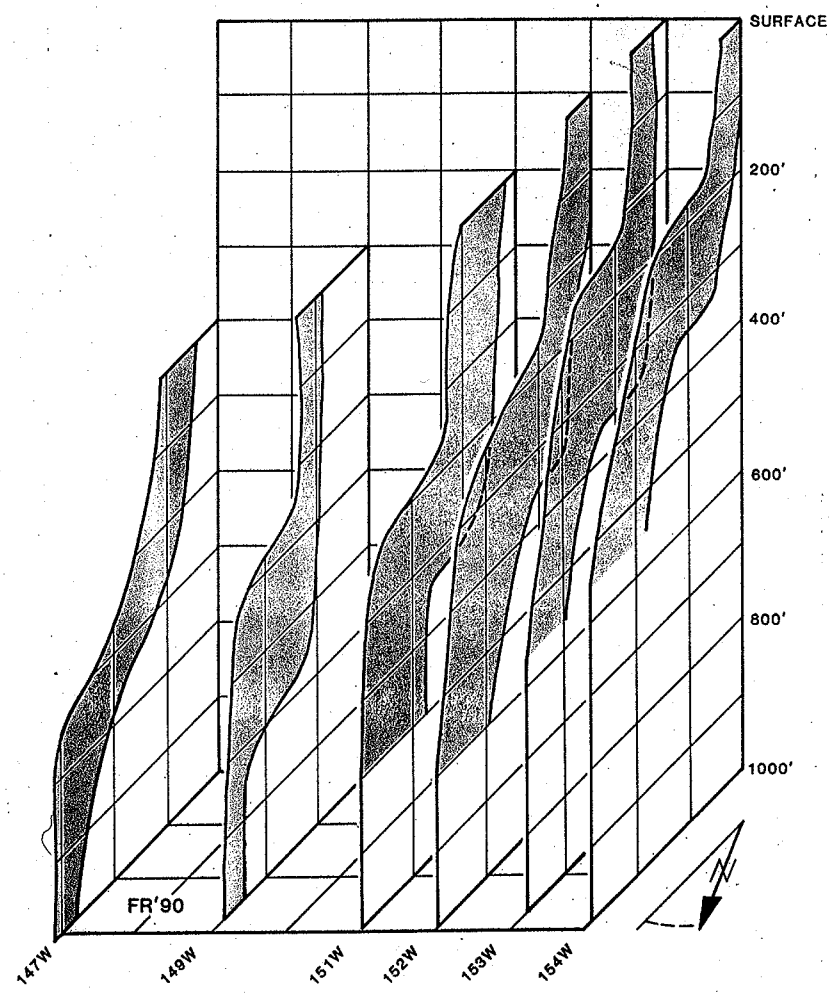

A

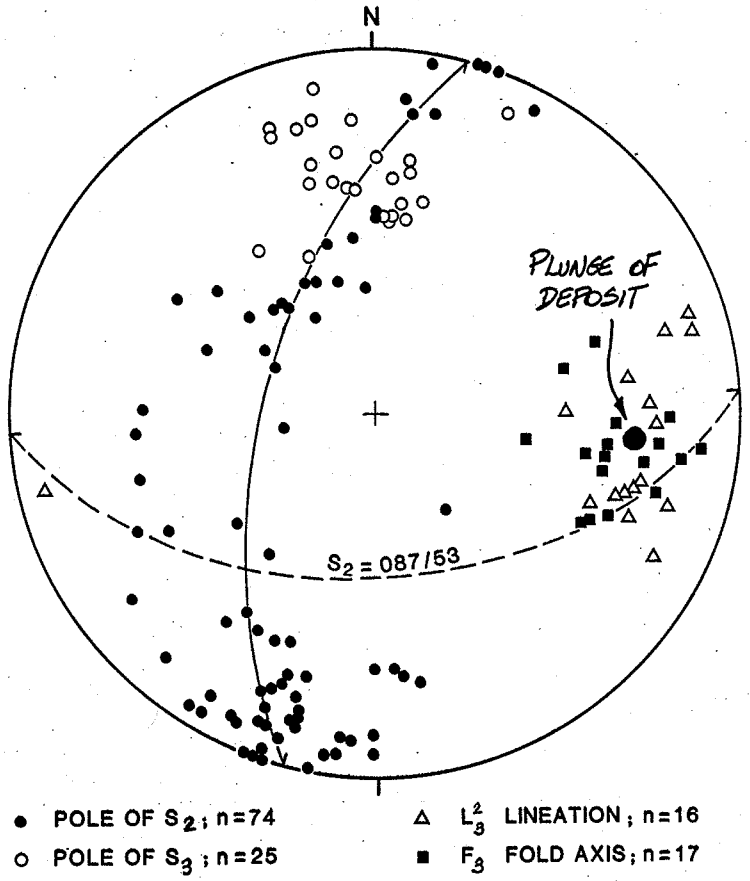

B

Figure 6.5. The Orenada Zone 4 deposit. (**A**) Three-dimensional projection showing the moderate easterly plunge of the F3 fold containing the deposit. (**B**) Stereographic projection of the structural elements of the deposit. From Robert et al. (1990).

shear veins. Concordant veins commonly display incipient boudinage and small extensional ladder veins perpendicular to their walls, both of which developed prior to the F3 folding (Robert et al., 1990). This indicates that the concordant veins have experienced some of the shortening related to the development of S2. Discordant V3 veins occupy narrow reverse-oblique (dextral) shear zones up to 30 m long which strike east-northeast and dip steeply to the south (Fig. 6.4B; Robert et al., 1990). V3 veins cut across both concordant veins and F3 folds and clearly represent a second mineralizing increment.

As a result of F3 folding, individual ore zones, as well as the deposit as a whole, have long axes subparallel to the plunge of the large F3 fold and that of the internal mesoscopic ones (Fig. 6.5B). In such deposits, recognition that mineralized veins are folded or at least overprinted, as indicated in core by variations in core angle and by a spaced cleavage overprinting the veins, is essential in correctly correlating mineralized intersections from one drill hole to the other.

DEFORMED SULPHIDIC GOLD DEPOSITS

The effects of overprinting deformation may also be such that shear zones and associated gold deposits can be folded on the property or regional scale. This will be the case of gold deposits formed prior to the last significant increment of deformation in a given area, or any ore deposit formed early in the evolution of greenstone terranes such as sulphidic gold deposits (see Robert 1990b), massive sulphide deposits or komatiite-hosted nickel deposits. In fact, syngenetic deposits will likely show the cumulated effects of all deformation increments affecting an area. This is the case for example in the sulphidic gold deposits of the Bousquet and D.J. LaRonde mines in the Bousquet district of Abitibi where gold mineralization occurs in massive to semi-massive sulphide lenses, overprinted by deformation within a 500 m wide shear zone (Tourigny et al., 1989; Marquis et al., 1990). As a result of complex deformation within the shear zone, the auriferous sulphide lenses have been boudinaged, transposed and elongated parallel to mineral lineations and inferred slip direction along the shear zone (Marquis et al., 1990; Tourigny et al, 1993). Two additional examples will serve to further illustrate structural elements and their relationships in deformed sulphide-type gold deposits.

Disseminated au sulfide deposits

Greywacke Lake deposit

Disseminated gold mineralization occurs at Greywacke Lake in the Stewart River area (Fig. 2.5) in a 100 m wide panel of clastic and volcaniclastic rocks (mainly

conglomerate and arenite) that are metamorphosed to assemblages (sillimanite + biotite + muscovite + plagioclase +/- microcline +/- garnet) indicative of the upper amphibolite facies. Gold occurs in irregular lenses of quartz-feldspar biotite schist that contain disseminated pyrrhotite and lesser pyrite and chalcopyrite and molybdenite. The lenses are aligned approximately parallel to the regional strike of their host rocks but, in detail, are actually discordant to primary lithological contacts. The para-concordant nature of the pre-deformational, discordant sulfide bodies is the result of their transposition, along with their host rocks, into an orientation (S1) parallel to the axial planes of an F1 intrafolial anticline pair of approximately 50 m wavelength (Fig. 6.6). The entire rock package has been re-folded to lie on the overturned southwest limb of a regional F2 synformal anticline that closes 1 km to the east (Fig. 6.7). The mesoscopic effects of the second deformation on the mineralization at the Greywacke Lake deposit are confined to rare minor F2 folds and a common S2 cleavage 10 to 20° clockwise to S1.

The nature and orientations of mesoscopic deformational fabric elements were recorded systematically across the deposit. Coupled with the distribution of lithologic units and observed overprinting relationships, three deformational increments D1, D2 and D3 were identified; these also appear to be in accord with the regional structural nomenclature of Lewry (1990; see Table 2.1).

D1 deformation dominates the map-scale structure at Greywacke Lake (Fig. 6.6). The prominent anticline defined by the distribution of map units are is a reclined intrafolial F1 fold that plunges 40 to 50° to the north (L1:355-45°). A down-plunge view shows the fold to be tight to isoclinal. The most penetrative planar fabric in most outcrops is S1 which is axial planar to F1 folds and displayed mainly by a micaceous pressure solution cleavage and extreme flattening of clasts. Careful examination of arenite units in the mesoscopic F1 antiformal hinge confirmed that S1 does not overprint earlier planar elements other than bedding. The shapes of trough crossbeds in the lithic arenite unit (Salx) confirm that the F1 folds are anticlinal and synclinal in a stratigraphic sense (Fig. 6.6) and that they face upwards (i.e. younger units are encountered upwards and northeastward along S1).

D2 deformation is less intense in these outcrops than D1. Most commonly marked by elongate faserkiesel, S2 cleavage (S2:240-65°) clearly crenulates S1 and transects F1 folds. Small downward-facing F2 folds are all S-shaped on the long limbs of F1 folds but no larger deposit-scale F2 folds were detected. Locally mineral and stretching lineations were recorded to lie in a down-dip orientation in S1. Most correspond to the intersection of S1,S0 with S2 and therefore are designated to be L2 of generation and coaxial with F2 folds. Some, however, are closer in orientation to the F1 hinge and may be related to D1.

F3 upright, open folds, up to 10 m in wavelength and trending 340°, deflect and overprint both S1 and S2 but have limited effect on the map-scale

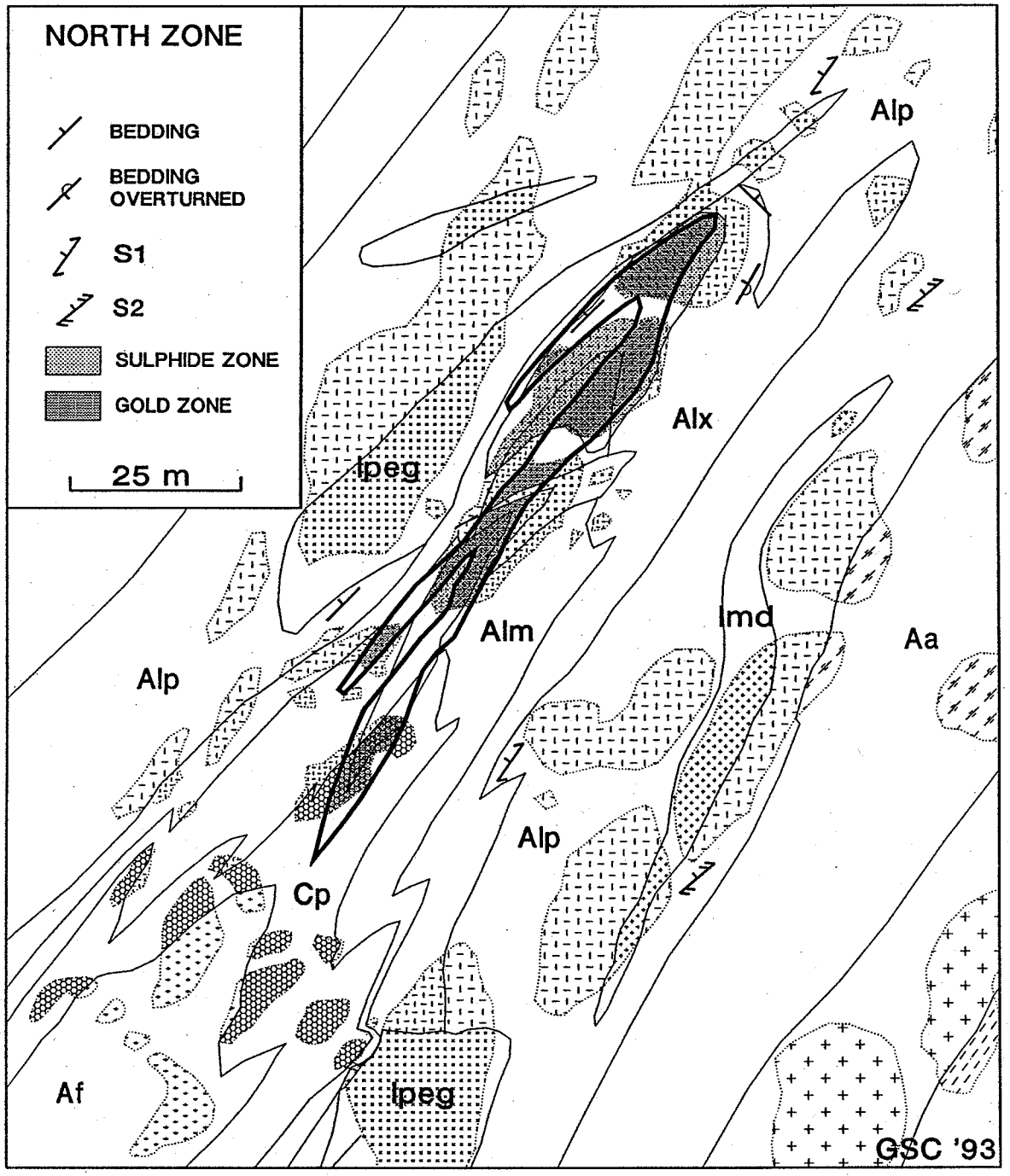

Figure 6.6. Geological map of folded (F1) metasedimentary gneisses (Af: feldspathic arenite; Cp: polymictic conglomerate; Alm: massive lithic arenite; Alx: cross-bedded lithic arenite; Alp: pebbly lithic arenite; Aa: arkose) at the Greywacke Lake deposit (after Poulsen and Robert, 1994). lpeg and lmd refer to pegmatite and monzodiorite respectively. Note that the auriferous zone of disseminated sulphides had originally an irregular shape and was discordant to layering; it has been passively folded with the enclosing rocks.

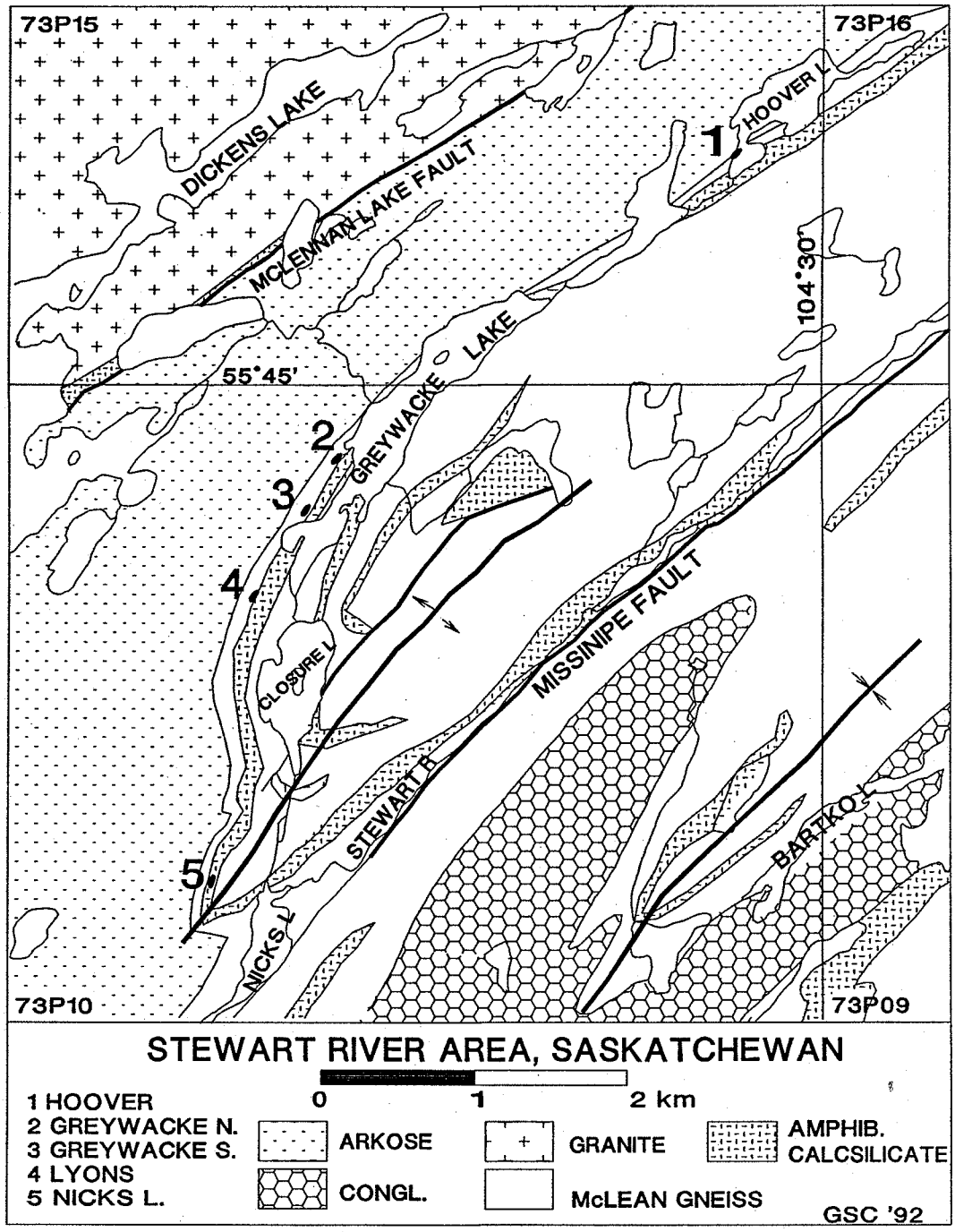

Figure 6.7. Geological map of the Stewart River area showing thelocation of the Greywacke Lake gold deposit with respect to the regional F2 fold centred near Closure Lake.

distribution of units. A small sinistral strike-slip fault, also with a 340° strike may be another manifestation of D3 deformation.

In addition to the mesoscopic folds described above, numerous others of similar size were observed in the outcrops at Greywacke Lake. These lack systematic axial plane orientations and invariably are associated with margins of pegmatitic intrusions. They appear to be of D2 and/or D3 generation in that they re-fold S1 but their localization and irregularity of orientation is attributable their common occurrence as indentations into necks of boudins in the pegmatite bodies.

Given the orientation of S2 and the position of the Greywacke Lake outcrops in relation to a major (S2?) synform that closes approximately one km to the east (Fig. 6.7), it is likely that the S2 cleavage and minor S-shaped F2 folds at greywacke are related to this larger structure. At Greywacke, F2 folds are small by comparison with the F1 folds, but it can be anticipated that elsewhere in the Stewart River area, where F1 and F2 folds may be of similar amplitude and wavelength, complex fold interference patterns might be encountered. The minimal effect of D2 at Greywacke Lake is fortunate, however, in that a relatively simple analysis is possible for the F1 folds which exert some control on mineralization.

Greywacke Lake falls into the broad category of disseminated gold deposits. The mineralization, although stratabound at the property-scale, occurs in discordant lenses at the local scale. The microscopic scale alignment of the sulfide minerals with S1 foliation and the macroscopic alignment of the sulfide-bearing lenses with F1 fold axial surfaces strongly suggests that mineralization was at least synchronous with, but more likely pre-dated, D1. We prefer the latter interpretation because, although the Greywacke North zone occupies the hinge of an F1 anticline, the Centre and South zones are located on its long limb. In addition, we could find no evidence of anomalous D1 deformation (higher strain zones for example) that would correlate directly with mineralization. The fact that the mineralized zones are now parallel to the axial surface of F1 folds is likely the result of their transposition, along with their host rocks, into the S1 orientation. The mineralized zones were certainly much more discordant to their host units than they now appear to be.

The apparent orientational control on the Greywacke mineralization by F1 folds is important for the planning of drill campaigns for mineralization of this type. Irrespective of genetic considerations, it is well known empirically that, where folding is a factor, it is common for gold orebodies to follow fold plunge for remarkably long distances. Examples include the "ledges" at the Homestake Mine, the vein, sulphide and porphyry orebodies at Geraldton and the complex vein orebodies on the Orenada property at Val D'Or. At Greywacke we have made a provisional estimate of 340-55° for the trend and plunge of the F1 anticline that contains the North zone. This estimate is constrained by the observed dips of

bedding, by the fact that the hinge line should lie in S1 and by the constraints imposed by the location of the conglomerate unit in drill sections (Poulsen and Robert, 1994). The known zones therefore should project down plunge in a north-northwestward ward direction relative to their surface positions. It must be stressed that the plunge estimate is for the stratigraphic fold hinge, not for the mineralization directly. It is only the co-incidence of the two at surface that suggests the possibility that they may have a common plunge.

Massive au sulfide deposits

Mosquito Creek deposit

The Mosquito Creek deposit in the Cariboo district (Fig. 2.7) is part of a more extensive deposit, composed of orebodies both pre-dating and post-dating a major deformation increment (Robert and Taylor, 1989, 1990). The deposit is hosted in a folded and overturned sequence of carbonaceous clastic sedimentary rocks which includes quartzite, phyllite, limestone and mafic sills or volcanic flows. Gold ores were mined from both pyritic lenses in limestone, or replacement orebodies, and from typical quartz-carbonate-pyrite veins (Figs. 6.8 A and B). Rock units at the mine parallel the regional NW-SE strike and moderate NE dip of an S1 foliation. Overturned beds suggest the presence of early F1 folds, and ductile faults developed within limestone beds are associated with D1. This foliation is overprinted by Z-shaped F2 folds plunging 10-20° to the northwest, with associated axial spaced S2 cleavage, which strikes E-W and dips 30° to the north (Figs. 6.9A and B). Development of a strong L2 elongation lineation, parallel to F2 fold axes, also characterizes D2.

Two sets of auriferous veins postdate F2 folds (Fig. 6.9A): diagonal veins are oblique to L2 strike east-west and are subvertical, whereas orthogonal veins are perpendicular to L2 and strike 030-040° and dip 70° to the southeast. Orthogonal veins may either cross-cut or splay from diagonal veins and are slightly younger. Both vein sets are interpreted to represent continued extension along L2. Pyritic orebodies occur exclusively within limestone layers. They range in shape from tabular bodies on limbs of F2 folds, to the more common pencil shape bodies parallel to L2 in the hinges of F2 folds (Fig. 6.9A). Previous workers considered the pyrite replacement of limestone as coeval with emplacement of the diagonal veins and viewed them as vein-related alteration products (Skerl, 1948; Alldrick, 1983). However, pyritic layers in F2 fold hinges are clearly overprinted and transposed by the S2 cleavage (Fig. 6.10), indicating that these orebodies predate the F2 folding and are earlier than the two sets of mineralized veins.

The overall geometry of the deposit is further complicated by a set of post-ore northerly trending faults dipping 40-70° to the east dextrally offset lithologic units (Fig. 6.8A). As for the Orenada Zone 4 deposit, folded orebodies at Mosquito Creek

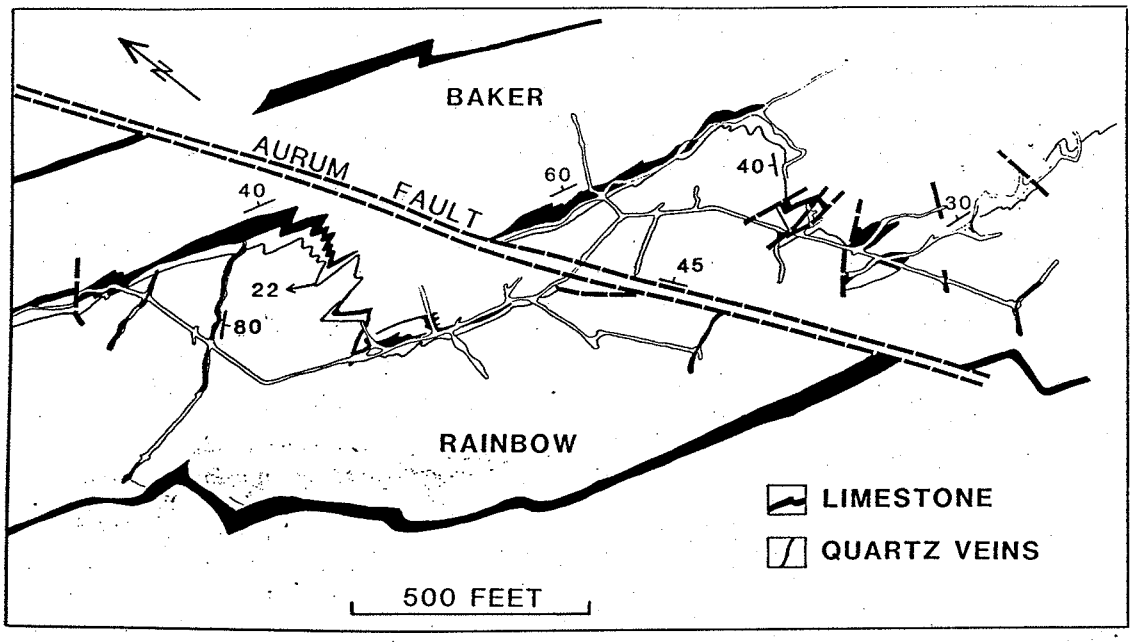

A

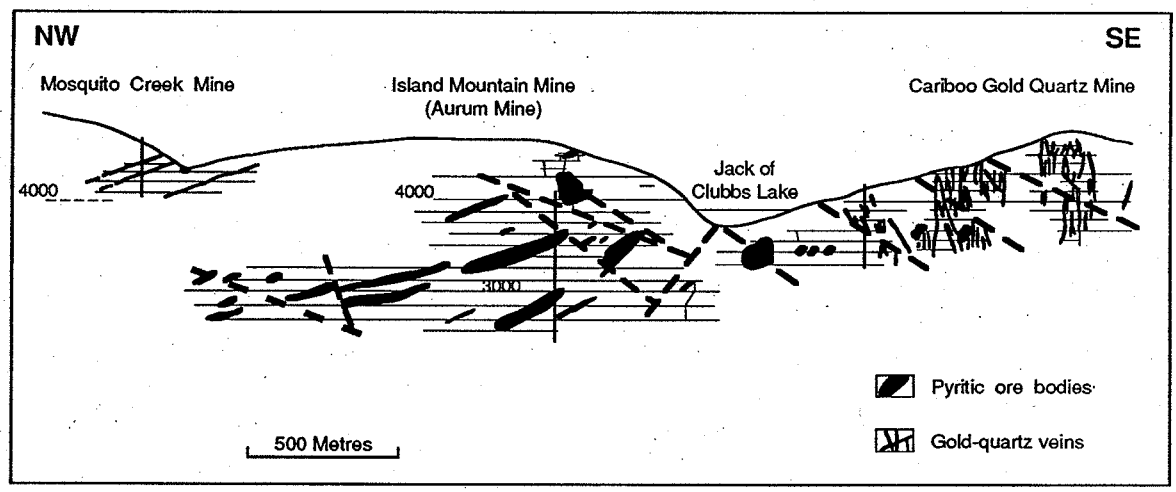

B

Figure 6.8. The Mosquito Creek, Island Mountain and Cariboo Gold Quartz deposits. (**A**) Simplified geological map of the 3500 foot level of the Island Mountain mine; from Benedict (1945). (**B**) Simplified longitudinal section through the three deposit showing the shallow NW plunge of the pyritic orebodies and the trace of the most significant quartz veins; from Alldrick (1983).

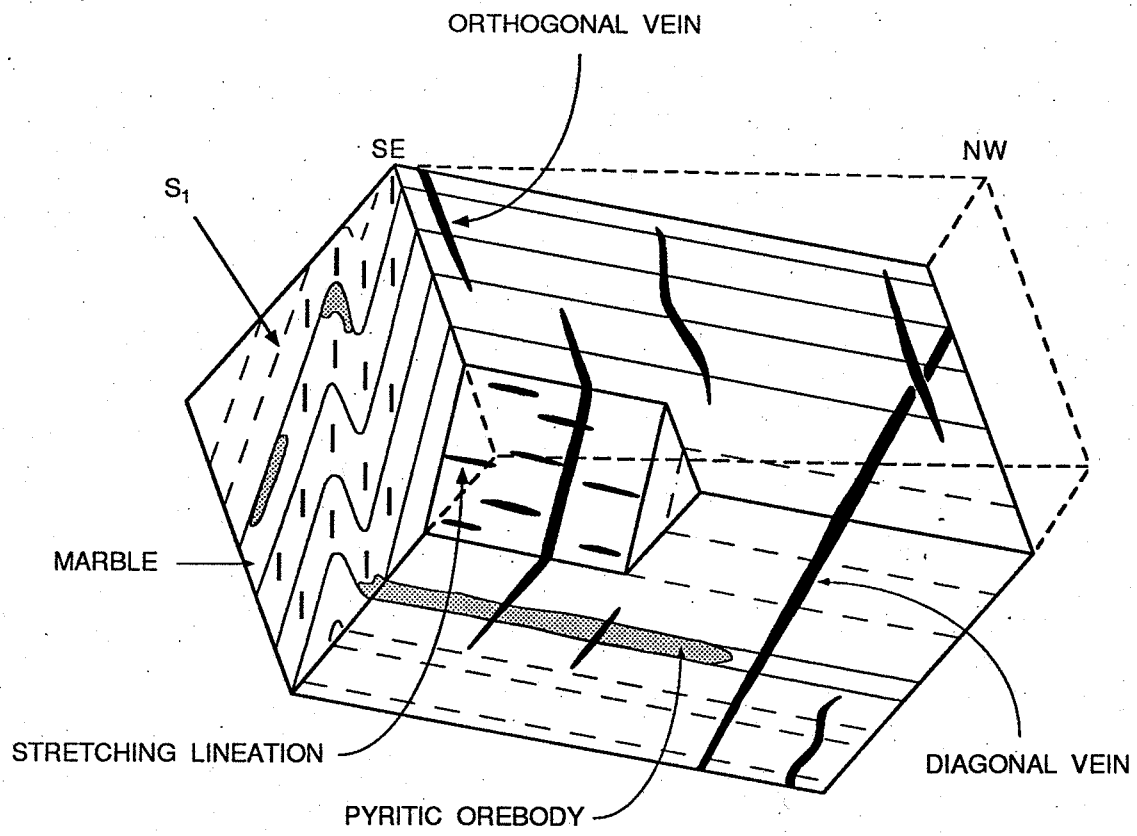

A

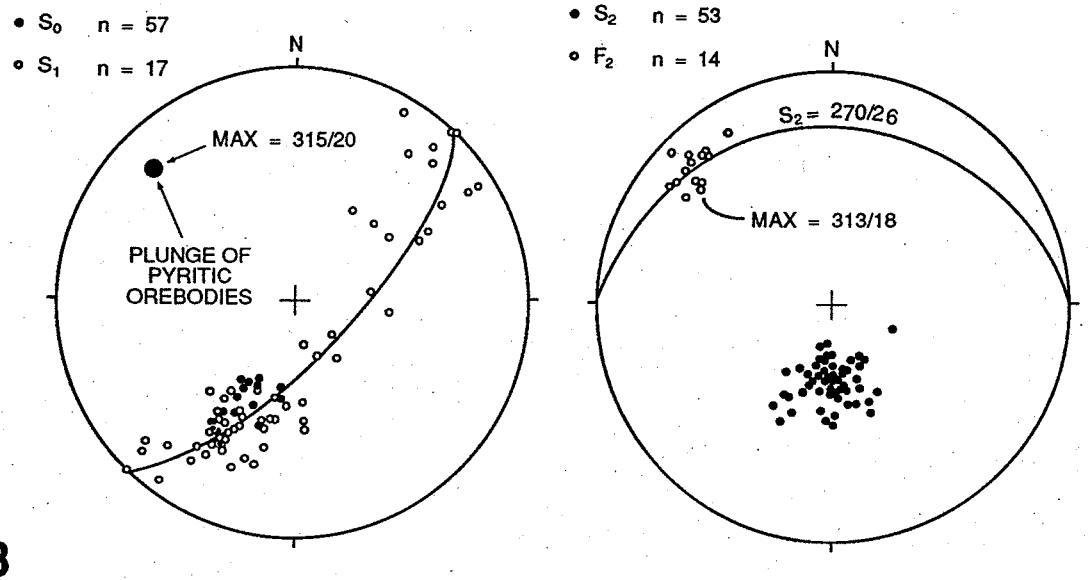

B

Figure 6.9. The Mosquito Creek deposit. (**A**) Block diagram illustrating relationships between pyritic orebodies, veins and structural features of the deposit. (**B**) Stereographic projections (equal area) of structural elements of the deposits.

are more abundant in the hinges of the folds and they have a long axis that is parallel to that of the folds. The fact that early, pyritic orebodies are deformed and folded is indicated the presence of a crenulation cleavage overprinting pyrite layers. In both cases, the plunge of the folded orebodies is parallel to the plunge of mesoscopic folds.

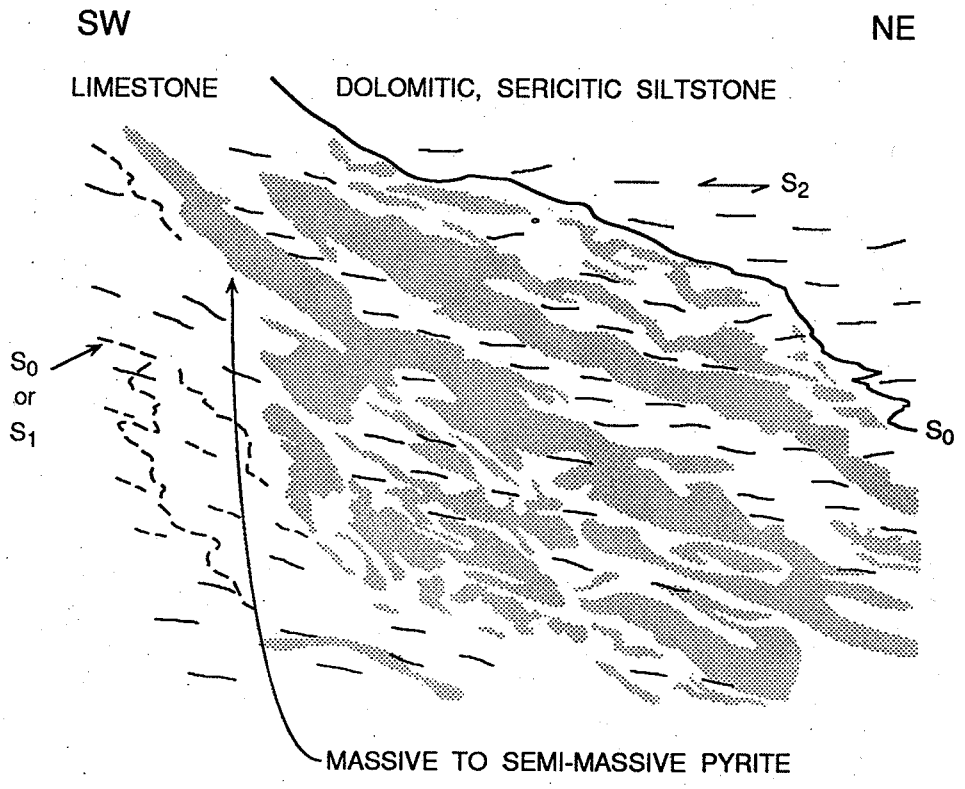

Figure 6.10. Cross-section of pyrite layers, parallel to the hangingwall contact of a limestone band, overprinted and partially transposed by S2.

REFERENCES

Aleksandrowski, P. 1985. Graphical determination of principal stress directions for slickenside lineation populations: An attempt to modify Arthaud's method. Journal of Structural Geology, v. 7, p. 73-82.

Alldrick, D.J. 1983. The Mosquito Creek Mine, Cariboo Gold Belt, B.C. Ministry of Energy, Mines and Petroleum Resources, Paper 83-1, p. 98-112.

Anderson, E.M. 1905. The dynamics of faulting. Transactions of the Edinburgh Geological Society, v. 8, p. 387-402.

Anderson, E.M. 1951. The dynamics of faulting. Edinburgh, Olivier Boyd, 183p.

Angelier, J., and Mechler, P. 1977. Sur une méthode graphique de recherche des contraintes principales également utilisable en tectonique et en séismologie: La méthode des dièdres droits. Bulletin de la Société Géologique de France, v. 7, p. 1309-1318.

Angelier, J. 1984. Tectonic analysis of fault slip data sets. Journal of Geophysical Research, v. 89, p. 5835-5848.

Arthaud, F. 1969. Méthode de détermination graphique des directions de raccourcissement, d'allongement et intermédiaire d'une population de failles. Bulletin de la Société Géologique de France, v. 7, sér. 1, p. 1309-1318.

Bédard, P. 1979. Compagnie Minière Lamaque Limitée. GAC-MAC Joint Annual Meeting, Excursion A2 Guidebook, p. 59-65.

Belkabir, A. 1990. Géologie du gisement filonien d'or, Dumont et géochimie de ces épontes altérées, Val d'Or, Québec. M.Sc.A. Thesis, École Polythechnique, Montréal, Quebec (Unpubl).

Belkabir, A., Robert, F., Vu, L., and Hubert, C. 1993. The influence of dikes on auriferous shear zone development within granitoid intrusions: the Bourlamaque pluton, Val d'Or district, Abitibi greenstone belt. Canadian Journal of Earth Sciences, v. 30, p. 1924-1933.

Bell, T.H., and Hammond, R.L. 1984. On the internal geometry of mylonite zones. Journal of Geology, v. 75, p. 273-296.

Benedict, P.C. 1945. Structure at Island Mountain Mine, Wells, B.C. Transactions of the Canadian Institute of Mining and Metallurgy, v. 58, p. 755-770.

Berger, A.R. 1971. Dynamic analysis using dikes with oblique internal foliations. Geological Society of America Bulletin, v. 82, pp. 781-786.

Berthé, D., Choukroune, P., and Gapais, D. 1979. Orthogneiss, mylonite and non-coaxial deformation of granites: the example of the South Armorican shear zone. Journal of Structural Geology, v. 1, p. 31-42.

Bott, M.H.P. 1959. The mechanics of oblique slip faulting. Geological Magazine, v. 96, p. 109-117.

Boullier, A.-M. and Robert, F. 1992. Paloeseismic events recorded in Archean gold-quartz vein networks, Val d'Or Abitibi, Quebec. Journal of Structural Geology, v. 14, p. 161-179.

Boulter, C.A., Fotios, M.G., and Phillips, G.N. 1987. The Golden mile, Kalgoorlie: A giant gold deposit localized in ductile shear zones by structurally induced infiltration of an auriferous metamorphic fluid. Economic Geology, v. 82, p. 1661-1678.

Brisbin, W.C., and Lau, M.H.S. 1990. Structural controls for the development of gold veins at the San Antonio Mine, Manitoba, Canada. Geological association of Canada, Program with Abstracts, vol 15, p. A-14.

Brommecker, R., Poulsen, K.H. and Hodgson, C.J. 1989. Preliminary report on the structural setting of gold at the Gunnar Mine in the Beresford Lake area, Uchi Subprovince, southeastern Manitoba. *In* Current Research, Part C, Geological Survey of Canada, Paper 89-1C, p.325-332.

Carey, E. 1979. Recherche des directions principales de contraintes associées au jeu d'une population de failles. Revue de géologie dynamique et de géographie physique, v. 21, Fascicule 1, p. 57-66.

CIMM. 1948. Structural Geology of Canadian Ore Deposits.

Clark, M.E., Archibald, N.J., Hodgson, C.J. 1986. The structural and metamorphic setting of the Victory gold mine, Kambalda, Western Australia. *In* Proceedings of Gold'86, an International Symposium on the Geology of Gold, *edited by* A.J. MacDonald, Toronto, p. 243-254.

Clark, M.E., Carmichael, D.M., Hodgson, C.J., Fu, M. 1989. Wall-rock alteration, Victory gold mine, Kambalda, Western Australia: Processes and P-T-X_{CO2} conditions of metasomatism. *In* The geology of gold deposits: The perpective in 1988, *edited by* R.R. Keays, W.R.H. Ramsay, D.I. Groves. Economic Geology Monograph 6, p. 445-459.

Cobbold, P.R. 1976. Mechanical effects of anisotropy during large finite deformation. Bulletin de la Société Géologique de France, v. 17, p. 1497-1510.

Coombe, W., Lewry, J.F. and Macdonald, R. 1986. Regional geological setting of gold in the La Ronge Domain, Saskatchewan. *In* Gold in the Western Shield, *ed.* L. A. Clark; Canadian Institute of Mining and Metallurgy, Special Volume 38, p. 26-56.

Cox, S.F. 1991. Geometry and internal structures of mesothermal vein systems: implications for hydrodynamics and ore genesis during deformation. University of Western Australia, Publication no. 25, p. 47-53.

Cox, S.F., Wall, V.J., Etheridge, M.E., and Potter, T.F. 1991. Deformational and metamorphic processes in the formation of mesothermal vein-hosted gold deposits - examples from the Lachland fold belt in Central Victoria, Australia. Ore Geology Reviews, v. 6, p. 391-423.

Craig, J.R., and Vaughan, D.J. 1981. Ore Microscopy and Ore Petrography. John Wiley & Sons, Inc., New York, 406 p.

Daigneault, R., St-Julien, P., and Allard, G.O. 1990: Tectonic evolution of the northeast portion of the Archean Abitibi greenstone belt, Chibougamau area, Quebec. Canadian Journal of Earth Sciences, v. 27, p.1714-1736.

Dion, C., Guha, J., and Fournier, R. 1990. Géologie de la mine Joe Mann. *In* Litho-tectonic Framework and Associated Mineralization of the Eastern Extremity of the Abitibi Greenstone Belt (field trip 3), *edited by* J. Guha, E.H. Chown and R. Daigneault. 8th IAGOD Symposium, Field trip guidebook. Geological Survey of Canada, Open File 2158, p. 97-103.

Donath, F.A. 1961. Experimental study of shear failure in anisotropic rocks. Geological Society of America Bulletin, v. 72, p. 985-990.

Donath, F.A. 1962. Role of layering in geological deformation. Transactions of the New York Academy of Sciences, ser II, 24, no 3, p. 236-249.

Dubé, B., Poulsen, K.H., and Guha, J. 1989. The effects of layer anisotropy on auriferous shear zones: The Norbeau Mine, Quebec. Economic Geology, v. 84, p. 871-878.

Dubé, B., and Guha, J. 1989. Étude métallogénique (aurifère) du filon-couche de Bourbeau, région de Chibougamau: synthèse finale. Ministère de l'Énergie et des Ressources du Québec, Mémoire MM 87-03, 156p.

Dubé, B., and Guha, J. 1992. Relationship between northeast-trending regional faults and Archean mesothermal gold-copper mineralization: Cooke Mine, Abitibi Greenstone belt, Quebec, Canada. Economic Geology, v. 87, p. 1525-1540.

Dubé, B., Lauzière, K., and Gaboury, D. 1992. Preliminary report on the structural control of the Rendell-Jackman gold deposit, Springdale Peninsula,

Newfoundland. *In* Current Research, Part D, Geological Survey of Canada, Paper 92-1D, p. 1-10.

Eisenlohr, B.N., Groves, D.I., and Partington, G.A. 1989. Crustal-scale shear zones and their significance to Archean gold mineralization in Western Australia. Mineralium Deposita, v. 24, p. 1-8.

Etheridge, M.A. 1983. Differential stress magnitudes during regional deformation and metamorphism - upper bound imposed by tensile fracturing. Geology, v. 11, p. 231-234.

Foxford, K.A., Nicholson, R., and Polya, D.A. 1991. Textural evolution of W-Cu-Sn-bearing hydrothermal veins at Minas da Panasqueira, Portugal. Mineralogical Magazine, v 55, p. 435-445.

Hanmer, S., and Passchier, C. 1991. Shear-sense indicators: A review. Geological Survey of Canada, Paper 90-17, 72 p.

Hibbard, J. 1983. Geology of the Baie Verte Peninsula, Newfoundland. Mineral Development Division, Newfoundland Department of Mines and Energy, Memoir 278 p.

Hobbs, B.E., Means, W.D., and Williams, P.F. 1976. An outline of structural geology. Wiley and Sons, 571p.

Hodgson, C.J. 1989. The structure of shear-related, vein-type gold deposits: A review. Ore Geology Reviews, v. 4, p. 231-273.

Hubert, C., Trudel, P., and Gelinas, L. 1984. Archean wrench fault tectonics and structural evolution of the Blake River Group, Abitibi Belt, Quebec. Canadian Journal of Earth Sciences, v. 21, p. 1024-1032.

Jackson, S.L., Sutcliffe, R.H., Ludden, J.N., Hubert, C., Green, A.G., Milkereit, B., Mayrand, L., West, G.F., and Verpaelst. 1990. Southern Abitibi greenstone belt: Archean crustal structure from seismis-reflection profiles. Geology. v. 18, p. 1086-1090.

Kerrich, R. 1989. Geodynamic setting and hydraulic regimes: shear zone hosted mesothermal gold deposits. *In* Mineralization and Shear Zones, *edited by* J.T. Bursnall, Geological Association of Canada, Short Course Notes v. 6, p. 89-128.

Lau, M.H.S. 1988. Structural geology of the vein system in the San Antonio Mine, Bissett, Manitoba, Canada. Unpublished M.Sc. thesis, Department of Geological Sciences, University of Manitoba, 154p.

Lewry, J.F., Thomas, D.J., Macdonald, R. and Chiarenzelli, J. 1990. Structural relations in Accreted terranes of the Trans-Hudson Orogen, Saskatchewan:

telescoping in a collisional regime? *in* The Early Proterozoic Trans-Hudson Orogen of North America, *edited by* J.F. Lewry and M.R. Stauffer. Geologiccal Association of Canada, Special Paper 37, p.75-94.

Lindgren, W. 1933. Mineral Deposits. McGraw-Hill Book Company, N.Y., 930 p.

Lisle, R.J. 1987. Principal stress orientations from faults: an additional constraint. Annales Tectonicae, v. 1, n. 2, p. 155-158.

Lisle, R.J. 1988. Romsa: A basic program for paleostress analysis using fault-striation data. Computers and Geosciences, v. 14, No 2. p. 255-259.

Lisle, R.J. 1989. Paleostress analysis from sheared dike sets. Geological Society of America Bulletin, v. 101, p. 968-972.

Lister, G.S., and Williams, P.F. 1983. The partitioning of deformation in flowing rock masses. Tectonophysics, v. 92, p. 1-33.

Mannard, G.N. 1990. La zone minéralisée de Paramaque. The Northwestern Quebec Polymetallic Belt, Excursion Guidebook, Canadian Institute of Mining and Metallurgy, p. 167-169.

Marquis, P., Hubert, C., Brown, A.C., and Rigg, D.M. 1990. An evaluation of genetic models for gold deposits of the Bousquet district, Quebec, based on their mineralogic, geochemical and structural characteristics. *In* The Northwestern Québec Polymetallic Belt: A Summary of 60 years of Mining Exploration. *Edited by* M. Rive, P. Verpaelst, Y. Gagnon, J.-M. Lulin, G. Riverin and A. Simard. Canadian Institute of Mining and Metallurgy, Special volume 43, p. 383-399.

McClay, K.R. 1987. The Mapping of Geological Structures. Geological Society of London Handbook, Open University Press, John Wiley and Sons, New York,

McKinstry, H. E. 1948. Mining Geology. Prentice-Hall Inc., New York. 680 p.

McKinstry, H.E. and Ohle, E.L. 1949. Ribbon structure in gold-quartz veins. Economic Geology, v. 54, p. 87-109.

Means, W.D. 1990. Kinematics, stress, deformation and material behavior. Journal of Structural Geology, v. 12, p. 953-972.

Newhouse, W.H. 1942. Structural features associated with the ore deposits described in this volume. *In* Ore Deposits as Related to Structural Features, *edited by* W.H. Newhouse, Princeton University Press, Princeton, New Jersey, p. 9-53.

Nicholson, R., and Pollard, D.D. 1985. Dilation and linkage of echelon cracks. Journal of Structural Geology, v. 7, p. 583-590.

Peters, S.G. 1993. Formation of oreshoots in mesothermal gold-quartz vein deposit: examples from Queensland, Australia. Ore Geology Reviews, v. 8, p. 277-301.

Picard, S. 1990. Le gisement Silidor. *In* The Northwestern Québec Polymetallic Belt: A Summary of 60 years of Mining Exploration. *Edited by* M. Rive, P. Verpaelst, Y. Gagnon, J.-M. Lulin, G. Riverin and A. Simard. Canadian Institute of Mining and Metallurgy, Special volume 43, p. 175-183.

Platt, J.P. 1983. Progressive refolding in ductile shear zones. Journal of Structural Geology, v. 6, p. 619-622.

Pollard, D.D., and Segall, P. 1987. Theoretical displacements and stresses near fractures in rocks: with applications to faults, joints, veins, dikes, and solution surfaces. *In* Fracture Mechanics of Rocks, *edited by* B.K. Atkinson, Academic Press, p. 277-349.

Pollard, D.D., Segall, P., and Delaney, P.T. 1982. Formation and interpretation of dilatent echelon cracks. Geological Society of America Bulletin, v. 93, p. 1291-1303.

Poulsen, K.H. 1986. Auriferous shear zones with examples from the Western Shield. *In* Gold in the Western Shield, *edited by* L.C. Clark, Canadian Institute of Mining and Metallurgy, Special Volume 38, p. 86-103.

Poulsen, K.H., Ames, D.E., Lau, M.H.S., and Brisbin, W.C. 1986. Preliminary report on the structural setting of gold deposits in the Rice Lake area, Uchi subprovince, southeastern Manitoba. *In* Current Research, part B, Geological Survey of Canada, Paper 86-1B, p. 213-221.

Poulsen, K. H., Ames, D. E., Galley, A. G., Derome, I., and Brommecker, R. 1987. Structural studies in the northern part of the LaRonge Domain. *In* Summary of Investigations 1987, Saskatchewan Geological Survey, Miscellaneous Report 87-4, pp. 107-114.

Poulsen, K. H., and Robert F. 1989. Shear zones and gold: practical examples from the southern Canadian Shield. *In* Mineralisation and Shear Zones, *edited by* J.T. Burnsnall, Geological Association of Canada, Short Course Notes v. 6, p. 239-266.

Poulsen, K.H., and Robert, F. 1994. Disseminated gold mineralization in the Stewart River area, La Ronge Domain, Saskatchewan. *In* Current Research 1994-C, Geological Survey of Canada, p. 103-112.

Poulsen, K.H., Card, K.D. and Franklin, J.M. 1992. Archean tectonic and metallogenic evolution of the Superior Province of the Canadian Shield. *In*

Precambrian Metallogeny Related to Plate Tectonics, *edited by* G. Gaal and K.J. Schultz, Precambrian Reseach, v. 58, p.25-54.

Ramberg, H. 1959. Evolution of ptygmatic folding. Norsk Geol.Tidsskr., v. 39, p. 99-151.

Ramberg, H. 1964. Selective buckling of composite layers with contrasted rheological properties, a theory for the simultaneous formation of several orders of folds. Tectonophysics, v. 1, p. 307-341.

Ramsay, J.G. 1980. Shear zone geometry: A review. Journal of Structural Geology, v. 2, p. 83-100.

Ramsay, J.G. 1983. Rock ductility and its influence on the development of tectonic structures in mountain belts. *In* Mountain Building Processes, *edited by* K.J. Hsü, Academic Press, p. 111-127.

Ramsay, J.G., and Huber, M.I. 1983. The Techniques of Modern Structural Geology. Volume 1: Strain Analysis. Academic Press, 307 p.

Ramsay, J.G., and Huber, M.I. 1987. The Techniques of Modern Structural Geology. Volume 2: Folds and Fractures. Academic Press, 700 p.

Ranalli, G., and Yin, Z.M. 1990. Critical stress difference and orientation of faults in rocks with strength anisotropies: the two-dimensional case. Journal of Structural Geology, v 12, p. 1067-1071.

Richard, M., Hubert, C., Brown, A.C., and Sirois, R. 1990. The Pierre Beauchemin gold mine: a structurally controlled deposit within a sub-horizontal layered composite granitoid. *In* The Northwestern Québec Polymetallic Belt: A Summary of 60 years of Mining Exploration, *Edited by* M. Rive, P. Verpaelst, Y. Gagnon, J.-M. Lulin, G. Riverin and A. Simard, Canadian Institute of Mining and Metallurgy, Special volume 43, p. 211-219.

Robert, F. 1989. The internal structure of the Cadillac tectonic zone southeast of Val d'Or, Abitibi Belt, Quebec. Canadian Journal of Earth Sciences, v. 26, p. 2661-2675.

Robert, F. 1990a. Structural setting and control of gold-quartz veins the Val d'Or area, southestern Abitibi Subprovince. *In* Gold and Base Metal Mineralisation in the Abitibi Subprovince, Canada, with Emphasis on the Quebec Segment, *Compiled by* S.E. Ho, F. Robert, and D.I. Groves. University of Western Australia, Publication 24, p.164-209.

Robert, F. 1990b. An overview of gold deposits in the Eastern Abitibi Subprovince. *In* The Northwestern Quebec Polymetallic Belt, *edited by* M. Rive, P. Verpaelst, Y. Gagnon, J.-M. Lulin, G. Riverin and A. Simard, Canadian Institute of Mining and Metallurgy, Special Volume 43, p. 93-105.

Robert, F. 1994a. Vein fields in gold districts: The example of Val d'Or, southeastern Abitibi. *In* Current Research 1994-C, Geological Survey of Canada, p. 295-302.

Robert, F. 1994. Timing relationships between Cu-Au mineralization, dykes and shear zones in the Chibougamau Camp, northeastern Abitibi Subprovince. *In* Current Research1994-C, Geological Survey of Canada, p. 287-294.

Robert, F., and Brown, A.C. 1986a. Archean gold-bearing quartz veins at the Sigma mine, Abitibi greenstone belt, Quebec. Part I. Geologic relations and formation of the vein system. Economic Geology, v. 81, p. 578-592.

Robert, F., and Brown, A.C. 1986b. Archean gold-bearing quartz veins at the Sigma mine, Abitibi greenstone belt, Quebec. Part II. Vein paragenesis and hydrothermal alteration. Economic Geology, v. 81, p. 593-616.

Robert F., and Taylor, B.E. 1990. Structural evolution and gold remobilization at the Mosquito Creek Gold Mine, Cariboo district, British Columbia; Geological Association of Canada, Mineralogical Association of Canada, Joint Annual Meeting, Vancouver 1990, Program With Abstracts, Vol. 15, p. A112.

Robert, F., and Poulsen, K.H. 1991. Practical applications of structural analysis of lode gold deposits. University of Western Australia Publication no. 25, p. 47-53.

Robert, F., Brommecker, R., and Bubar, D. S. 1990. The Orenada Zone 4 deposit: deformed vein-type gold mineralization within the Cadillac Tectonic Zone SE of Val d'Or. *In* The Northwestern Quebec Polymetallic Belt, *edited by* M. Rive, P. Verpaelst, Y. Gagnon, J.-M. Lulin, G. Riverin, and A. Simard, Canadian Institute of Mining and Metallurgy, Special Volume 43, p. 255-268.

Sansfaçon, R. and Hubert, C. 1990. The Malartic gold district, Abitibi greenstone belt, Quebec: Geological setting, structure and timing of gold emplacement at Malartic Goldfields, Barnat, East-Malartic, Canadian Malartic and Sladen mines. *In* The Northwestern Quebec Polymetallic Belt, *edited by* M. Rive, P. Verpaelst, Y. Gagnon, J.-M. Lulin, G. Riverin, and A. Simard. Canadian Institute of Mining and Metallurgy, Special Volume 43, p. 221-235.

Sauvé, P., Imreh, L., and Trudel, P. 1993. Description des gîtes d'or de la région de Val d'Or. Ministère de l'Énergie et des Ressources, Québec, MM 91-03, 178 p.

Scholz C.H. 1989. Mechanics of faulting. Annual Review of Earth and Planetary Sciences, v. 7, p. 309-334.

Sibson, R.H. 1977. Fault rocks and fault mechanisms. Journal of the Geological Society of London, v. 133, p. 191-213.

Sibson, R.H. 1986. Brecciation processes in fault zones: inferences from earthquake rupturing. PAGEOPH, v. 124, p. 159-175.

Sibson, R.H. 1990. Faulting and fluid flow. *In* Short Course on Fluids in Tectonically Active Portions of the Crust, *edited by* B.E. Nesbitt. Mineralogical Association of Canada, p. 93-129.

Sibson, R.H., Robert, F., and Poulsen, K.H. 1988. High-angle reverse faults, fluid-pressure cycling and mesothermal gold-quartz deposits. Geology, v. 16, p. 551-555.

Stewart, P.W. 1992. The origin of the Hope Brook mine, Newfoundland: a shear zone-hosted acid-sulphate gold deposit. PhD thesis, University of Western Ontario, London, Ontario, 398 p.

Struik, L.C. 1988. Structural geology of the Cariboo Mining District, east-central British Columbia. Geological Survey of Canada, Memoir 421, 100p.

Struik, L.C. 1986. Imbricated terranes of the Cariboo gold belt with correlations and implications for the tectonics of southeastern British Columbia. Canadian Journal of Earth Sciences, v. 23, 1047-1061.

Talbot, C., and Sokoutis, D. 1992. The importance of incompetence. Geology, v. 20, p. 951-953.

Taylor, B.E. and Robert, F. 1989. Structural and geochemical studies at the Mosquito Creek gold mine, Cariboo district, B.C. Cordilleran Geology and Exploration Roundup, Vancouver, Feb. 7-10, 1989, Program with Abstracts, p. A 121.

Tourigny, G., Hubert, C., Brown, A.C., and Crépeau, R. 1988. Structural geology of the Blake River Group at the Bousquet Mine, Abitibi, Québec. Canadian Journal of Earth Sciences, v. 25, p. 581-592.

Tourigny, G., Hubert, C., Brown, A.C., and Crépeau, R. 1989. Structural control of gold mineralization at the Bousquet mine, Abitibi, Quebec. Canadian Journal of Earth Sciences, v. 26, p. 157-175.

Tourigny, G. Doucet, D., and Bourget, A. 1993. Geology of the Bousquet #2 mine: An example of a deformed, gold-bearing, polymetallic sulphide deposit. Economic Geology, v. 88, p. 1578-1597.

Treagus, S.H., 1981. A theory of stress and strain variations in viscous layers, and its geological implications. Tectonophysics, v. 70, p. 75-103

Treagus, S.H. 1983. A theory of finite strain variation through contrasting layers and its bearing on cleavage refraction. Journal of Structural Geology, v. 5, p. 351-368.

Treagus, S.H. 1988. Strain refraction in layered systems. Journal of Structural Geology, v. 3, p. 517-527.

Treagus, S.H., and Sokoutis, D. 1992. Laboratory modelling of strain variation across rheological boundaries. Journal of Structural Geology, v. 14, p. 405-424.

Turner, F.J., and Weiss, L.E. 1963. Structural Analysis of Metamorphic Tectonites. McGraw-Hill Book Company, Inc., New York.

Twiss, R.J., and Moores, E.M. 1992. Structural Geology. W.H. Freeman and Company, New York, 532 p.

Vu, L., Darling, R., Béland, J., and Popov V. 1987. Structure of the Ferderber gold deposit, Belmoral Mines Ltd, Val d'Or, Quebec. Canadian Institute of Mining and Metallurgy Bulletin, v. 80, p. 68-77.

Vu L., 1990. Geology of the Ferderber gold deposit and gold potential of the Bourlamaque batholith, Belmoral Mines Ltd., Val d'Or, Quebec. *In* The Northwestern Quebec Polymetallic Belt, *edited by* M. Rive, P. Verpaelst, Y. Gagnon, J.-M. Lulin, G. Riverin, and A. Simard, Canadian Institute of Mining and Metallurgy, Special Volume 43, p. 237-244.

Walker, S.D., and Cregheur, P. 1982. The Chadbourne mine, Noranda, Quebec: A gold-bearing breccia. *In* Geology of Canadian Gold Deposits, *edited by* R.W. Hodder and W. Petruk. Canadian Institute of Mining and Metallurgy, Special Volume 24, p. 58-66.

Wallace, R.E. 1951. Geometry of shearing stress and relation to faulting. Journal of Geology, v. 59, p. 118-130.

Williams, P.F. 1979. The development of asymmetrical folds in a cross-laminated silstone. Journal of Structural Geology, v. 1, p. 19-30.

Wilson, H.S. 1948. Lamaque Mine. In Structural Geology of Canadian Ore Deposits. Canadian Institute of Mining and Metallurgy, p. 882-889.

Yin, Z.M., and Ranalli, G. 1992. Critical stress difference, fault orientation and slip direction in anisotropic rocks under non-Andersonian stress systems. Journal of Structural Geology, v. 14, p. 237-244.